

The Formation and Characterisation of Protein Bigels



A thesis submitted to the National University of Ireland in
fulfilment of the requirements for the degree of

Master of Science

by

Lucy Moran, B. Sc.

Department of Chemistry

Maynooth University

October 2017

Research Supervisor: Dr. Jennifer McManus

Head of Department: Dr. Jennifer McManus

Declaration

I hereby certify that this thesis has not been submitted before, in whole or in part, to this or any university for any degree and is, except where otherwise stated, the original work of the author.

Signed: _____

Date: _____

Acknowledgments

Firstly, I would like to express my sincere gratitude to my supervisor Dr. Jennifer McManus, for the continuous support during my masters, for her patience, motivation, and immense knowledge which she generously shared with me. Her guidance helped me in all the time of research and writing of this thesis. I could not have imagined having a better supervisor for my masters study.

I would also like to thank Carol and Donna and all of the technical staff in the Chemistry Department for their help over the past year.

Thanks to all the members of the McManus group, past and present, without which I would not have gotten through the past year! Michelle, Mark, and Alice, thank you for all your help and support in my early days of pursuing my masters, I learned so much from you all and it was a pleasure to have crossed paths with you. Matthew, Judith, Sarah, Alessandro and My, thank you all for your help, advice and support, many coffee breaks and occasional yoga class, I am very lucky to have worked with such a fantastic group of researchers.

A huge thank you to my parents for their support over the past year! Yvonne, thank you for your sympathetic ear, and always having a hot dinner waiting for me! Peter, thank you for meeting me for the many walks along the canal and hikes further afield with BB and Connie to help clear my head. Thank you to Hannah, Sean, Declan, Bino and all my friends for all your support and encouragement over the past year.

Finally, thank you to Science Foundation Ireland for funding this work.

Abstract

Bigels can be described as double network systems that consist of two discrete but interpenetrating gel networks that each contribute to the mechanical properties of the gel producing a much stronger more robust gel. The first protein-protein bigel consisting of BSA and gelatin in a 9:10 ratio, was previously described by my colleagues in 2015 (Blumlein and McManus, 2015). The method of preparation for these bigels was optimised and standardised for consistency amongst future measurements. New proteins were then explored as potential candidates for the bigels. New proteins were carefully chosen based on their physio-chemical properties. Then, by tuning the conditions of the protein solution it is possible to control the kinetics of the gelation procedure, ensuring that both gel systems form independently of one another. A new bigel was formed from ovalbumin and gelatin with an elastic modulus of 67 kPa, much greater than previously recorded. In addition, the gels exhibited a high degree of elasticity, with 85 % reversibility recorded. These mechanical properties were all determined using cavitation rheology. As previously reported with the original BSA/gelatin bigel, these newly formed bigels are much stronger than the combined elastic moduli of their parent gels.

Preliminary cellular studies showed a positive growth response towards the bigels when compared with collagen scaffolds and untreated wells, which in combination with their biocompatibility, biodegradability and mechanical strength highlights the huge potential these bigels have for biomedical applications such as drug delivery, wound healing and in particular stress-bearing applications such as replacement bone, ligament and cartilage.

Abbreviations

ACS	absorbable collagen sponge
BSA	bovine serum albumin
CGM	complete growth medium
CPP	central precocious puberty
CR	cavitation rheology
DMEM	Dulbecco's Modified Eagle's Medium
DMSO	dimethyl sulfoxide
DN	double-network
DNACC	DNA coated colloid
DSC	differential scanning calorimetry
ECM	extracellular matrix
EGF	epidermal growth factor
FESEM	field emission scanning electron microscopy
Gel-75g	gelatin; bloom number 75g
Gel-225g	gelatin; bloom number 225g
HA	hydroxyapatite
HEK	human embryonic kidney
IPN	interpenetrating network
LH	luteinizing hormone
LOD	limit of detection
MSC	mesenchymal stem cells
MTT	3-(4,5-dimethylthiazol-2-yl)-2,5-diphenyltetrazolium bromide
OVA	ovalbumin
PB	Presto Blue viability assay
PBS	Phosphate buffered saline
P_c	critical pressure
PEG	polyethylene glycol

RFU	relative fluorescence units
SDS	sodium dodecyl sulphate
SEM	scanning electron microscopy
T _m	melt transition temperature
XTT	(2,3-bis-(2-methoxy-4-nitro-5-sulfophenyl)-2H-tetrazolium-5-carboxanilide)

Table of Contents

Declaration	i
Acknowledgments	ii
Abstract	iii
Abbreviations	iv
Chapter 1: Introduction	10
1.1 Soft matter	11
1.1.1 Protein structure	11
1.2 Self-assembly of proteins	12
1.2.1 The thermodynamics of protein self-assembly	13
1.2.2 Intermolecular interactions.....	14
1.2.2.1 Electrostatic interactions	14
1.2.2.2 Van der Waals forces.....	15
1.2.2.3 Hydrogen bonding	15
1.2.2.4 The hydrophobic effect	16
1.3 Phase transitions in proteins	16
1.3.1 Protein phase diagram	16
1.3.2 Protein aggregation	18
1.3.3 Spinodal decomposition in proteins	19
1.4 Gelation	20
1.4.1 Chemical gels	20
1.4.2 Physical gels.....	20
1.4.2.1 Colloidal gelation	21
1.4.3 Double network gels	22
1.5 Model proteins.....	24
1.5.1 Bovine Serum Albumin (BSA)	24
1.5.2 Ovalbumin (OVA)	25
1.5.3 Gelatin	26
1.5.4 Collagen	27
1.6 Cells and Tissues	28
1.6.1 HEK 293T cell line	28
1.6.2 Hydrogel scaffolds	28

1.6.2.1	Design criteria	29
1.6.2.1.1	Biodegradation	29
1.6.2.1.2	Biocompatibility	30
1.6.2.1.3	Porosity	30
1.6.2.1.4	Mechanical properties	30
1.6.2.1.5	Surface properties	31
1.6.2.2	Applications of hydrogel scaffolds.....	32
1.6.2.2.1	Wound healing	32
1.6.2.2.2	Tissue engineering	33
1.6.2.2.3	Drug delivery	34
1.6.3	Cell viability assays	35
1.6.3.1	Tetrazolium reduction assays	35
1.6.3.2	Resazurin reduction assays.....	36
1.7	Thesis Motivation.....	37
Chapter 2: Materials and Methods		38
2.1	Preparation of materials.....	39
2.1.1	Reagents	39
2.1.2	Gel preparation.....	39
2.1.2.1	Single component gels.....	39
2.1.3	Bigels	39
2.1.3.1	Initial bigel preparation procedure	39
2.1.3.2	Optimised bigel preparation procedure	39
2.1.4	Collagen gel preparation	40
2.2	Methods used to characterise protein gels.....	40
2.2.1	Cavitation Rheology	40
2.2.1.1	Background	40
2.2.1.2	Instrumentation.....	43
2.2.2	Optical Microscopy	43
2.2.2.1	Background	43
2.2.2.2	Imaging of protein gels.....	44
2.2.3	Differential scanning calorimetry	44
2.2.3.1	Background	44
2.2.3.2	Instrumentation.....	46
2.2.3.3	Sample preparation.....	46

2.3	Mammalian cell culture	46
2.3.1	Reagents for mammalian cell culture.....	46
2.3.1.1	Complete growth medium	47
2.3.1.2	Phosphate buffered saline.....	47
2.3.1.3	Trypsin-EDTA solution.....	47
2.3.1.4	Sodium hydroxide	47
2.3.1.5	Acetic acid	47
2.3.2	Growing cells from frozen stocks	47
2.3.3	Sub-culturing or passaging of cells	48
2.3.4	Cell counting	48
2.3.5	Freezing cells	48
2.3.6	Collagen Scaffold.....	49
2.3.6.1	2D collagen coating.....	49
2.3.6.2	3D collagen scaffold.....	49
2.3.7	Bigel Scaffolds	49
2.3.7.1	Preparation of bigel scaffold covering entire well surface.....	50
2.3.7.2	Preparation of hollow cylindrical bigel scaffold	50
2.3.8	Presto Blue assay - description	51
2.3.8.1	Fluorescence spectroscopy	51
2.3.8.2	Optimisation of PB	52
2.3.8.3	Use of PB to assess impact of various scaffolds on cell growth	52
2.3.8.4	Imaging cells	53
Chapter 3: Cavitation rheology of protein bigels.....		54
3.1	Introduction	55
3.2	Aims of this study.....	57
3.3	Results	57
3.3.1	Cavitation rheology (CR) instrument.....	57
3.3.2	BSA/Gelatin Bigel	58
3.3.2.1	The impact of needle depth on measurements of the elastic modulus ..	59
3.3.2.2	Preparation conditions for bigel formation	62
3.3.2.3	The impact of pH on the formation and characteristic of bigels	63
3.3.3	New bigel candidates	64
3.3.3.1	Single component ovalbumin gels	65
3.3.3.1.1	Differential Scanning Calorimetry.....	65

3.3.3.1.2	Cavitation Rheology	66
3.3.3.1.3	Reversibility.....	67
3.3.3.1.4	Effect of pH on mechanical properties of the gels.....	68
3.3.3.2	Single component gelatin gels.....	69
3.3.3.2.1	Differential Scanning Calorimetry.....	70
3.3.3.2.2	Cavitation Rheology	70
3.3.4	Ovalbumin/Gelatin-225g Bigels	71
3.3.4.1	Cavitation rheology	71
3.3.4.2	Reversibility	73
3.3.4.3	Light Microscopy:	74
3.4	Discussion	75
3.5	Conclusion.....	80
Chapter 4: Bigels as cell scaffolds.....		81
4.1	Introduction	82
4.2	Aims of this study.....	85
4.3	Results	85
4.3.1	Analysis of the mechanical properties of collagen gel.....	85
4.3.2	In vitro assessment of different cell scaffolds.....	86
4.3.2.1	Optimisation of Presto Blue assay.....	87
4.3.2.2	Preparation of bigel scaffolds for cell culture	88
4.3.2.3	Impact of various scaffolds on cell growth, determined using presto blue assay	89
4.4	Discussion	92
4.5	Conclusion.....	94
Final Conclusions		96
References		98

Chapter 1:

Introduction

1.1 Soft matter

Soft matter can be defined as material that is neither liquid nor crystalline solid, and can be identified by its sensitive response to mechanical and thermal stress. Soft matter is concerned with the study of polymers, gels surfactants and colloidal dispersions. Many biological systems are also composed of soft matter. Globular proteins sometimes behave as colloids (Valente *et al.*, 2005), DNA is a stiff polymer (Peters *et al.*, 2013), membrane lipids can be considered surfactants (Lee *et al.*, 2009). There have been numerous studies done on the colloidal behaviour of proteins (Rosenbaum *et al.*, 1996; Valente *et al.*, 2005). Proteins are polymeric biomolecules consisting of amino acid chains. Small globular proteins have a radius of approximately 1 -2 nm (García De La Torre *et al.*, 2000), and therefore on the lower end of the colloidal length scale. In addition, the net overall charge of a protein is responsible for many important physical properties and phase behaviours such as aggregation, solubility and the formation of colloidal gels (Rosenbaum *et al.*, 1996; Asherie, 2004; Dumetz *et al.*, 2008).

1.1.1 Protein structure

Proteins are complex molecules consisting of four different levels of structure, primary, secondary, tertiary and quaternary. The primary structure of a protein consists of the sequence of amino acids in a polypeptide chain, composed from twenty commonly occurring amino acids. These are small molecules primarily composed of nitrogen, oxygen and hydrogen and can be classified according to their specific properties, whether they are hydrophobic, hydrophilic, acidic or basic. Each protein has a unique sequence of amino acids that determines the folding of the protein and consequently its function. The secondary structure of a protein involves the folding of the amino acid chain. The main secondary structure features include α -helices and β -sheets, which are stabilised through hydrogen bonding. The protein will orient in space to form its most stable structure, stabilised by hydrogen bonds, salt bridges and disulphide bridges. This is known as the tertiary structure of the proteins and along with the secondary structure, is what determines the function of the protein. In a physiological environment, the hydrophobic residues such as alanine, valine, leucine and isoleucine will reside within the interior of the protein, to avoid contact with the hydrophilic medium. The polar and hydrophilic residues such as Asp, Glu, Lys and Arg will dominate at the surface of the

protein. The quaternary structure of a protein is the arrangement of multiple protein molecules held together by disulphide bonds, salt bridges, hydrogen bonds and hydrophobic interactions (Whitford, 2005).

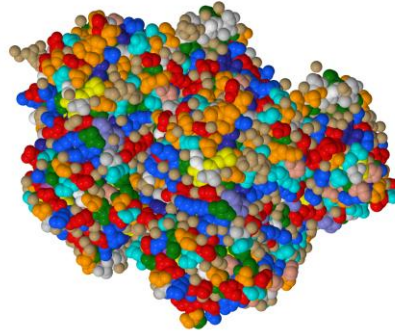


Figure 1.1: 3D representation of ovalbumin, showing complex surface chemistry, where each amino acid is coloured differently. Rendered using Jmol from PDB ID: 1OVA.

1.2 Self-assembly of proteins

The self-assembly of proteins is essential to many biological processes. Proteins only function when they have folded into their correct configuration. In addition, globular proteins can also self-assemble into larger complexes such as crystals, amorphous aggregates or amyloid fibrils, figure 1.2, (McManus *et al.*, 2016), mediated through non-covalent interactions. Failure to assemble correctly can impact biological processes (Ahnert *et al.*, 2015), ultimately leading to disease. Alzheimer’s disease, Parkinson’s disease, cataract formation and sickle-cell anaemia are all associated with protein condensed phases. (Knowles *et al.*, 2014).

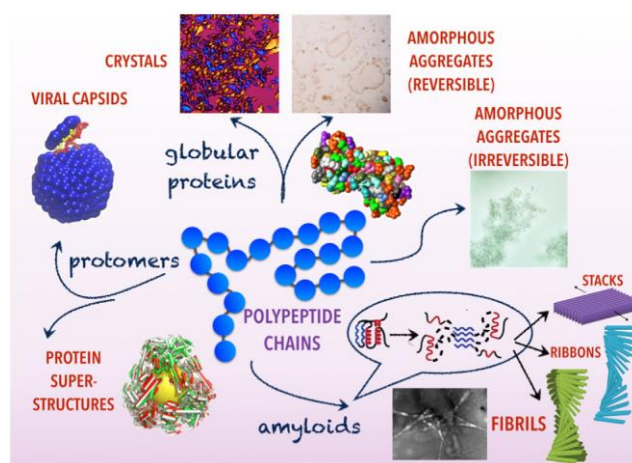


Figure 1.2: An overview of the different condensed phases that can occur from the self-assembly of proteins. Taken from (McManus *et al.*, 2016).

1.2.1 The thermodynamics of protein self-assembly

Thermodynamics involves the relationship between different forms of energy, including; heat, work and temperature and the conversion between these different states (Atkins, 1988). It may be considered the driving force behind the self-assembly of any colloidal system, including that of proteins (Grzybowski *et al.*, 2009). The first law of thermodynamics is concerned with the conservation of energy within a system, stating that energy cannot be created or destroyed within a system and is governed by the following equation;

$$\Delta U = q + w \quad [\text{Eqn. 1.1}]$$

where ΔU is the change in internal energy of the system, q is the heat supplied to the system and w is the work done by the system.

The second law states that the sum of entropies (S) where the entropy represents disorder, of a system will always increase and can be represented by;

$$\Delta S = \frac{q}{T} \quad [\text{Eqn. 1.2}]$$

where ΔS is the change in entropy, T is the temperature of the system in Kelvin. The enthalpy (H) of a system depends on the internal pressure (p), volume (V) and internal energy (U) of a system;

$$H = U + pV \quad [\text{Eqn. 1.3}]$$

The Gibbs free energy of a system ΔG , is related to the enthalpy (H) and entropy (S) of a system by the following equation;

$$\Delta G = \Delta H - T\Delta S \quad [\text{Eqn. 1.4}]$$

When ΔG is equal to zero, a system is said to be in thermodynamic equilibrium, when ΔG is less than zero a system is said to be spontaneous (Atkins, 1988). Proteins will assemble to reduce the entropy and free energy of the system.

1.2.2 Intermolecular interactions

Intermolecular forces are responsible for the existence of different phases of matter, such as liquid, solids and gases. These can be divided into attractive forces and repulsive forces. These non-covalent interactions all work synergistically for the self-assembly of proteins. The four main non-covalent interactions include hydrogen bonding, van der Waals interactions, the hydrophobic effect and electrostatic interactions. The length-scale between the particles is a key parameter in determining the dominant interactions.

1.2.2.1 Electrostatic interactions

Electrostatic interactions occur between charged atoms. They are based on coulombic attractions and are much stronger than hydrogen bonds. Attractive interactions occur between oppositely charged ions, and repulsive interactions occur between similarly charged ions. Salt bridges form between cationic and anionic amino acid residues, contributing to the overall stability of a protein (Whitford, 2005).

Protein molecules also undergo electrostatic forces. In solution, protein molecules either have a net positive or negative charge depending on the pH of the solution. An electric double layer forms around the surface of the protein consisting of a stern layer of strongly bound counter-ions, and a diffuse layer further from the surface with less tightly bound counter-ions, figure 1.3. The zeta potential is the potential difference across the boundary between the diffuse layer and bulk solution, known as the slipping plane, figure 1.3. It is an important measure for the electrostatic interactions between colloidal particles or protein molecules (Liang *et al.*, 2007).

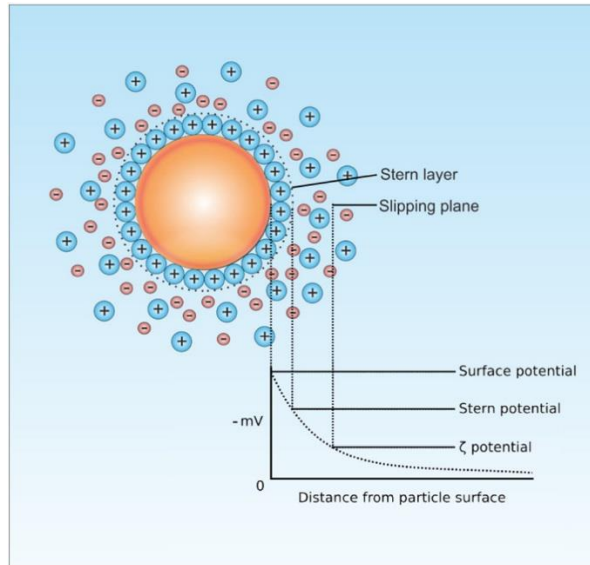


Figure 1. 3 Representation of the electric double layer surrounding a colloid or protein. Taken from (An et al., 2017).

1.2.2.2 Van der Waals forces

Unlike the electrostatic interactions described previously, van der Waals forces exist between neutral atoms and molecules. Otherwise known as dispersion forces, charge fluctuation forces, or induced dipole forces, they involve the interaction between fluctuating dipoles that arise from the outer electrons on two molecules (Everett, 2007). These forces are weak and typically have a long range of between 0.2 nm and 10 nm and increase in magnitude as the molecules approach one another. It can be simplified between two non-polar identical atoms or molecules using the following equation;

$$W(r) = \frac{-C}{r^6} \quad [\text{Eqn 1.5}]$$

where $W(r)$ is the van der Waals potential and r is the distance between the two molecules. The energy associated with van der Waals interactions is approximately 1 kcal/mol (Everett, 2007).

1.2.2.3 Hydrogen bonding

Hydrogen bonding is an attractive interaction that occurs between a hydrogen (H) atom on one group and another highly electronegative atom such as nitrogen (N), oxygen (O) or fluorine (F) on another group. Hydrogen bonding is one of the key driving forces responsible for self-organisation in proteins due to the abundance of relevant atoms in

the amino and carboxyl side-chains and in the backbone of proteins. It plays a significant role in both the secondary and tertiary structure of proteins as well as in protein aggregation. Its importance is illustrated in amyloid fibrils, which are a feature of Alzheimer's disease, and which are governed by the formation of hydrogen bonds between β -sheets, (Knowles *et al.*, 2007). The strength of most hydrogen bonds varies between 10 and 40 kJ mol⁻¹ and are typically short ranged (Israelachvili, 1991).

1.2.2.4 The hydrophobic effect

Hydrophobic forces occur between water molecules and non-polar groups and are driven by entropy. Water in bulk assembles into large clusters of hydrogen-bonded water molecules that may orient themselves into an ordered structure (Liang *et al.*, 2007). When hydrophobic molecules come into contact with water, they disturb the structured orientation of the water molecules resulting in an entropically unfavourable situation. The hydrophobic molecules will therefore re-assemble, in order to minimise their surface area in contact with water, and to achieve equilibrium, expelling the water molecules and thus reducing the total free energy of the system. Amphipathic molecules will re-arrange so that the hydrophobic parts are not exposed to the water resulting in the formation of micelles (Wang *et al.*, 2016).

1.3 Phase transitions in proteins

Water-soluble globular proteins undergo phase transitions in response to various stimuli such as temperature, pH or mechanical stress. Globular proteins are capable of forming various different condensed phases; crystals, gels, amorphous aggregates, dense liquids and amyloid fibrils (Asherie *et al.*, 1996; Dumetz *et al.*, 2008). Gibbs free energy is the driving force behind phase transitions in protein solutions (Prausnitz and Foose, 2007).

1.3.1 Protein phase diagram

Phase diagrams show the different states of a protein as a function of the protein concentration, temperature and solution conditions, such as pH and ionic strength. The most common phase diagrams are two dimensional in which the protein concentration is displayed as a function of another variable, although multi-dimensional phase diagrams

do exist (Asherie, 2004). Depending on these conditions, the protein may form condensed phases or states, such as crystals or aggregates, or it may undergo liquid-liquid phase separation whereby the solution splits into protein-rich and protein-poor regions, figure 1.4, (Asherie *et al.*, 1996; McManus *et al.*, 2016). While relatively few phase diagrams for proteins exist, there has been extensive done on the phase diagram for a few globular proteins including γ -crystallins (Berland *et al.*, 1992; McManus *et al.*, 2007) and lysozyme (Broide *et al.*, 1996; Rosenbaum *et al.*, 1996).

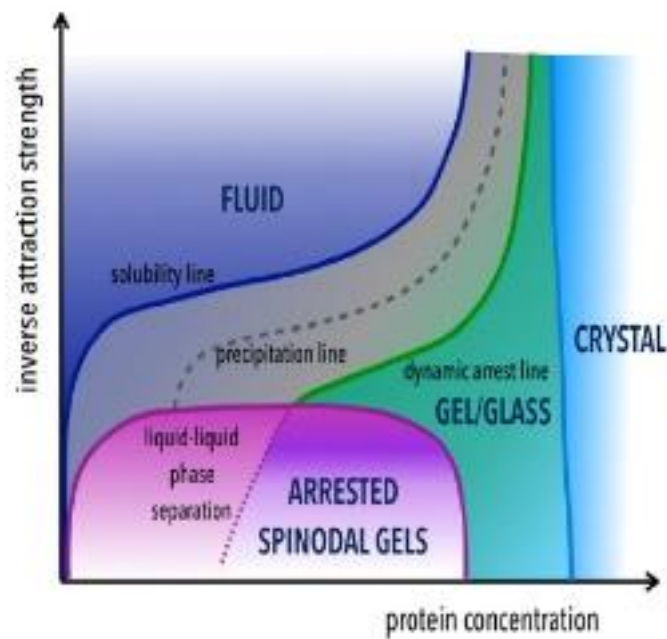


Figure 1.4: Schematic of a state diagram for a globular protein showing the different condensed phases it may form, taken from (McManus *et al.*, 2016).

The phase diagram for lysozyme is shown in figure 1.5. The coexistence curve, also known as the binodal line or liquid-liquid phase separation line indicates the boundary between the protein existing as a single homogenous state, or as two distinct phases, protein rich and protein poor. The solubility curve illustrates how the solubility of the protein varies according to different variables, in this instance temperature and protein concentration. The spinodal line indicates the division between biphasic region into metastable and unstable regions. By quenching the protein solution to deep within the unstable region, spinodal decomposition occurs (Asherie *et al.*, 1996; Cardinaux *et al.*, 2007; Vekilov, 2012). Multiple solubility lines occur when a protein solution of a

certain composition forms more than one crystal phase, for the case of lysozyme tetragonal and rhombohedral crystals can both be formed (Vekilov, 2012).

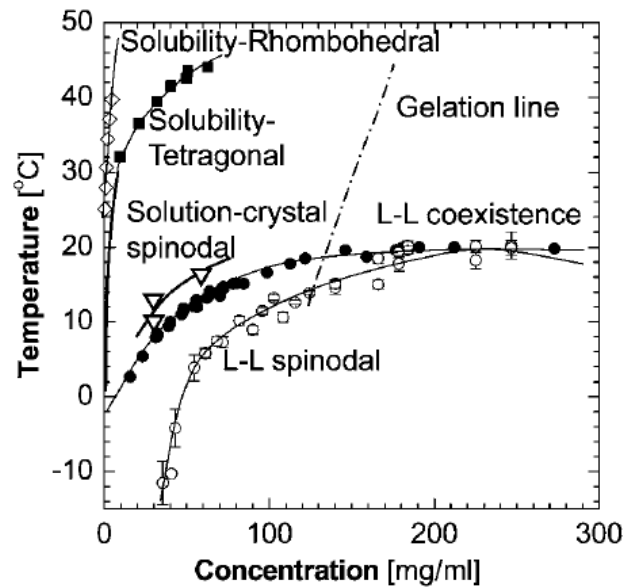


Figure 1.5: Phase diagram for lysozyme. Taken from (Vekilov, 2012).

1.3.2 Protein aggregation

Protein aggregation involves the assembly of proteins into a condensed phase and may be reversible or irreversible (Morris *et al.*, 2009). Protein aggregation can have huge implications for many processes. Many diseases involve protein aggregation such as the formation of amyloid fibrils in Alzheimer's, Huntington's and Parkinson's disease (Knowles *et al.*, 2014), it also leads to many technical problems for biotechnology and pharmaceutical industries such as the aggregation of protein components in drug products which occurs when the proteins are at high concentrations (Wang, 2005).

Protein aggregation may occur from natively folded proteins, unfolded proteins or partially folded protein intermediates (Morris *et al.*, 2009). The aggregation of natively folded proteins involves the self-association of protein monomers to form small oligomers due to specific and non-specific intermolecular interactions between amino acid residues on the surface of the protein. This process is generally reversible however over time as the oligomer grows in size, covalent bonds may form, rendering it irreversible (Philo and Arakawa, 2009).

The self-association of unfolded or partially unfolded protein may also result in aggregates and is generally the dominant mechanism in protein aggregation (Wang, 2005). By altering the solution conditions for the protein such as pH, temperature or ionic strength, it is possible to induce a conformational change in the protein. Solution pH also influences the stability and aggregation of proteins. At the isoelectric point (pI) of a protein, the protein has no overall net charge. However, as the pH of a protein solution is altered, so is the net charge on the protein. As the pH is lowered, the carboxyl and amine groups become protonated resulting in an overall positive charge and as the pH is raised, these groups are deprotonated resulting in a net negative charge. These charges have an impact on the electrostatic interactions between the proteins, and can prevent aggregation from occurring (Li *et al.*, 2016). Temperature also has a strong impact on protein aggregation. Once the temperature of a protein solution is raised above its melting temperature, this causes the protein to unfold exposing hydrophobic residues. In order to reduce the free energy of the system, these residues may form intermolecular bonds such as disulphide covalent bonds, resulting in an aggregated structure (Wang, 2005).

1.3.3 Spinodal decomposition in proteins

Spinodal decomposition occurs in colloidal solutions, including that of proteins, whereby material flows from regions of low concentration to regions of high concentration resulting in two distinct phases consisting of high-density and low-density regions. Unlike aggregation, spinodal decomposition is characterised by a much more defined phase separation which occurs rapidly and uniformly throughout the material (Gibaud and Schurtenberger, 2009). This phenomenon is dependent on certain key parameters including volume fraction (ϕ) and the interparticle interaction strength $U_a/k_B T$ between the colloidal particles. These conditions can be controlled so that the colloidal particles initially undergo spinodal decomposition, whereby the protein solution undergoes liquid-liquid phase separation, followed by a jamming between the high-density and low-density regions, whereby the process of spinodal decomposition becomes arrested. This results in a solid-like percolated network (Cardinaux *et al.*, 2007; Lu *et al.*, 2008; Zaccarelli *et al.*, 2008; Gibaud and Schurtenberger, 2009; Gibaud *et al.*, 2011; Blumlein and McManus, 2015).

1.4 Gelation

Gels are a class of material that have been defined in many ways, incorporating anything from the biopolymer network formed by gelatin, to colloidal silica gels. What these gels have in common is that they each consist of a three-dimensional structure that consists primarily of solvent while still possessing a solid-like consistency (Zaccarelli, 2007). They can be described as a low-density disordered arrested state that possesses shear properties. A sol-gel transition occurs when a liquid mixture of sol particles suspended in a solvent, transforms into a gel through the aggregation of the sol particles, forming a percolating network. (Chambon and Winter, 1987). Hydrogels occur when the liquid solvent is water. Gels can be classified as either chemical, physical or a combination of both depending on the type of bonding present between the particles (Zaccarelli, 2007).

1.4.1 Chemical gels

Chemical gels are formed from cross-linking polymers, through chemical bonds, often with the use of a crosslinker such as glutaraldehyde (Distantina *et al.*, 2012). Natural and synthetic polymers are often crosslinked through reacting their functional groups with a cross-linker. Chemical gels also include epoxy resins and sol-gel glasses. Epoxy resins consist of a short polymer containing reactive groups at either end, which mediate a step-wise growth resulting in a three-dimensional, fully connected network (Corezzi *et al.*, 2005). Another example of a cross-linked polymeric gel are sol-gel glasses. These are formed from the hydrolysis of certain organic derivatives of silicon oxide and metal oxides in the presence of water (Zaccarelli, 2007).

1.4.2 Physical gels

Physical gels occur when the particles interact reversibly through intermolecular forces such as hydrogen bonding, electrostatic interactions and hydrophobic forces. Ionic-cross-linked gels are formed by combining ionic polymers with di- or tri-valent counterions. Alginate gels are very popular in the biomedical industry due to their biocompatibility and their ability to retain structural similarity to the extracellular

matrix (ECM) (Lee and Mooney, 2012). Alginate is a naturally occurring ionic polysaccharide, obtained from brown seaweed. By combining alginate polymers with divalent cations such as Ca^{2+} , it is possible to obtain a cross-linked gel. The cations bind solely to guluronate blocks that occur on the alginate chain, which then form junctions with guluronate blocks on adjacent alginate polymer chain, resulting in a cross-linked gel structure (Lee and Mooney, 2012).

Thermo-reversible gels are formed by cooling hot solutions of gelatin above its melt transition temperature and upon cooling, gelatin transforms from a random coil structure to a helical structure (Yannas, 1972).

1.4.2.1 Colloidal gelation

Colloidal gels consist of clusters of colloidal particles suspended in a liquid solvent where the particles exhibit short-range attraction, and that have aggregated to form a branched, percolated network, capable of sustaining mechanical stress (Lu and Weitz, 2013). They only occur when the distance between the particles is less than the range of attraction. They can be classified as either equilibrium gels or non-equilibrium gels (Zaccarelli, 2007). The former involves gels that don't phase separate, where a stable gel network is formed following a series of equilibrium states (Biffi *et al.*, 2015; Ruzicka *et al.*, 2013). Non-equilibrium routes involve phase separation including that of arrested spinodal decomposition and unlike equilibrium gels, are irreversible (Manley, Wyss, *et al.*, 2005; Lu *et al.*, 2008; Gibaud *et al.*, 2011; Varrato *et al.*, 2012; Di Michele *et al.*, 2014; Blumlein and McManus, 2015; Mahmoudi and Stradner, 2015; Olais-Govea *et al.*, 2015). DLCA (diffusion-limited cluster aggregation) gels occur in low-density colloidal systems and have low fractal dimensions of ~ 1.76 (Zaccarelli, 2007). They involve particles sticking irreversibly to each other and the system's behaviour is determined by the diffusion of the particle (Dinsmore and Weitz, 2002).

As globular proteins can be considered as colloidal particles (Valente *et al.*, 2005), these gelation mechanisms can extend to protein gels. Protein gels have been described that were formed via arrested spinodal decomposition (Cardinaux *et al.*, 2007; Gibaud and Schurtenberger, 2009; Gibaud *et al.*, 2011; Blumlein and McManus, 2015; Mahmoudi and Stradner, 2015). There have been numerous studies on the formation of lysozyme gels via spinodal decomposition (Cardinaux *et al.*, 2007; Gibaud and Schurtenberger,

2009; Gibaud *et al.*, 2011). Cardinaux *et al.* located the gel boundary and glass line, below the coexistence curve in the phase diagram for lysozyme, figure 1.6. through centrifugation experiments (Cardinaux *et al.*, 2007).

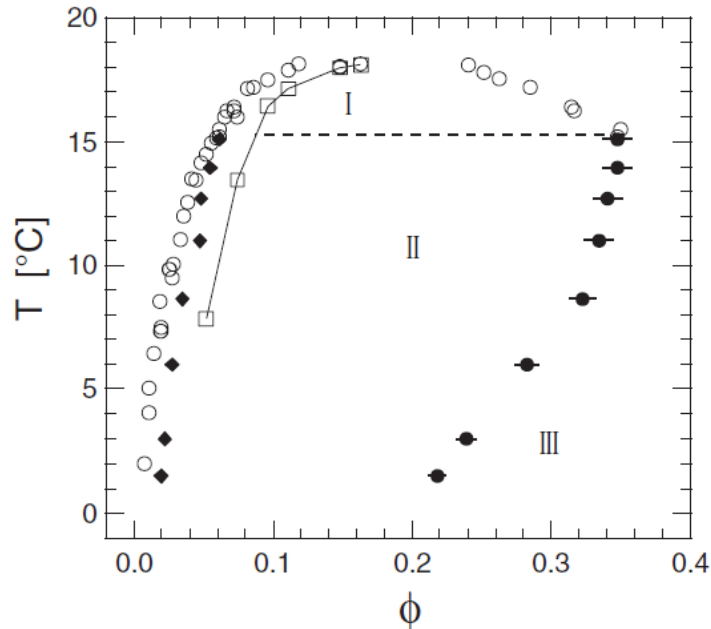


Figure 1.6: Kinetic phase diagram of lysozyme solutions showing regions of I: complete demixing, II: gel formation through an arrested spinodal decomposition, III: homogenous glass. Taken from (Cardinaux *et al.*, 2007).

At specific volume fractions, when the lysozyme solution is quenched into region II, figure 1.6, the lysozyme undergoes phase separation followed by dynamical arrest resulting in a gel with clusters that has length scales in the order of a few micrometres, given lysozyme has an approximate size of 2 nm (Gibaud and Schurtenberger, 2009).

1.4.3 Double network gels

Double network gels are formed from two gel networks and have been of interest due to mechanical enhancements which are particularly useful for certain stress-bearing applications such as replacement cartilage. They can be formed by sequential or covalent networking between different polymers resulting in a bicontinuous gel network (Dragan, 2014) or the two gel networks can be completely separate forming a bigel (Varrato *et al.*, 2012; Di Michele *et al.*, 2014; Blumlein and McManus, 2015).

Interpenetrating gel networks (IPNs), involve the synthesis of one polymeric gel network in the immediate presence of the other, without the formation of any covalent

bonds between the two polymers (Dragan, 2014). Double network (DN) IPNs were initially described by Gong *et al.* in 2003, whereby hydrogels with extremely high mechanical strength of up to 17 times that of the individual component networks with an elastic modulus of 0.4-0.9 MPa. The DN system consisted of a first brittle network of poly(2-acrylamido-2-methylpropanesulfonic acid) (PAMPS) that was interpenetrated with a second soft system of poly(acrylamide) (PAAM) with the optimal molar ratio 1:2 whereby the second system is in excess (Gong *et al.*, 2003).

A bigel consists of two discrete interpenetrating networks whereby each network contributes to the overall mechanical properties of the material in a synergistic manner (Di Michele *et al.*, 2014; Blumlein and McManus, 2015). In 2012, the Foffi Group described a binary colloidal gel consisting of DNA-coated colloids (DNACCs), showing how arrested spinodal decomposition of the complementary coated colloidal particles may lead to bigel formation (Varrato *et al.*, 2012). They used computer simulations to investigate the phase behaviour of bigels, in which phase separation occurs due to the thermodynamic instability that arises as a result of an interplay in the density and composition fluctuations of the particles. These computer simulations were confirmed using confocal microscopy images of DNA-coated colloids (DNACCs) in which interspecies attraction could be controlled. Later studies in 2014 supported their findings on the kinetics of the bigel formation and examined the structural and mechanical properties of the bigels. It was found that bigels are more resistant to strain than a single-component gel at the same volume fraction due to the steric repulsion between the bigel components preventing further demixing (Di Michele *et al.*, 2014).

In 2012, the Suo group reported a synthetic double network gel, formed from an ionically cross-linked alginate gel and a covalently cross-linked polyacrylamide gel. Both networks were shown to work synergistically to create a gel with stronger properties, with the new gel capable of being stretched over twenty times its original length. In addition, the gels showed a 74 % recovery of the original fracture energy, owed to the polyacrylamide network bridging a crack in the gel system, stabilising deformation (Sun *et al.*, 2012).

The first protein-only bigel consisting of BSA and gelatin was described in 2015 (Blumlein and McManus, 2015). These gels exhibited very strong mechanical properties, much stronger than either parent gel, similar to what was seen by Foffi *et al.*

and Sun *et al.* (Sun *et al.*, 2012; Di Michele *et al.*, 2014). The first percolated gel network was formed from the arrested spinodal decomposition of BSA and the second was formed from the physical entanglement of gelatin around the BSA (Blumlein and McManus, 2015). Once heated above its melt transition temperature, unfolded BSA rapidly undergoes spinodal decomposition, followed by irreversible aggregation mediated by disulphide bond formation, in its arrested state. Environmental scanning electron microscopy (ESEM) indicated uniform spherical structures of $\sim 1 \mu\text{m}$ and confocal and light microscopy revealed a branched structure of spherical particles, consistent with the formation of a gel by arrested spinodal decomposition. In addition the confocal microscopy also revealed two discrete networks, satisfying the requirement for a bigel (Blumlein and McManus, 2015).

1.5 Model proteins

The proteins for the bigels were chosen based on their physical and chemical properties. It was important to minimise intermolecular interactions between each protein pair to ensure the formation of two discrete gel networks. In addition to this they are all commercially readily available at low-cost.

1.5.1 Bovine Serum Albumin (BSA)

BSA is a member of the albumin family of globular proteins. BSA is an abundant protein that accounts for approximately 10 % of whey proteins. It has a molecular weight of 66kDa and with 580 amino acids (Boye *et al.*, 1996). It is stabilized by 17 disulphide bridges, with one free cysteine residue at Cys34 (Carter and Ho, 1994), which plays a crucial role in the redox properties of BSA (Kurotsu *et al.*, 2015). BSA consists of approximately 54 % α -helices and 40 % β -sheets and turns. It contains three homologous domains (I-III) each made up of two sub-domains (A and B), which organise to form a heart-shaped protein (Carter and Ho, 1994). The crystal structure for dimeric BSA is shown in figure 1.7.

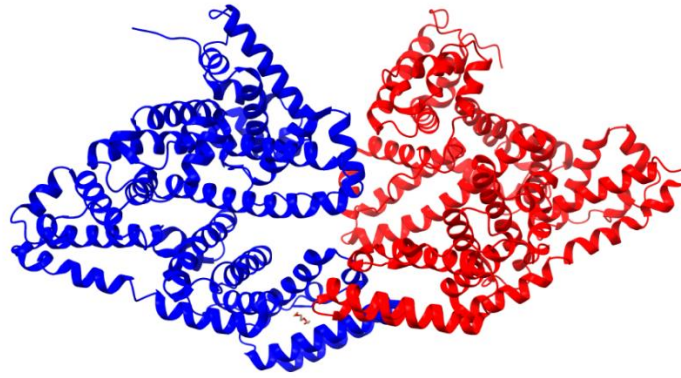


Figure 1.7. Cartoon representation of the crystal structure of dimeric BSA rendered using Jmol (PDB ID: 4f5s).

1.5.2 Ovalbumin (OVA)

Ovalbumin is the main protein constituent of egg-white, comprising 54 % (Abeyrathne *et al.*, 2013) of egg white protein. Interestingly, OVA is a member of the serpin superfamily (Hunt and Dayhoff, 1980), despite showing no protease inhibitory activity as seen with many members of the serpin family. As of yet, its function has not yet been determined (Huntington and Stein, 2001). Ovalbumin has an isoelectric point of 4.7 – 5.2 (Bhattacharjee and Bansal, 2005) and a molecular weight of 45 kDa with 386 amino acids (Thompson and Fisher, 1978). OVA contains six cysteine residues with a single disulphide bond between Cys74 and Cys121 (Thompson and Fisher, 1978). OVA is a glycoprotein with a carbohydrate group attached to its N-terminal (Abeyrathne *et al.*, 2013). The secondary structure of OVA is composed of 41 % α -helices 34 % β -sheets, 13 random coils, 12 % β -turns (Ngarize *et al.*, 2004). The crystal structure for tetrameric OVA is shown in figure 1.8.

Upon heating, OVA undergoes a conformational change from its serpin structure to an insoluble form consisting of only β -sheets with exposed hydrophobic residues. Serpins are unusual in that their most stable state is not their native state but an intermediate metastable S-state that differs from the native state in its conformational structure (Smith, 1964). The conversion of N-Ovalbumin to S-Ovalbumin can be identified by a 2-5 % loss of α -helix content and a small increase in anti-parallel β -sheets, as well as a shift in T_m from 78 to 86 °C (Huntington and Stein, 2001). S-Ovalbumin is unable to form aggregates (Weijers *et al.*, 2003).

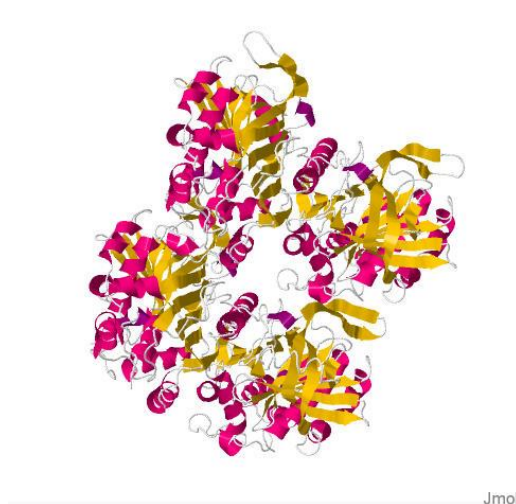


Figure 1.8: Cartoon representation of the crystal structure of four OVA molecules rendered using Jmol (PDB ID: 1OVA), the alpha helices are pink and beta sheets are yellow.

1.5.3 Gelatin

Gelatin, is a naturally occurring biopolymer that is derived from denatured collagen. This degradation can be achieved through acidic or alkaline treatment. The former involves breaking crosslinks between strands in addition to hydrolysing the strands, producing gelatin type A, which is characterised by a broad molecular weight distribution. Under basic conditions gelatin type B is formed (Djabourov *et al.*, 1988). Gelatin consists of a heterogeneous mixture of polypeptides. Its structure is dependent on its collagen precursor. The isoelectric point of Type A is 7.0 – 9.0 while that of Type B is only 4.7 – 5.2. The melt transition temperature, T_m , of gelatin is approximately 40 °C, with little variation for different molecular weights (Bigi *et al.*, 2004). Gelatin is primarily used to form thermoreversible gels, which due to their mechanical properties and biocompatibility provide good candidates for food or biomedical industries. Gelatin gels are formed by dissolving the gelatin in water, which is only soluble above its T_m , following which a helix to coil transition is observed. On cooling the gelatin solution, a reverse transition from coil to helix is then formed with the strands becoming physically entangled with one another (Hayashi and Oh, 1983) as seen in figure 1.9. The strength of gelatin gels depend on their molecular weight and structure and commercially is referred to as its bloom number. The bloom number of gelatin is determined by the force, in grams, required to impress a standard 0.500 +/- 0.001 inch diameter plunger to a depth of 4 mm into the surface of a 6.67 % gelatin gel. The bloom number is directly proportional to the strength of the gel, with that of commercial

gelatin ranging from 50 to 300. The triple-helix content and strength of gelatin has shown to increase in relation to its bloom number (Bigi *et al.*, 2004).

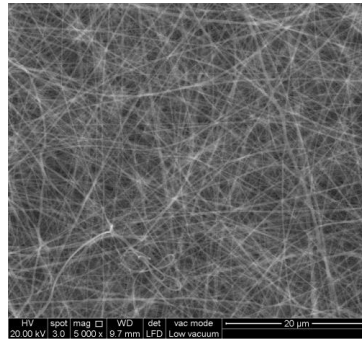


Figure 1.9: SEM images of randomly oriented gelatin based hydrogel. Taken from Hoque (Hoque *et al.*, 2014)

1.5.4 Collagen

Collagen is the main component of skin, tendons, ligaments, teeth and bones, constituting a major component of the connective tissue. It is commonly used in biomedical applications including drug delivery and tissue engineering due to its biodegradability, biocompatibility and weak antigenicity (Lee *et al.*, 2001).

Collagen has an approximate molecular weight of 285 kDa (Whitford, 2005). There have been 28 different forms of collagen identified (Shoulders and Raines, 2009), with the majority belonging to one of the four major collagen groups, type 1, type 2, type 3 and type 4. The function and location of these four major groups is summarised in table 1.2.

Table 1.1: The functions of the four major collagen groups, adapted from (Whitford, 2005).

Type	Function
Type I	Major component of tendons, ligaments and bones
Type II	Comprises over 50 % of cartilage
Type III	Provides strength to artery, intestine and uterus walls
Type IV	Forms the basal lamina of epithelia

The well-established triple helix structure of collagen was initially elucidated by Ramachandran and Kartha in 1954 using X-ray crystallography (Ramachandran and Kartha, 1954). Collagen consists of three polypeptide chains, which have on average a

length of 1000 amino acids, figure 1.10. The three individual polypeptide chains adopt a polyproline II structure that each combine to form a super helix, known as tropocollagen. This structure is primarily stabilised by hydrogen bonding between adjacent carbonyl and amide groups (Bhattacharjee and Bansal, 2005). For collagen types I, II, III and V, the triple helices subsequently assemble to form collagen fibrils, which in turn self-assemble to form collagen fibres, and hydrogel networks in a hierarchal manner, figure 1.10, (O’Leary *et al.*, 2011).

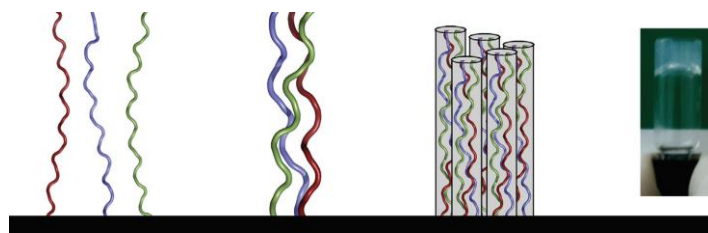


Figure 1.10: The self-assembly of polypeptide chains to form a hydrogel. Taken from (O’Leary *et al.*, 2011).

1.6 Cells and Tissues

1.6.1 HEK 293T cell line

Cells from the Human Embryonic Kidney (HEK) 293 cell line were used for all of the experiments in chapter 4 due to their ease of growth and transfection and they are commercially readily available (Thomas and Smart, 2005). This cell line was originally initiated by Van der Eb in 1973, by transforming normal HEK cells with sheared adenovirus type 5 DNA, that deregulates the cell cycle (Graham and Van Der Eb, 1973). The cell line was then transfected with the large T antigen of simian virus 40 which deactivates p53, a tumour suppressing protein resulting in further deregulation to the cell cycle allowing the cell line to be grown for long periods *in vitro*.

1.6.2 Hydrogel scaffolds

Hydrogels scaffolds are emerging as a very important class of 3D scaffold for biomedical applications such as tissue engineering (Dhandayuthapani *et al.*, 2011), cell encapsulation (Annabi *et al.*, 2010), and wound healing (Jones *et al.*, 2006). Hydrogels are composed of hydrophilic polymeric networks and can be classified as chemical, physical or a combination of both. Chemical hydrogels involve crosslinking polymers

using a chemical crosslinker such as glutaraldehyde (Distantina *et al.*, 2012), however this introduces a source of toxicity towards the cells. Physical hydrogels are formed from non-covalent interactions such as hydrogen bonding, hydrophobic interactions and electrostatic interactions (Zhu and Marchant, 2011) and are often formed from natural polymers such as proteins and polysaccharides (Jonker *et al.*, 2012).

1.6.2.1 Design criteria

When designing 3D scaffolds, it is desirable to have a structure that mimics the natural extracellular matrix (ECM). Cells *in vivo* are surrounded by the ECM, a complex network consisting of proteins and proteoglycans (Zhu and Marchant, 2011). Some of the most important factors to consider in the design of scaffolds include the biocompatibility and biodegradability of the scaffold, the degree of porosity, the mechanical properties and the surface features of the material.

1.6.2.1.1 Biodegradation

For the purpose of tissue engineering applications, it is important that a scaffold can maintain cellular proliferation for the lifetime of the scaffold and subsequently degrade without producing any harmful by-products (El-Sherbiny and Yacoub, 2013). Studies have been conducted to determine the importance of scaffold degradation for tissue engineering scaffolds, by examining cellular activity in non-degradable scaffolds (El-Sherbiny and Yacoub, 2013). PEG and PEG-dimethacrylate (PEGDMA) were photopolymerised to produce non-degradable scaffolds encapsulating bovine and ovine chondrocytes for cartilage regeneration. Although the cells initially maintained viability, overtime, the cell viability significantly decreased with time (Elisseef *et al.*, 1999). However studies examining the impact of degradable poly(propylene fumarate-co-ethylene glycol) scaffolds on cellular growth showed that cells maintained high levels of proliferation and were more evenly dispersed (Suggs and Mikos, 1999). Degradation of hydrogels is generally achieved by enzymatic digestion (Knipe *et al.*, 2015).

1.6.2.1.2 Biocompatibility

Biocompatibility is a key feature in the design of a scaffold to ensure that there is limited harmful immunological or toxic effects because of the scaffold. In the case of tissue engineering, the purpose of the hydrogel or scaffold is to encourage healing and regeneration amongst the cells. If the hydrogel is not biocompatible, this could result in permanent damage or scarring to the tissues. Irgacure is a free radical photo-initiator, commonly used in the synthesis of hydrogels that has been shown to have a direct negative impact on cell viability (Bryant *et al.*, 2000). In order to overcome this limitation, for the purpose of chemically synthesised hydrogels, it would be necessary to purify the material to remove any harmful unreacted chemicals or by-products through extensive solvent washing or dialysis. Another method to overcome this is through the use of natural hydrogels which do not require a chemical cross-linker (Jonker *et al.*, 2012).

1.6.2.1.3 Porosity

A highly porous hydrogel is essential for the encouragement of cell growth, uniform cell distribution and interconnection between the different tissues. In addition, it is important that the pore size is large enough to prevent pore blocking by the cells which would inhibit cell penetration (Annabi *et al.*, 2010). The effect of scaffold pore size on the extent of ECM secretion and cell growth has been reported in recent studies (Brauker *et al.*, 1995; Lien *et al.*, 2009). It has been found that genipin-crosslinked gelatin scaffolds with larger pore sizes showed better balance between cell growth and ECM secretion when compared with those with a smaller pore size, where cell growth dominated, resulting in over-confluency and decreases ECM secretion. The optimal pore size for chondrocytes was reported between 250-500 μm (Lien *et al.*, 2009). The extent of porosity must also be sufficient to allow neovascularization to occur, the formation of new blood vessels which is a necessity for cell survival through nutrient exchange and elimination of waste products (Brauker *et al.*, 1995).

1.6.2.1.4 Mechanical properties

Cells have also been shown to respond to the mechanical properties of their scaffold (Discher, 2005). Adherent cells along with the extracellular matrix combine to form an

elastic microenvironment *in vivo*, which is evident in many soft tissues including brain, muscle and skin. The formation of an elastic cell culture scaffold mimics this environment encouraging the growth of cells. Studies have shown that mesenchymal stem cells (MSCs) respond to the stiffness of their environment (Engler *et al.*, 2006; Park *et al.*, 2012). Soft matrices resembling the brain have encouraged the differentiation of MSCs into neurons, stiffer matrices resembling muscle tissue have encouraged the differentiation of MSCs into myoblasts and the use of matrices resembling the elasticity of collagenous bone have encouraged the differentiation of MSCs into osteoblasts (Engler *et al.*, 2006). In addition, scaffolds with strong mechanical properties are desirable for the purpose of replacement bone and cartilage, whereby the scaffold must withstand the stresses that the new tissue will ultimately bear (Dhandayuthapani *et al.*, 2011).

1.6.2.1.5 Surface properties

The surface of a scaffold is the initial and primary site of interaction with cells and tissues, and consequently is key feature in the design of 3D scaffolds. The surface properties of a scaffold have been shown to have a direct impact on cellular attachment and proliferation (Boyan *et al.*, 1996). Various different methods have been employed to alter the surface features of scaffolds in an attempt to improve cellular attachment and proliferation, figure 1.11. Incorporation of the integrin-binding arginine-glycine-aspartic acid (RGD) peptide on the surface of a scaffold has been shown to facilitate cellular adhesion and proliferation (Pierschbacher and Ruoslahti, 1984; Hersel *et al.*, 2003). The ability of this peptide to promote cell attachment was originally identified by Pierschbacher and Ruoslahti through examining the peptide sequence of fibronectin, a glycoprotein with strong cell attachment properties (Pierschbacher and Ruoslahti, 1984). The RGD peptides are recognised by integrin ligands which in turn bind to adhesive cell surface proteins (Ruoslahti, 1996). This peptide is also present in other proteins including collagen, gelatin (Hoque *et al.*, 2014), laminin, fibrinogen and entactin (Ruoslahti, 1996).

Other methods used to improve cellular adhesion to the surface of scaffolds include the use of thin film depositions such as hydroxyapatite (HA) (Dhandayuthapani *et al.*, 2011). Studies have shown that calcium phosphate films deposited onto nanostructured

titanium surfaces can induce osteogenic differentiation in mesenchymal stem cells (McCafferty *et al.*, 2014). Various growth factors such as heparin (Kallapur and Akeson, 1992) and epidermal growth factor (EGF) (Tıǧlı *et al.*, 2011) have also been attached to the surface of scaffolds as well as being incorporated into the scaffold to encourage cell adhesion and proliferation.

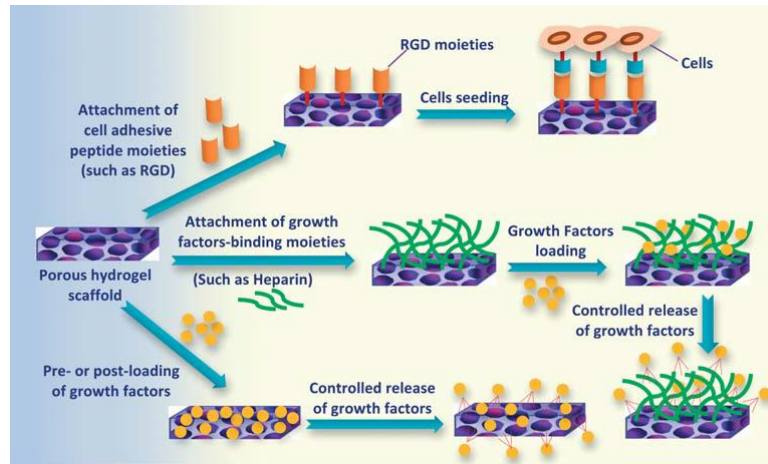


Figure 1.11: Some of the approaches for altering the surface properties of a scaffold for cell adhesion purposes. Taken from (El-Sherbiny and Yacoub, 2013).

1.6.2.2 Applications of hydrogel scaffolds

Hydrogels are widely used in various biomedical applications including tissue engineering (Dhandayuthapani *et al.*, 2011), drug delivery (Chung and Park, 2009), and wound healing (Jones *et al.*, 2006) due to their hydrophilic character and flexibility and biocompatibility with many commercial products on the market (Caló and Khutoryanskiy, 2015).

1.6.2.2.1 Wound healing

Hydrogels provide an ideal candidate for wound dressings due to their physical and chemical properties such as their high water content, their ability to swell and absorb moisture and their porosity. Wound dressings must be able to maintain a certain degree of moisture between the wound and the dressing, protect the wound from any sources of infection, absorb any excess toxins and exudate, be able to provide sufficient diffusion for gases and be easily removable (Jones *et al.*, 2006). Hydrogels satisfy all of these

requirements and are increasingly being used for wound dressings in place of gauze, which although is cheap, it is not have the same desirable properties of hydrogels and often causes problems in its removal, with trauma occurring to the wound.

Intrasite Gel[®] is an amorphous sterile hydrogel produced by Smith & Nephew, consisting of modified carboxymethylcellulose (2.3 %), propylene glycol (20 %) and water (77.7%), used for granulating open cavity wounds (Vernon, 2000). The high water content and porosity, ensures the transmission of water vapour and oxygen, proving effective rehydration to the surface of the wound, as well as debridement, removal of unhealthy tissue away from the wound, essential to recovery (Vernon, 2000). Granugel[®] is a combination of a hydrogel and hydrocolloid consisting of pectin, carboxymethylcellulose and propylene glycol marketed by CanvaTec (Williams, 1996). The presence of the hydrocolloid provides the ability to absorb larger amounts of exudate, which can help speed up the healing process (Caló and Khutoryanskiy, 2015). Woundtab[®] is a hydrogel formed from carboxymethylcellulose, glycerol and a sulphonated copolymer used for chronic wounds. Due to its superabsorbent properties, it is capable of absorbing bacteria and retaining them within the hydrogel (Caló and Khutoryanskiy, 2015).

1.6.2.2.2 Tissue engineering

Tissue engineering involves the repair, regeneration or replacement of tissues or organs using engineered materials. The potential biocompatibility of hydrogels is a very desirable feature for the purpose of tissue engineering since the hydrogel will most likely be in direct contact with various organs and tissues, in addition to its similarity to the extra-cellular matrix and potential mechanical strength which is required for replacement bone and cartilage. There are multiple collagen based products on the market due to its biocompatibility. CondroColl[®] and HydroxyColl[®] are both collagen based scaffolds marketed by SurgaColl[™] (Gleeson *et al.*, 2010; Levingstone *et al.*, 2014). HydroxyColl[®] is a collagen and hydroxyapatite based scaffold for bone regeneration (Gleeson *et al.*, 2010). CondroColl[®] is a multi-layered scaffold, for osteochondral repair, designed to mimic the gradient structure of osteochondral tissue. The first layer consists of type 1 collagen and hydroxyapatite (HA), the major components of bone, the second layer is composed of type 1 and type II collagen and

HA and the third layer is composed of type I and type II collagen with hyaluronic acid, mimicking cartilage. The physical properties of this material provides optimal cellular growth and distribution facilitating rapid healing (Levingstone *et al.*, 2014). Infuse® Bone Graft is another collagen based product produced by Medtronic that has been approved as an autograft replacement for certain spinal fusion procedures, open tibial fractures and for sinus augmentation. Its composed from a recombinant human bone morphogenetic protein-2 (rhBMP-2) applied to an absorbable collagen sponge (ACS) carrier (McKay *et al.*, 2007). Infuse bone graft provides an alternative to harvesting autogenous bone which often involves complications.

1.6.2.2.3 Drug delivery

Hydrogels are commonly used for drug delivery applications due to their physical properties. The high porosity provides the ability to load drugs for the later release *in vivo*. In addition, it is possible to tune the degree of porosity for various different delivery mechanisms. This release may occur through diffusion, swelling, or else it may be chemically or environmentally mediated (Chung and Park, 2009). They can also be adapted for sustained drug release, which involves maintaining high concentrations of drug over extended periods of time. Reservoir and matrix devices are used for diffusion-controlled delivery systems. Reservoir systems involve a drug reservoir in the core of the system, surrounded by a hydrogel membrane. Drug release occurs at a constant rate. Matrix systems involve dispersing the drug throughout the hydrogel. Drug release occurs through the pores of the hydrogel at a rate proportional to the square root of time (Chung and Park, 2009).

There have been many studies done regarding the potential use of hydrogels in drug delivery systems, however there are only a few that have reached commercialisation (Caló and Khutoryanskiy, 2015). Supprelin® LA, is a subcutaneous insert produced by Endo Pharmaceuticals Inc., used for the treatment of central precocious puberty (CPP) in both male and female children. It consists of a hydrogel reservoir system that releases histrelin acetate, a gonadotropin-releasing hormone that reduces luteinizing hormone (LH) levels and sex steroids concentration (Davis *et al.*, 2014). Cervidil® is a drug-delivery system used for cervical ripening to induce labour in patients. The hydrogel is

composed of crosslinked polyethylene oxide/urethane polymer and drug release is stimulated by hydrogel swelling in the vagina (Mozurkewich *et al.*, 2011).

1.6.3 Cell viability assays

Cell viability assays are an essential tool for analysing cellular response to a particular scaffold or the impact of different test molecules on cellular action, whether they have a positive effect on cell proliferation or have any cytotoxic effects that lead to cell death. They provide initial data prior to performing any *in vivo* studies. They're also widely used for the study of receptor binding effects (Hulme and Trevethick, 2010). They allow the direct quantification of viable cell numbers. Reduction assays are some of the most commonly used assays, including those that are tetrazolium based and resazurin based. The reduction of these molecules only occurs in metabolically active cells by mitochondrial activities. The signal generated from the fluorescence or absorbance of the reduced molecule can be directly related to the number of viable cells (Xu *et al.*, 2015). The ATP assay is another cell viability assay, however it is different to the reduction based assays in that it immediately ruptures the cell membranes and monitors ATP production. (Riss *et al.*, 2013).

1.6.3.1 Tetrazolium reduction assays

MTT (3-(4,5-dimethylthiazol-2-yl)-2,5-diphenyltetrazolium bromide) is one of the most commonly used cell viability assays, since its development in 1983 for high throughput-screening (Mosmann, 1983). The MTT solution must be prepared prior to use by dissolving in a physiological buffer, and is then incubated with cells for 1 to 4 hours (Riss *et al.*, 2013). The tetrazolium is reduced to formazan, figure 1.12 (a), which is purple in colour and absorbs at a wavelength of 570 nm. The signal intensity due to the absorbance of formazan is directly proportional to viable cells. The reduction of tetrazolium occurs by mitochondrial dehydrogenase enzymes which transfer electrons to the tetrazolium molecule (Mosmann, 1983). Formazan is an insoluble precipitate that accumulates within the cells, on the cell surface and in the medium. In order to measure the absorbance, the formazan must be solubilised with a suitable organic solvent such as dimethylsulfoxide (DMSO), sodium dodecyl sulphate (SDS) or isopropanol (Xu *et al.*, 2015). There have been numerous other tetrazolium compounds also used for assessing

cell viability including MTS, XTT and WST-1 (Riss *et al.*, 2013). Unlike MTT which is positively charged, these compounds are negatively charged preventing them from directly penetrating viable cells and they must be used with an intermediate electron acceptor that facilitates the reduction of tetrazolium (Riss *et al.*, 2013).

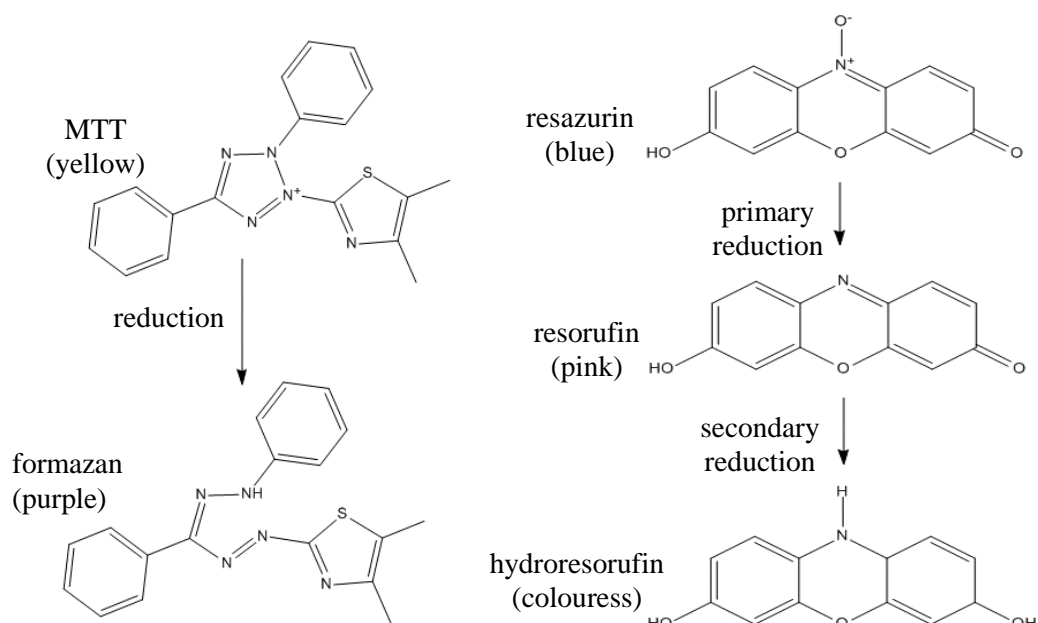


Figure 1.12: (a) Structures of MTT and its reduced form, formazan. (b) Structures of resazurin, resorufin and hydroresorufin. Rendered using Chemdraw.

1.6.3.2 Resazurin reduction assays

Resazurin based reduction assays are more recent and are often used in place of MTT and other tetrazolium based assays due to their ease of use and reduced toxicity towards cells, allowing further usage of cells in subsequent experiments (Yu *et al.*, 2003). They are also water soluble and so do not require an organic solvent, rather they can be dissolved in any physiological buffer which can be added directly to cells. The mechanism by which resazurin is reduced to resorufin, figure 1.12 (b) is not fully understood however it is believed to occur during cellular respiration by NADPH and NADH (Candeias *et al.*, 1998) which is strongly fluorescent and red in colour. Similarly to the production of formazan, the signal intensity of the resorufin is directly proportional to the number of metabolically active cells. A further reduction from resorufin (pink) to non-fluorescent hydroresorufin (colourless), figure 1.12 (b), can occur after extended periods of incubation time which can lead to artefactual results. AlamarBlue was the first resazurin based product produced in 1994 (Ansar Ahmed *et*

al., 1994), however PrestoBlue is a more recent product and is claimed to offer distinct advantages over AlamarBlue due to its shorter incubation times of as little as ten minutes with higher levels of sensitivity (Xu *et al.*, 2015).

1.7 Thesis Motivation

The motivation for this work was to investigate new proteins for the formation of the new protein bigels that can potentially be used as biomaterials for biomedical applications. A bigel consists of two discrete interpenetrating networks that each contribute to the overall mechanical properties of the gel resulting in enhanced strength (Varrato *et al.*, 2012; Blumlein and McManus, 2015). The first protein-only bigel composed of BSA and gelatin was described in 2015 with very strong mechanical properties (Blumlein and McManus, 2015), by exploring new protein pairs there is the potential for form new protein bigels with even stronger mechanical properties.

The first part of the research involved examining the preparation procedure for the protein bigels with a view to optimizing it for consistency for future measurements. New proteins were explored as potential candidates for the bigels with the hopes of producing a gel that satisfied the requirements for bigel and displayed even more enhanced mechanical properties. Natural hydrogels consisting of proteins or polysaccharides are increasingly being used in biomedical applications due to their biocompatibility and biodegradation however these often lack the mechanical strength required for stress-bearing applications such as replacement cartilage. The formation of a protein bigel could potentially overcome this limitation. Cavitation rheology was used to characterise the new materials. The second part of this research involved examining the impact of different cellular scaffolds on cellular proliferation, preliminary tests on the potential use of the bigels *in vivo*.

Chapter 2:

Materials and Methods

2.1 Preparation of materials

2.1.1 Reagents

Chicken egg white albumin (OVA), bovine serum albumin (BSA), gelatin (bloom number 75g), gelatin (bloom number 225g) and collagen type 1 were purchased from Sigma-Aldrich and used without further purification. All buffers were prepared using ultrapure (Type 1, Milli-Q) water and analytical grade solvents and reagents.

2.1.2 Gel preparation

2.1.2.1 Single component gels

To prepare single component OVA and BSA gels, protein solutions were made up to the desired concentration in the appropriate buffer and allowed to fully hydrate overnight. 300 μ l of the protein solutions were aliquoted into eppendorf tubes and heated at 90 °C in a water bath for 3 min. The heated samples were then quenched in ice for 30 min.

To prepare gelatin gels, gelatin solutions were heated at 90 °C for 30 min. The heated solution was then removed from the water bath and aliquoted into 300 μ l samples which were cooled in ice, forming the physical gel on cooling.

2.1.3 Bigels

The bigel was prepared as follows;

2.1.3.1 Initial bigel preparation procedure

The individual protein solutions were made at twice the desired concentration and mixed in a 50:50 ratio. The protein solution was heated at 80 °C for 1 hr and then allowed to cool at room temperature.

2.1.3.2 Optimised bigel preparation procedure

The individual protein components were prepared at twice the concentration and equilibrated at 45 °C in a water bath. The two components were then mixed to create a homogeneous protein mixture and a pH check was conducted. The pH was adjusted to pH 5.5 with 0.1 M NaOH as required. The samples were sealed and heated in a water bath at 90 °C for 3 minutes (optimised time) and then quenched in ice.

2.1.4 Collagen gel preparation

Collagen Type 1 derived from rat tail was purchased from Sigma-Aldrich as a 3.9 mg/ml solution in 0.02 N acetic acid. The following procedure was carried out on ice to slow the gelation process. The stock solution of collagen (3.9 mg/ml) was mixed with phosphate buffered saline (PBS), previously prepared by dissolving one PBS tablet (Fisher Scientific, UK) in ultrapure water, to prepare a final solution at 2mg/ml. The pH was adjusted with 1 M NaOH (Fisher Scientific, UK) as required to achieve a physiological pH of approximately 7. The final solution was mixed by gently aspirating using a pipette. To allow gelation to occur, the solution was aliquoted into the required volume (usually 300 μ l) and then incubated at 37 °C for 1 hour.

2.2 Methods used to characterise protein gels

2.2.1 Cavitation Rheology

2.2.1.1 Background

Cavitation rheology (CR) is a recently developed technique that can be used to measure the mechanical properties of a material (Zimmerlin *et al.*, 2007; Kundu and Crosby, 2009), particularly those of certain biological soft materials including cell spheroids, the eye lens and vitreous (Crosby and McManus, 2011; Cui *et al.*, 2011; Chin *et al.*, 2013; Blumlein *et al.*, 2017).

CR has multiple advantages over other forms of rheology such as shear rheology due to the fact that a large amount of material is not required to determine the elastic modulus, heterogeneities can be probed and the instrumentation for CR is more straightforward and less costly (Zimmerlin *et al.*, 2007). CR has been used to determine the mechanical properties of tissues *in vivo*, including that of the eye lens (Zimmerlin *et al.*, 2010; Chin *et al.*, 2013). This is highly useful for the analysis of disease progression and how the mechanical properties of tissues change during these processes.

Since CR can be used to measure the elastic modulus very locally, at the tip of the needle, it is possible to explore the heterogeneities within a sample as well as the presence of a gradient (in terms of mechanical properties) within the sample (Zimmerlin

et al., 2010). In addition, it can also be used for turbid samples (Blumlein and McManus, 2015) since it is not necessary to monitor deformation visually as the drop in pressure within the system indicates that cavitation has occurred. The ability to vary the needle diameter also provides the ability to measure samples at length scales ranging from 0.1 – 1000 μm , including intracellular, cellular and intercellular length-scales (Zimmerlin *et al.*, 2010; Cui *et al.*, 2011; Blumlein *et al.*, 2017).

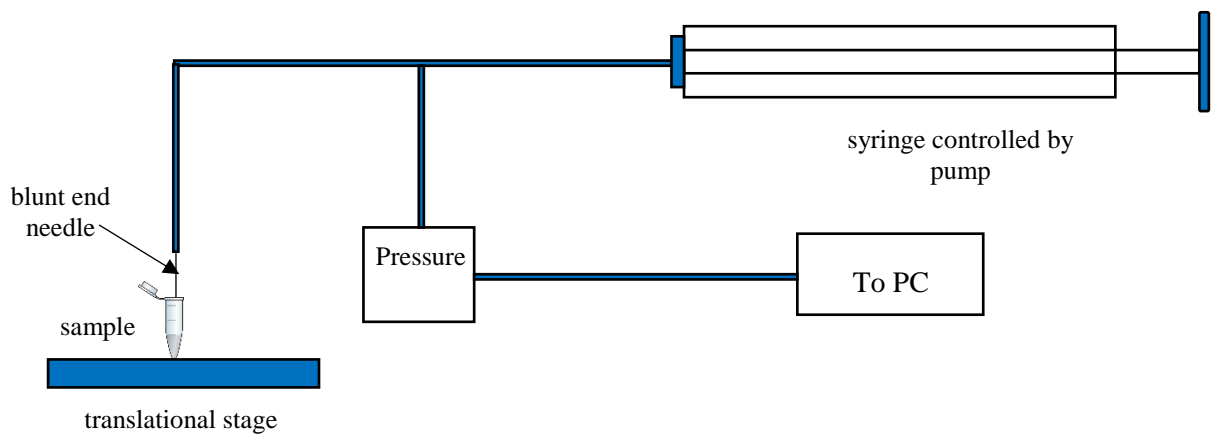


Figure 2.1: Set-up of a typical CR experiment.

The set up for a typical CR experiment is shown in figure 2.1. A typical experiment involves inserting a blunt end needle into the sample which is positioned on a translational stage. Once the needle is in position, the pressure of the closed system is gradually increased by compressing the medium (typically air or water) within the syringe at a constant rate (chosen to ensure no back pressure), until a bubble or cavity is formed at the tip of the needle. The formation of this cavity causes a drop in pressure of the system, associated with the critical pressure, P_c , figure 2.2.

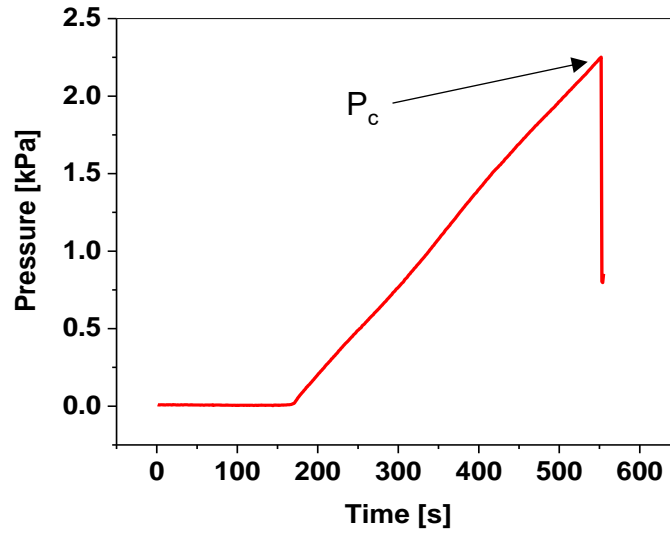


Figure 2.2: A typical pressure plot during a cavitation rheology experiment.

For a liquid, the formation of this cavity or unstable expansion is resisted by the surface tension between the liquid and the cavitating medium where this critical pressure can be defined by;

$$P_c = \frac{2\gamma}{r} \quad [\text{Eqn. 2.1}]$$

where γ is the surface tension and r is the needle internal radius (Zimmerlin *et al.*, 2007).

For an elastic material, the formation of the cavity is resisted by two forces, the surface tension between the elastic material and the cavitation medium, and the elastic restoring force of the sample. Gent and his colleagues have shown that this force can be represented by $5/6E$ (Gent and Tompkins, 1969; Gent and Wang, 1991), so that at the tip of a syringe, these combined forces have been shown to relate to the critical pressure (P_c) of the system by the equation;

$$P_c = \frac{5}{6}E + \frac{2\gamma}{r} \quad [\text{Eqn 2.2}]$$

where γ is the surface tension of the material and r is the internal needle radius (Zimmerlin *et al.*, 2007). The error bars for each needle size in all experiments were

determined by calculating the standard deviation of the critical pressures measured for at least 10 replicates of each sample at each needle size.

2.2.1.2 Instrumentation

The cavitation rheology instrument was previously built in-house. It comprises of a syringe pump (New Era) regulating a syringe (Hamilton GASTIGHT®), connected to a High Accuracy Silicon Ceramic pressure sensor HSCDANT001PG3A3 (Honeywell) and blunt end Hamilton needles (Fisher Scientific, UK). A custom written programme was used to record the pressure at the needle tip during the experiment (Blumlein *et al.*, 2017).

For the purpose of the cavitation rheology experiments in chapters 3 and 4, the cavitating medium was air and the flow rate was set to 400 $\mu\text{l}/\text{min}$ for all experiments. The elasticity of the material was determined through successive pressurization and depressurization cycles using a syringe pump.

2.2.2 Optical Microscopy

2.2.2.1 Background

Microscopy is commonly used in molecular biology due to its ability to visualise objects in greater detail. Optical microscopy uses visible light and a system of lenses to magnify and visualise images. The resolution of an optical microscope is defined as the smallest distance visible between two separate particles that can still be distinguished as separate entities and is limited by the numerical aperture of the system (Cooper, 2011). The resolving power is one of the key limiting factors of a microscope. For optical microscopy the greatest resolution is typically close to the wavelength of light, 400-700 nm and even those resolutions only occur at high magnifications of 600x. As a result is not possible to view specimens at a molecular (Cooper, 2011). Electron microscopes offer an alternative to optical microscope due to their greater resolving powers. It involves passing a beam of electrons through the sample (Cooper, 2011).

Some of the main forms of optical microscopy include bright field, phase contrast, fluorescence and polarization microscopy. In order to be perceived by the eye and distinguished from its surroundings, the specimen being analysed must exhibit contrast.

Bright field microscopy involves passing light directly through the sample. The ability to distinguish between different phases or components of the sample is dependent on the contrast that occurs from the absorption of visible light by the sample, as a result it can often be difficult to distinguish between the different components. Phase contrast microscopy is very useful for visualising samples that have small differences between the refractive index of the different components. It uses phase shifts from the differences in refractive index and converts them into amplitude shifts resulting in enhanced contrast between the components. Fluorescence microscopy is very useful for viewing cellular components and processes that cannot be visualised by bright field or phase contrast microscopy. It can be used to visualise specimens that exhibit autofluorescence, or by adding fluorescent labels that attach to the specimen. It involves the excitation of the fluorescence species, and the subsequent separation of the emitted light (weaker) from the excitation light (brighter), resulting in a high contrast image (Cooper, 2011). Polarization microscopy can be used to visualise birefringent samples and involves exploiting the optical anisotropic behaviour of the molecules for their analysis (Oldenbourg, 2013).

2.2.2.2 Imaging of protein gels

Bright field microscopy and phase contrast microscopy were used to observe the microstructure of the gels at micrometre length scales. The gels were examined and imaged using an Olympus BX61 upright microscope, equipped with a digital imaging system at a magnification of 100x. Cell^F software was used to view and record the images and all image analysis was done using ImageJ software. Phase contrast microscopy was used to give enhanced contrast between the different components of the gels.

2.2.3 Differential scanning calorimetry

2.2.3.1 Background

Differential Scanning Calorimetry (DSC) is a technique used to determine the thermal properties of a material. Some of the many applications of DSC include the determination of the purity and detection of polymorphism in compounds (Reubke and Mollica, 1967), and determining glass transition temperatures, crystallization and

polymerization kinetics in polymers (Bruylants *et al.*, 2005). DSC is also used to determine different thermodynamic parameters associated with the denaturation of proteins including the thermal melt temperature (T_m) excess heat capacity (ΔC_p) and the transition enthalpy (ΔH_{cal}) for the process (Johnson, 2013). During a typical DSC experiment, the DSC instrument monitors the amount of power required to maintain the same temperature in a reference cell, filled with solvent, and a sample cell filled with protein and solvent. As the temperature of both cells is gradually increased, the protein begins to unfold, an endothermic process which results in heat being absorbed, producing a change in the temperature difference between the sample and reference cell. The heat flow required to maintain the same temperature between both cells is proportional to the excess heat capacity (ΔC_p) of the thermally induced process, the protein unfolding (Johnson, 2013).

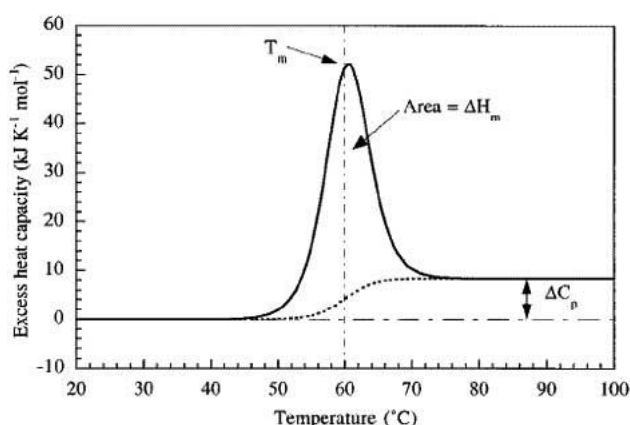


Figure 2.3: A typical thermogram from a DSC experiment for a two-state unfolding of a globular protein, taken from (Bruylants *et al.*, 2005).

A typical DSC plot for a globular protein undergoing an ideal-two state unfolding process is shown in figure 2.3. The maximum of the endothermic peak is related to the thermal transition temperature or melt temperature (T_m) of the protein, which is defined as the temperature at which 50 % of the protein is unfolded. The integration of the peak yields the enthalpy of the process and the post-transition baseline indicates the heat capacity for the protein.

2.2.3.2 Instrumentation

DSC was used to determine the melt transition temperature of the starting materials, OVA and gelatin and to determine if OVA underwent any reversible denaturation. A Perkin Elmer Pyris-6 Differential Scanning Calorimeter (Perkin Elmer, Ireland) was used for all DSC measurements. The samples were equilibrated at 25 °C for 5 min before the temperature increased from 25 °C to 100 °C at a scan rate of 1 °C min⁻¹. For the reversibility measurements, three heating cycles and three cooling samples were carried out, all at a rate of 1 °C min⁻¹. The heat flow required to keep the sample and the reference sample at the same temperature was recorded. The data was analysed using Origin software.

2.2.3.3 Sample preparation

Sample preparation involved fully hydrating the protein in the appropriate buffer (ultrapure water) at a concentration of 100 mg ml⁻¹ and aliquoting 55 µl of the sample into a stainless steel DSC pan which was then sealed. A reference sample was also prepared containing the same mass of buffer only.

2.3 Mammalian cell culture

All cell culture work was performed in a SafeFAST Classic 212 biological safety cabinet (BSC) (SafeFast Classic, Faster S.r.l., Italy) under aseptic conditions.

HEK293T/17 cells were used in all experiments purchased from LGC, UK. These cells are derived from the human embryonic kidney cell line. All cells were grown in a Memmert INCO 153 (Schwabach, Germany) CO₂ incubator. The incubator was operated at 5% CO₂, 90% relative humidity and at a temperature of 37 °C.

2.3.1 Reagents for mammalian cell culture

The reagents for mammalian cell culture were all prepared using sterile reagents and solvents in a BSC. The reagents were autoclaved at 121 °C for 20 minutes in a SX-500E TOMY autoclave and filter sterilized through a 0.22 µm Millex-GV syringe filter (Millipore, Ireland).

2.3.1.1 Complete growth medium

Complete growth medium (CGM) was prepared by supplementing Dulbecco's Modified Eagles Medium (DMEM) which contains 4,500 mg/ml L-Glucose and 4.00mM L-Glutamine, purchased from GE Healthcare Life Sciences (USA) with the following; 10% Bovine Calf Serum (BCS) 10,000 units/ml Penicillin, 10mg/ml Streptomycin, 1.5 mg/ml sodium bicarbonate and 1 mM sodium pyruvate, all purchased from Sigma-Aldrich (USA).

2.3.1.2 Phosphate buffered saline

1X PBS was prepared by dissolving one PBS table (Fisher Scientific, UK) in 100 ml ultrapure water.

2.3.1.3 Trypsin-EDTA solution

10X trypsin-EDTA (5 g/l porcine trypsin, 2 g/l EDTA-4Na, 0.9 % NaCl) (Sigma-Aldrich, USA) was diluted to 1X trypsin-EDTA using 1X PBS.

2.3.1.4 Sodium hydroxide

Sodium hydroxide buffer was prepared at concentration of 1 M using 40 g NaOH (Fisher Scientific, UK) per litre of ultrapure water.

2.3.1.5 Acetic acid

Glacial acetic acid (Fisher Scientific,UK) was diluted to a concentration of 0.02N using ultrapure water.

2.3.2 Growing cells from frozen stocks

Cells were stored in cryotubes in a Statebourne Biorack 750 (Statebourne, USA), liquid nitrogen cryopreservation tank. For recovery of cells, the frozen cells were directly thawed in a water bath at 37 °C for approximately 2 minutes. Complete growth medium (CGM) was heated to 37 °C in a water bath. The contents of the cryotube was transferred to a sterile 15 ml centrifuge tube containing 10 ml of the warmed CGM. The tube containing the suspended cells was centrifuged at 125g for 10 minutes to pellet cells. The supernatant was then removed and the cells were resuspended in 7 ml of pre-warmed medium. Cells were then transferred to the required vessel (T25 cell culture flask or 6-well plate) and seeded at a concentration of 1×10^5 cells/ml.

2.3.3 Sub-culturing or passaging of cells

CGM was changed every few days as required. Metabolising cells release acidic by-products which causes the phenol red in DMEM to change colour from pink to orange indicating that a change in medium is required. When 90 % confluency was reached, assessed using a light optical microscopy, the cells were passaged. Prior to cell passage, the CGM was removed, and the cells were washed with pre-warmed 1X phosphate buffered saline (PBS) to remove any remaining serum. For a T25 culture vessel (growth surface area of 25 cm²), 300 µl of trypsin-EDTA was added to the vessel and incubated at 37 °C for up to 10 minutes to detach the cells. Following this, 7 ml of CGM was added to the flask and the cells were harvested by gently aspirating the cells to dislodge all cells from the vessel walls. The cell suspension was then transferred to a 15 ml centrifuge tube and centrifuged at 125g for 10 minutes to pellet the cells. Following centrifugation, the supernatant was discarded, and the cells were resuspended at the appropriate concentration for the required vessel. Volumes were adjusted depending on the vessel in use.

2.3.4 Cell counting

Cells were counted using a bright-line haemocytometer (Hausser Scientific, USA) and Trypan Blue 0.4 % solution (Sigma, Aldrich, USA), a blue stain that is only absorbed by dead cells, allowing viable cells to be identified and quantified. Suspended cells were mixed to ensure the cells were evenly distributed and 10 µl were removed and added to 90 µl of Trypan Blue giving a 1/10 ratio. 10 µl was added to the haemocytometer and cells were viewed under the light microscope. Dead cells (blue) were excluded from the cell count and the total number of viable cells were determined using the following equation;

$$\text{Number cells/ml} = \text{cell count (average)} \times 10^4 \text{ cells/ml} \times \text{dilution factor}$$

2.3.5 Freezing cells

Cell stocks were prepared for freezing by harvesting the cells from the vessel and centrifuging the cells at 125g for 10 minutes. The pelleted cells were then re-suspended

in cryopreservation medium, consisting of 95 % CGM and 5% dimethyl sulfoxide, at a density of 3×10^6 cells/ml. The solution was then aliquoted into Nalgene cryogenic vials (ThermoScientific) in 1 ml volumes. The vials were then transferred into a Mr. Frosty Freezing Container (ThermoScientific), a polycarbonate container, containing 100 % isopropanol, which when placed at $-80\text{ }^\circ\text{C}$ claims to achieve a cooling rate of approximately $-1\text{ }^\circ\text{C}/\text{minute}$, the optimum rate for freezing cells. After 3 hours the frozen tubes were then transferred to a liquid nitrogen cryopreservation tank for long-term storage.

2.3.6 Collagen Scaffold

2.3.6.1 2D collagen coating

The stock collagen solution (concentration of 3.9 mg/ml), was diluted to 50 $\mu\text{g}/\text{ml}$ using 0.02N acetic acid. 200 μl of the diluted collagen solution was added to each well to coat the dishes with $5\mu\text{g}/\text{cm}^2$. The plate was incubated for 1 hour at room temperature. Following this, any excess collagen solution was carefully removed from the well. The well was then rinsed using PBS. Plates were then air dried for ~ 2 hrs and stored at $2 - 8\text{ }^\circ\text{C}$ until required.

2.3.6.2 3D collagen scaffold

To prepare a three-dimensional collagen scaffold, the collagen gel was prepared as described in section 2.1.2, using aseptic conditions. 300 μl was aliquoted into each well of a 24 well plate for incubation. The plates were incubated at $37\text{ }^\circ\text{C}$ for 1 hour or until a gel had formed. Prior to use, the collagen gels were dialysed with CGM. 500 μl of CGM was added to each well and allowed to dialyse for ~ 2 hours. The CGM was then removed and replaced with fresh CGM. This process was repeated three times.

2.3.7 Bigel Scaffolds

BSA/gelatin-75 and OVA/gelatin-225 bigels were prepared in a 24-well plate. The following is the procedure for the BSA/gelatin bigel. The OVA/gelatin bigel was prepared in a similar manner.

2.3.7.1 Preparation of bigel scaffold covering entire well surface

The BSA samples were prepared at a volume fraction of $\phi = 0.132$ by hydrating the protein in ultrapure water (previously autoclaved at 121 °C). The gelatin samples were prepared at a volume fraction of $\phi = 0.146$ in ultrapure water (previously autoclaved at 121 °C) and heated to 90 °C for 30 min to dissolve. The two separate protein solutions were equilibrated at 45 °C in a water bath. Following equilibration, the heated solutions were mixed in the biological safety cabinet (BSC) resulting in a combined volume fraction of $\phi = 0.139$. The pH was checked to ensure a pH of 5.5. 300 μ l was aliquoted per well into a 24-well plate. The plate was then sealed using sealing tape (Thermo Scientific, USA) and heated at 90 °C for 3 minutes. Prior to use, the gels were dialysed by adding 500 μ l CGM to each well and allowing to dialyse for ~2 hours. The CGM was then removed and replaced with fresh CGM. This process was repeated three times.

2.3.7.2 Preparation of hollow cylindrical bigel scaffold

To create the bigel scaffold, a cylindrical insert was created from layered silicone thermal pads, figure 2.4 (b). The insert had a diameter of 11.3 mm and a surface area of 1 cm², half the total surface area of the well (2 cm²). The insert was placed in the centre of the well and 300 μ l of the OVA/gelatin-225 homogeneous protein solution, as prepared above, was aliquoted into the well, around the insert. The plate was sealed using sealing tape and heated at 90 °C for 3 min in a water bath, allowing the gel to form around the insert. After bigel formation, the silicon insert was removed, leaving a free standing bigel in the shape of a hollow cylinder around the outside of the well, as depicted in figure 2.4 (a). As before, the bigel scaffold was dialysed with three 500 μ l rinses with CGM prior to use.

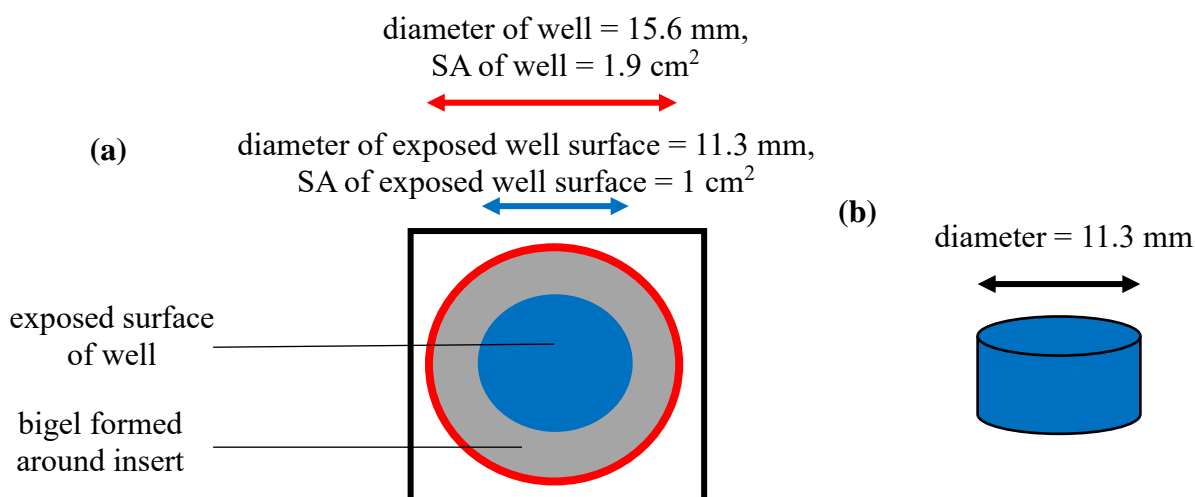


Figure 2.4 (a): Top plan view of hollow cylindrical bigel (grey) formed around edge of well (in 24 well plate) with exposed cell surface in the centre (blue) with dimensions. (b) 3D plan of silicone insert.

2.3.8 Presto Blue assay - description

Presto Blue (PB) was purchased from BioSciences (Ireland) as a 10X solution. PB is cell viability assay used to assess cell proliferation *in vitro*. This is done by monitoring the reduction of resazurin to resorufin which only occurs in metabolically active cells (Lall *et al.*, 2013). Resorufin is fluorescently active at an excitation wavelength of 560 nm and an emission wavelength of 590 nm, allowing the growth of cells to be quantified.

2.3.8.1 Fluorescence spectroscopy

The reduction of resazurin to resorfin was monitored with fluorescence spectroscopy using a SpectraMax M2e (Molecular Devices, USA) plate reader at wavelengths of 560 nm excitation and 590 nm emission in bottom-read mode. Fluorescence spectroscopy measures the intensity of photons emitted from a sample as it transitions from its excited state to the ground state.

2.3.8.2 Optimisation of PB

Prior to use, it was necessary to determine the optimal incubation time for HEK 273 cells. Cells were seeded with CGM in a standard clear-bottom 24 well plate (Nest, China) at concentrations ranging from 5×10^4 cells/ml to 2.5×10^5 cells/ml (total well volume 500 μ l) and allowed to adhere overnight. The following day, 50 μ l of the medium was removed and replaced with 50 μ l PB. The final concentration of PB in contact with the cells is 1X PB. The cells were then incubated at 37 °C, 5% CO₂, 90% relative humidity and the fluorescence was taken at incubation times of 10, 20, 30 and 60 minutes with a plate reader using bottom-read mode. The fluorescence was recorded at an excitation wavelength of 560nm and an emission wavelength of 590 nm. As PB is a live assay, it is possible to take readings at multiple time points from the same wells/plate. All measurements were taken as an average of three separate wells and corrected for any background fluorescence by including control wells containing only CGM with no cells on each plate. 30 minutes was chosen as the incubation time.

2.3.8.3 Use of PB to assess impact of various scaffolds on cell growth

The bigel scaffolds were formed as described in section 2.3.7.1 and the collagen scaffolds as described in section 2.3.6, all in a 24 well plate under aseptic conditions.

The cells were then seeded at a concentration of 1×10^5 cells/ml and allowed to adhere for 24h. 50 μ l of the medium was removed and replaced with 50 μ l of PB. The cells were allowed to incubate with the reagent for 30 min at 37 °C. 100 μ l aliquots were removed from each well and transferred to a 96 well plate (VWR, Ireland) for measurement. The remaining PB and medium in the 24 well plate was removed and replaced with 500 μ l CGM and the cells were returned to the incubator until the following day.

The fluorescence was recorded at an excitation wavelength of 560nm and an emission wavelength of 590 nm using a SpectraMax M2e plate reader. All measurements were taken as an average of three separate wells and corrected for any background fluorescence by including control wells containing only CGM and the scaffolds with no cells on each plate. This process was repeated daily for 11 days.

2.3.8.4 Imaging cells

Cells were visualised under an Olympus CRX31 inverted microscope with a microscope USB digital camera used to image the cells. Images were processed and analysed using ISCapture and ImageJ software. In order to calibrate the size scale of the micrographs, photos of a grid with known partition dimensions were taken for each magnification used.

Chapter 3:
Cavitation rheology of protein bigels

3.1 Introduction

Hydrogels consist of 3D hydrophilic polymeric networks in which water is a major component. They are widely used in cell encapsulation, tissue engineering, wound healing and regenerative medicine (Hoffman, 2002; Chung and Park, 2009; El-Sherbiny and Yacoub, 2013; Zhang *et al.*, 2015). Natural polymers including proteins, are ideal candidates for these hydrogels, owing to their biocompatibility and biodegradability. Chemical hydrogels are formed by covalent cross-linking between polymer chains whereas physical hydrogels form from the entangled chains or intermolecular interactions such as hydrogen bonding or hydrophobic forces which hold the gel together (Zhu and Marchant, 2011).

Historically, one of the limitations for using hydrogels in biological applications was a lack of mechanical stability, which is required for advanced biomedical applications such as replacement cartilage, ligaments and tendons (Hutmacher, 2001). Since then, new materials have been developed by various methods to overcome this limitation. These include the formation of interpenetrating networks (IPN) that involve the synthesis or cross-linking of multiple polymers sequentially (Sperling and Mishra, 1996; Zhang *et al.*, 2015), double-network (DN) gels, which consist of two polymeric gels in network form (Nakayama *et al.*, 2004; Sun *et al.*, 2012) and bigels, which can describe two discrete interpenetrating gel networks whereby both networks contribute to the overall mechanical strength of the gel (Varrato *et al.*, 2012; Blumlein and McManus, 2015).

In 2012 the Foffi Group described a binary colloidal gel consisting of DNA-coated colloids (DNACCs), showing how arrested spinodal decomposition of the complementary coated colloidal particles may lead to bigel formation (Varrato *et al.*, 2012). Sun *et al.* reported a synthetic alginate and polyacrylamide double network gel, whereby both networks were shown to work synergistically to create a gel with stronger properties, with the new gel capable of being stretched over twenty times its original length (Sun *et al.*, 2012).

A protein-only bigel was described for the first time in 2015. This consisted of two proteins, BSA and gelatin, which formed a double network gel with interesting mechanical properties. These gels had elastic moduli of up to 24.3 kPa, four times greater than the combined modulus of the two parent proteins. Confocal microscopy analysis of the gels revealed a percolated network of uniform spherical BSA aggregates surrounded by a second discrete network of the gelatin, figure 3.1.

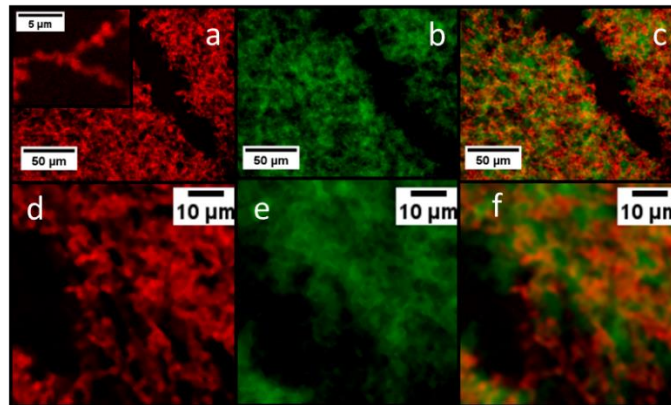


Figure 3.1: Confocal microscopy image (20x magnification) of a protein bigel, $\phi = 0.139$ composed of gelatin, $\phi = 0.073$ and BSA, $\phi = 0.066$. Gelatin labelled with FITC appears green, BSA labelled with Dylight 633 appears red. Insert in panel 1 is at 100x magnification. The overlay of the two images indicates that the gel networks are discrete but interpenetrating. Taken from (Blumlein and McManus, 2015).

Based on confocal microscopy, environmental scanning microscopy and elasticity measurements, it was concluded that the bigel structure was consistent with an arrested particle gel of BSA forming the first component of the bigel, followed by the formation of a second physical gelatin gel entangled around the BSA gel. These gels also demonstrated swelling behaviour, indicating a promising potential to be used in different biomedical applications such as drug delivery, wound healing or as biomimetics in tissue culture (Blumlein and McManus, 2015). New proteins could contribute to an even stronger gel which would offer even more opportunities for biomedical applications.

3.2 Aims of this study

The aim of this study was to explore if other protein pairs could be used to create protein bigels and to examine if the enhanced mechanical properties observed in the BSA/gelatin double network persist in other bigel systems. The procedure to produce the bigels was also examined with a view to optimising the process for consistency. Cavitation rheology was used to measure the mechanical properties of the new double network materials.

3.3 Results

3.3.1 Cavitation rheology (CR) instrument

Previous work has indicated that small differences in the inner radii of needles used in CR measurements can lead to significant variation in the measurement of the elastic modulus. However, the surface tension of water can reliably be measured using CR and can be used to identify needles with the correct inner diameter measurements to be used for further measurements. The critical pressure for water at a particular needle size is related to the surface tension by;

$$P_c = \frac{2\gamma}{r} \quad [\text{Eqn 3.1}]$$

where γ is the surface tension and r is the needle internal radius (Zimmerlin *et al.*, 2007).

Table 3.1: Some of the values obtained for the surface tension of water at different needle sizes

Needle radius (mm)	Average P_c (kPa)	Surface tension (Nm^{-1})
0.42	0.351 +/- 0.023	73.7
0.30	0.497 +/- 0.009	74.5
0.21	0.688 +/- 0.027	72.2
0.16	0.936 +/- 0.016	74.8

The values obtained for several different needle sizes are listed in table 3.1 and are comparable to the literature values for the surface tension of water, of 72.75 mNm^{-1} at 20°C (Vargaftik *et al.*, 1983).

3.3.2 BSA/Gelatin Bigel

A protein bigel consisting of BSA and gelatin was initially described in 2015 (Blumlein and McManus, 2015). This bigel had enhanced mechanical properties when compared with the parent gels it was composed of. It was found to have an elastic modulus of 24.3 kPa using cavitation rheology. Based on confocal microscopy, environmental scanning microscopy and elasticity measurements, it was concluded that the bigel was formed via spinodal decomposition of unfolded BSA, followed by the formation of a second physical gelatin gel surrounding the BSA gel (Blumlein and McManus, 2015).

As part of this project, these experiments were repeated a number of times and variability in the determination of the elastic modulus as determined using cavitation rheology was initially found (figure 3.2). Although the same bigel preparation procedure as described in the paper was used, a range of values for the elastic modulus, E , were determined using cavitation rheology, whereby the critical pressure (P_c) across a range of needle sizes can be related to E using the equation;

$$P_c = \frac{5}{6}E + \frac{2\gamma}{r} \quad [\text{Eqn 3.2}]$$

where γ is the surface tension and r is the needle internal radius (Zimmerlin *et al.*, 2007). These values for E ranged from 12.77 to 21.19 kPa, lower than the original value of 23.4 kPa for the same protein compositions. In addition, error bars were larger than expected, suggesting more heterogeneity within the sample than in the earlier experiments.

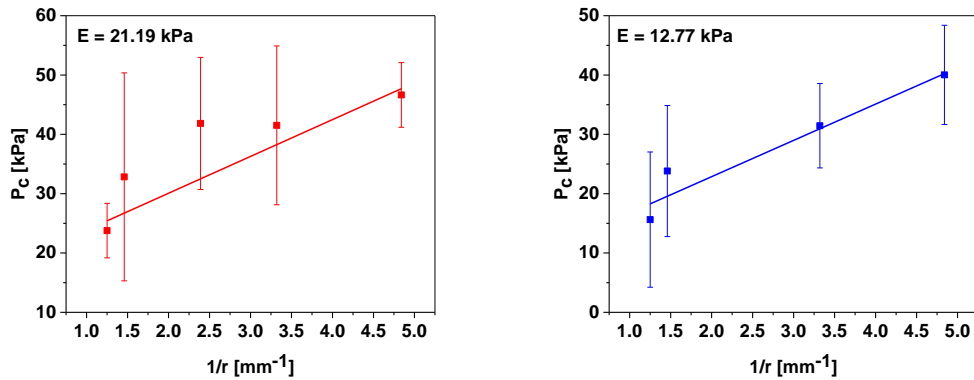


Figure 3.2: The elastic moduli of BSA gelatin bigel $\phi = 0.139$ was found to be 21.19 kPa and 12.77 kPa using equation 3.1. The bigels were both formed using the same preparation procedure.

In an attempt to understand the source of these inconsistencies, a number of studies were carried out to examine the method of preparation for the bigels. It also became clear that the needle placement within the sample during measurement was important in the determination of E , which was further probed.

3.3.2.1 The impact of needle depth on measurements of the elastic modulus

The larger than expected error bars observed in the BSA/gelatin data, figure 3.2, suggested a more heterogeneous gel than previously observed. To determine the source of the variability, several factors related to both the preparation of the material and the measurement of the elastic modulus using CR were considered. We observed that the value for E varied, depending on the placement of the needle inserted into the sample (typically prepared in an Eppendorf tube). This led to an investigation regarding the depth at which the needle was placed within the sample.

The critical pressure was measured using CR at different points within the sample. During the cavitation rheology experiment, the needle was inserted into the sample at two different levels, 1 and 3 cm, measured from the top of the vial, and the critical pressure for two different needle sizes was recorded. The first experiment involved heating the BSA and gelatin-75 mixture at 90 °C for 15 min (less than the incubation time for the original preparation method, which heated for 1 hour). The gel formed was completely opaque. The critical pressures as well as the error, determined by the standard deviation, are listed in table 3.2. Higher pressures were observed when the needle was placed at the bottom of the sample, compared with the pressures observed when the needle was placed towards the top of the sample, figure 3.3. The second experiment involved heating the mixture for 3 min. Once again, the sample was completely opaque in appearance. This time there was a smaller difference noticed between the different needle placements as well as smaller errors recorded, table 3.3, figure 3.4.

Table 3.2: The critical pressures and their associated errors measured at different needle placements following a 15 minute incubation.

	15 minute incubation			
Needle size	14g (r = 0.8 mm)		20g (r = 0.3 mm)	
Needle placement from top of sample	1 cm	3 cm	1 cm	3 cm
P_c [kPa]	26.5 +/- 5.9	55.3 +/- 8.1	31.1 +/- 10.5	77.8 +/- 26.9

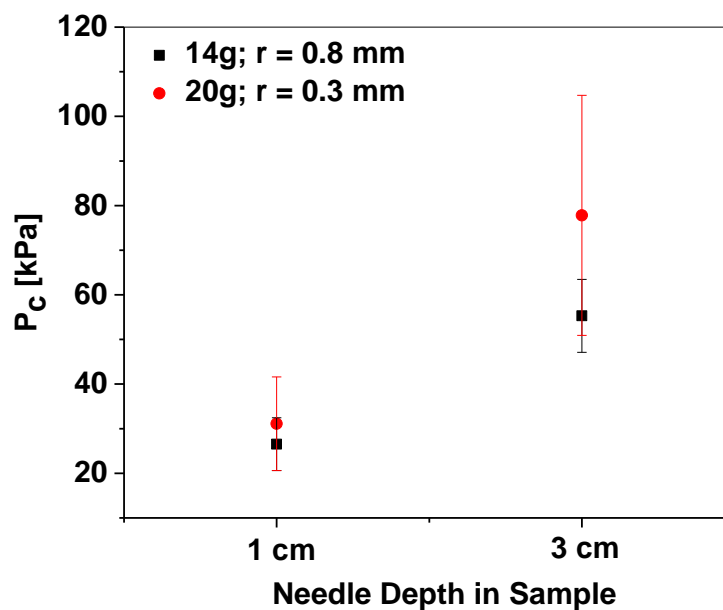


Figure 3.3: A comparison of the critical pressure depending on the placement of the needle in the sample of BSA/gelatin bigel $\phi = 0.139$ following a 15 min incubation at 90 °C.

Table 3.3: The critical pressures and their associated errors measured at different needle placements following a 3 minute incubation.

	3 minute incubation			
Needle size	14g (r = 0.8 mm)		20g (r = 0.3 mm)	
Needle placement from top of sample	1 cm	3 cm	1 cm	3 cm
P_c [kPa]	29.3 +/- 3.9	35.6 +/- 5.5	42.1 +/- 4.3	43.8 +/- 4.6

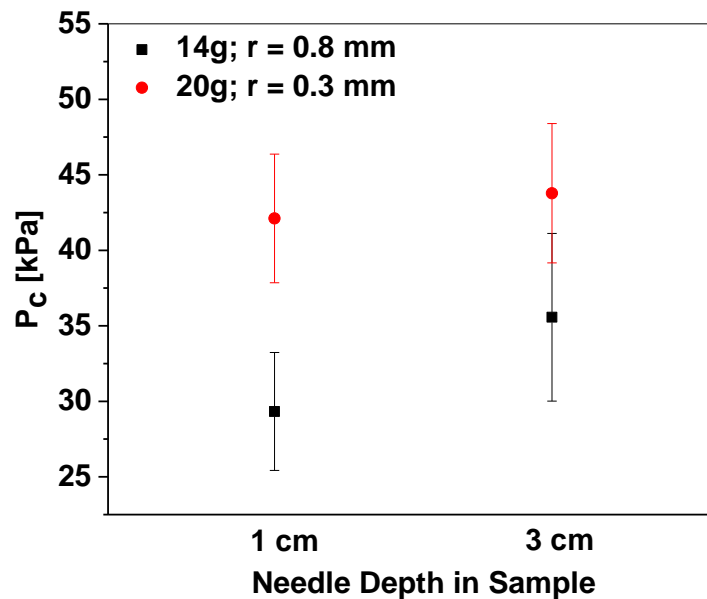


Figure 3.2: A comparison of the critical pressure depending on the depth of the needle in the sample of BSA Gelatin bigel $\phi = 0.139$ following a 3 min incubation at 90 °C.

As previously stated, the mechanism for gelation of the BSA component of the bigel was proposed to be due arrested spinodal decomposition, which is consistent with the rapid opacity on heating and the very uniform size of the particles formed within the gel (1 – 2 μm). Since spinodal decomposition occurs very rapidly, it is likely that the BSA gel forms during the first few minutes of incubation. This is supported by the observation that the sample turns completely turbid within the first ~ 90 sec of heating. For the remaining incubation time, while the gelatin is still in its molten state, it is possible that the BSA gelled network had begun to sediment to the bottom of the tube, which is not unreasonable given the relatively large size of the particles containing aggregated protein which form. This sedimentation would lead to a concentration gradient in the sample and would explain the higher critical pressures observed when the needle was placed towards the bottom of the sample. To test this hypothesis, the heating time (and cooling time) were shortened so that there was less time for sedimentation to occur in the heating phase and the sample was cooled by placing on ice, to shorten the time required for gelation of gelatin to occur. When the sample was heated for 3 minutes this difference in the elastic modulus at different depths was much

smaller. To create a more consistent procedure for future bigels, the heating time was reduced to 3 minutes and after removing the sample from heating, it was immediately quenched in ice to speed up the formation of the gelatin gel, which is formed on cooling.

3.3.2.2 Preparation conditions for bigel formation

Given the importance of preparing a relatively homogeneous sample (to minimise gradients due to sedimentation etc), the procedure to produce the bigels was optimised, to ensure greater consistency in the sample preparation and less variability in CR measurements. The new procedure is summarized in table 3.4.

Table 3.4: A summary of the new preparation procedure for the bigels

Step 1: Mixing	<ul style="list-style-type: none"> • Equilibrate & mix two components at 45 °C • pH Check: 5.5 • (pI BSA: 4.7, pI Gelatin: 4.7 – 5.2)
Step 2: Heating	<ul style="list-style-type: none"> • Heated at 90 ° C for 3 min
Step 3: Cooling	<ul style="list-style-type: none"> • Immediately quenched in ice water

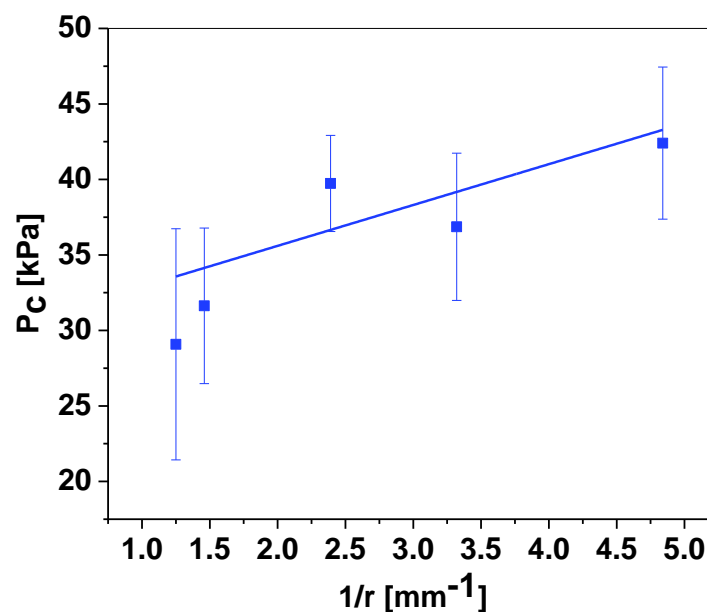


Figure 3.5: The elastic modulus for the 9:10 BSA Gelatin bigel formed using the new conditions (summarized in table 3.2) was found to be 36.2 kPa using equation 3.2.

BSA:gelatin-75g 9:10 gels were formed using the new preparation procedure, as summarized in table 3.4. The elastic modulus for a gel prepared in this way was determined to be 36.2 kPa using cavitation rheology, figure 3.5. This value was much more reproducible than before, with less variability observed in the data. This value is also higher than the value previously reported for the BSA/gelatin-75 bigel of 24.3 kPa. This is most likely a reflection of a more homogeneous gel throughout the sample.

3.3.2.3 The impact of pH on the formation and characteristic of bigels

Since a bigel consists of two interpenetrating discrete gel networks, it is important that there is no inter-species attraction between the two proteins. To ensure this, it is necessary to adjust solution conditions so that the pH of the homogeneous protein solution is close to their respective isoelectric points, so there is no charge attraction between the two proteins, but sufficient residual charge to ensure that limited self-association occurs prior to gelation. The isoelectric point of a protein is the pH at which it has no net electrical charge. The isoelectric point of BSA is 4.7 (Ge et al. 1998) and varies from 4.7-5.2 for gelatin (Bhattacharjee and Bansal, 2005), depending on the type of gelatin used. Therefore, at a pH of 5.5 there is little net charge on either protein in the mixture. For the BSA/gelatin bigel initially described, there was no need for a pH adjustment as the resulting pH when the proteins were dissolved in water and mixed together was approximately 5.5. Due to the fluctuations in the pH of water however, the effect of the pH on the BSA/gelatin bigel was also explored to determine what impact a higher pH might have on the bigel. A homogeneous protein solution was prepared at total volume fraction of $\phi = 0.139$, consisting of gelatin, $\phi = 0.073$ and BSA, $\phi = 0.066$. The pH was adjusted to 7 and the solution was incubated at 90 °C for 3 min. The elastic modulus was found to be 31.02 kPa using cavitation rheology, figure 3.6, slightly lower than the value of 36.2 kPa measured for the bigel at pH 5.5 using the optimised procedure, figure 3.5. In addition, the gels were less opaque in appearance compared with gels prepared at a pH of 5.5, figure 3.7.

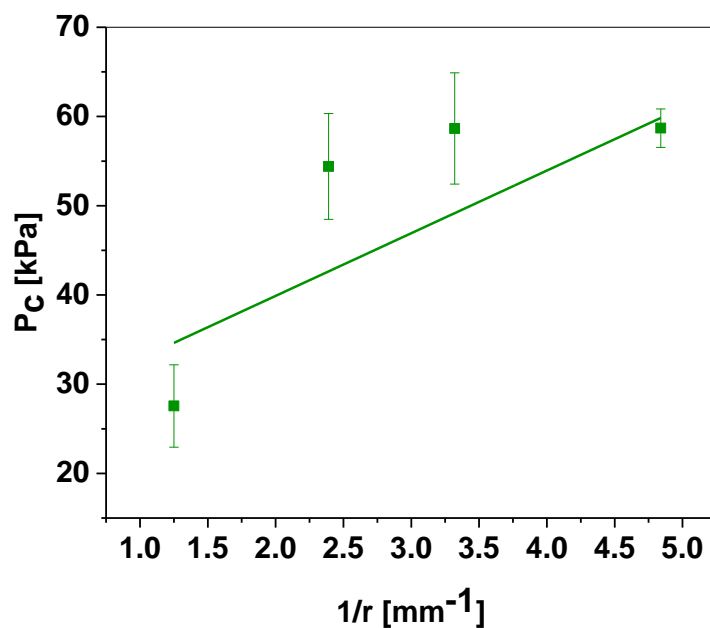


Figure 3.6: The elastic modulus of BSA/gelatin bigel; $\phi = 0.139$ at a pH of 7 was found to be 31.02 kPa using equation 3.2



Figure 3.7: A comparison of the BSA/gelatin bigel; $\phi = 0.139$, at a pH of 5.5 (left) and a pH of 7 (right).

3.3.3 New bigel candidates

To improve any future development of products based on the formation of protein bigels, it is important to ensure that it is possible to make bigels from other protein pairs. When choosing the new proteins to prepare bigels from, it was important to consider their properties to ensure inter-species attraction could be kept at a minimum, so that two discrete interpenetrating networks could be produced. The mechanical properties of

these new gels were probed to determine if the same enhanced mechanical properties seen in the BSA/gelatin bigel can be reproduced for a different protein bigel. Before attempting to produce a double network gel, the mechanical properties of the single component gels were measured using cavitation rheology.

3.3.3.1 Single component ovalbumin gels

Ovalbumin (OVA) was the first protein explored as a potential bigel candidate. OVA was chosen due to its similarity in structure and properties to BSA. It has an isoelectric point of 4.58 – 4.75 (Feeney, 1957) and a melt transition temperature of ~77 °C (Photchanachai *et al.*, 2002) It is also very similar in amino acid content to BSA (Lewis *et al.*, 1950). In addition to its properties, it is readily available at low-cost.

3.3.3.1.1 Differential Scanning Calorimetry

Differential Scanning Calorimetry (DSC) was used to determine the melt transition temperature (T_m) of ovalbumin. The temperature was increased/decreased at 1 °C/min while the change in heat capacity of the sample was measured. There was an endothermic peak observed at 77.26 °C, figure 3.8, indicating the melt transition temperature of OVA. This is consistent with the literature values for T_m for OVA (Photchanachai *et al.*, 2002).

Two heating cycles and cooling cycles were carried out to determine if the protein underwent any reversible unfolding. There was no change in heat capacity detected following the first heating cycle indicating irreversible aggregation following protein unfolding.

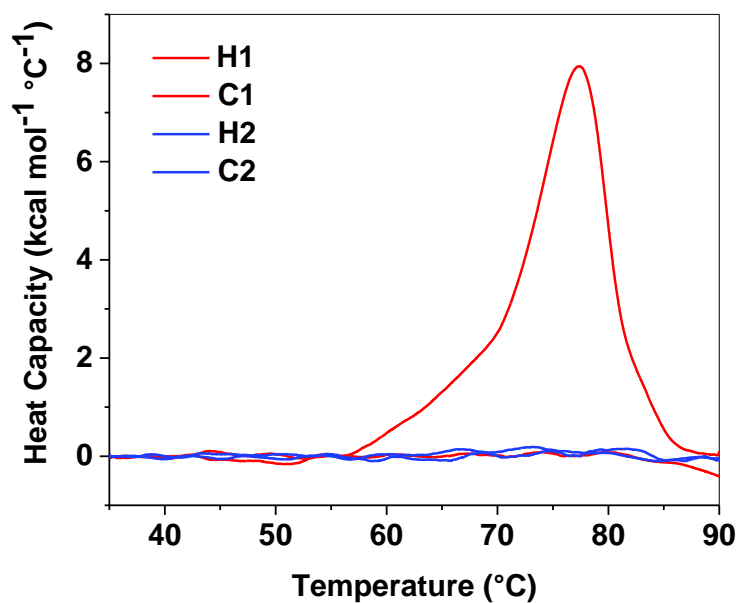


Figure 3.8: The normalised and baseline subtracted DSC thermogram for ovalbumin (100 mg/ml) in water during two heating and two cooling cycles showing T_m of ~ 77.4 °C.

3.3.3.1.2 Cavitation Rheology

The elastic moduli of single component OVA gels were measured using cavitation rheology. At a volume fraction of $\phi = 0.066$, the elastic modulus was found to be 5.67 kPa, figure 3.9. Below a volume fraction of $\phi = 0.066$, the OVA gels were extremely weak. As the volume fraction of the gels increased, the elastic moduli also increased.

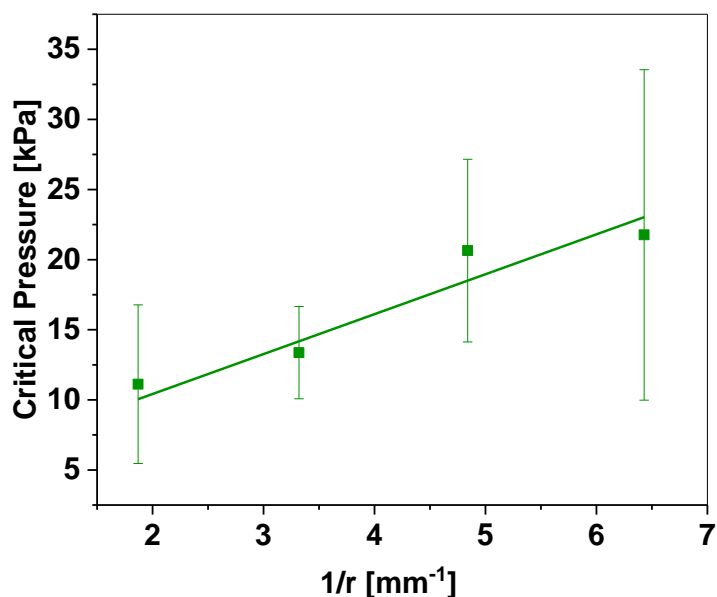


Figure 3.9: The elastic modulus of OVA, $\phi = 0.066$ was found to be 5.67 kPa using equation 3.2, measured using cavitation rheology.

3.3.3.1.3 Reversibility

One way to determine the degree of elastic character of a gel using cavitation rheology is to measure the degree to which the deformation of the gel due to bubble formation is reversible. For certain stress-bearing applications, having a high degree of elasticity is required (Sun *et al.*, 2012). The reversibility as determined using CR of the single component OVA gels was explored by subjecting the system to successive pressurisation and depressurisation cycles, which can help to distinguish elastic deformation and irreversible fracture. If the critical pressure returns to the same critical pressure following the second pressurization cycle, this would indicate a fully elastic material. In addition to this, the critical pressure will scale linearly with r^{-1} , whereas for a material that undergoes irreversible fracture following cavitation, the critical pressure will scale linearly with $1/r^{1/2}$. Following the initial pressurization cycle (critical pressure of 13.4 kPa, for a 20 gauge needle) for the OVA gels, the critical pressure was measured as 6.09 kPa on a second pressurization cycle 45 % of its original critical pressure, figure 3.10, indicating that the deformation process is partially reversible (Kundu and Crosby, 2009).

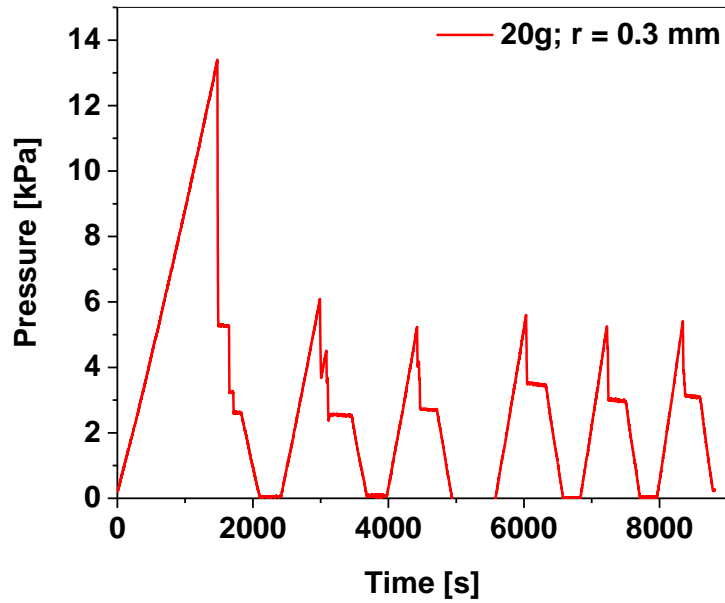


Figure 3.10: Cavitation rheology of OVA, $\phi = 0.066$ (83 mg ml^{-1}) indicates deformation process is 45 % reversible.

3.3.3.1.4 Effect of pH on mechanical properties of the gels

As previously mentioned, for the formation of the BSA/gelatin double network gels, the pH was critically important to ensure that there is no inter-charge attraction between the two proteins. However, the pH also plays an important role in the gelation of the single component BSA and OVA gels. The OVA gels were prepared at $\phi = 0.066$ in water. After heating at 90°C for 3 min, the gels were very weak in consistency and not very opaque, figure 3.11 (b). To determine the source of this, the gel was prepared again, however this time a pH check was conducted. The pH was at 7, meaning there was a net negative charge on the protein. The ovalbumin gel was then prepared at pH of 5.5 and the resulting gel appeared more turbid, figure 3.11 (a).

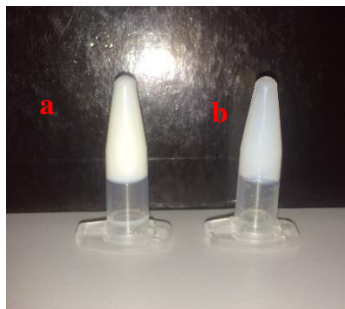


Figure 3.11: The OVA gels at a pH of 5.5 (a), were more turbid than those formed at a pH of 7 (b).

The effect of pH on the mechanical properties of OVA gels was also probed using cavitation rheology. At a pH of 7, the OVA gels formed were very weak with an elastic modulus of 0.05 kPa. When the pH was adjusted to 5.5, stronger gels were formed with an elastic modulus of 5.64 kPa, figure 3.12. These results suggest that the OVA underwent amorphous aggregation at a pH of 7, emphasising the need to control solutions conditions to ensure that gel formation occurs by spinodal decomposition rather than amorphous protein aggregation, which is generally diffusion limited.

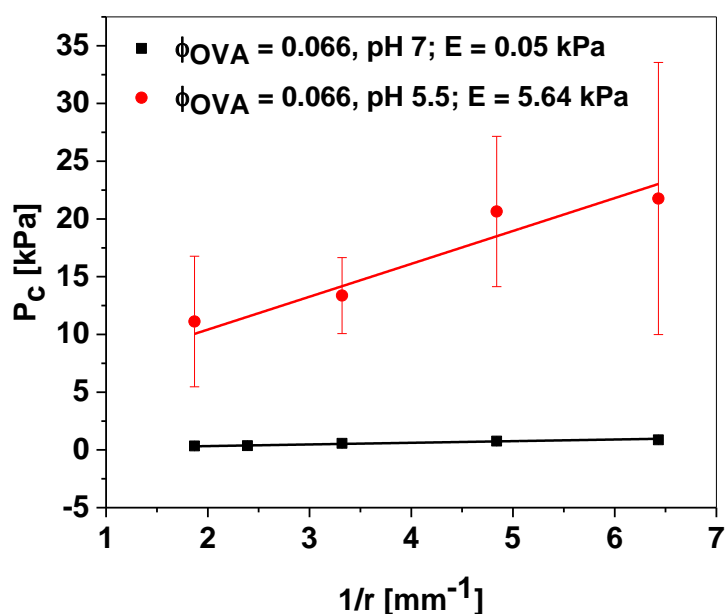


Figure 3.12: A comparison of the elastic modulus for OVA, $\phi = 0.066$ at a pH of 7 and 5.5 was found to be 0.05 kPa and 5.64 kPa respectively, using equation 3.2.

3.3.3.2 Single component gelatin gels

When choosing the bigel components, it is important to consider the properties of the proteins so that no intermolecular attraction occurs to ensure the formation of a discrete double network. Gelatin has an isoelectric point of 4.7 -5.2, similar to that of ovalbumin, 4.58 - 4.7 (Rhodes *et al.*, 1958). It also does not contain any cysteine residues that could form disulphide bridges which the free cysteines present on ovalbumin can do. For the BSA/gelatin bigel, gelatin with a bloom number of 75g was used (where the bloom number is directly proportionate to the molecular weight). It has been shown that the molecular weight has a direct impact on the mechanical strength of

gelatin gels (Ferry and Eldridge, 1948). For these reasons, gelatin with a bloom number of 225g, was chosen as another potential bigel component.

3.3.3.2.1 Differential Scanning Calorimetry

Differential Scanning Calorimetry was used to determine the melt transition temperature (T_m) of the higher molecular weight gelatin, Gel-225 at a concentration of 100 mg/ml was prepared. The baseline subtracted DSC plot indicates a T_m of ~ 31 °C, figure 3.13, consistent with the published values for the melting transition temperature of gelatin (Bigi *et al.*, 2004).

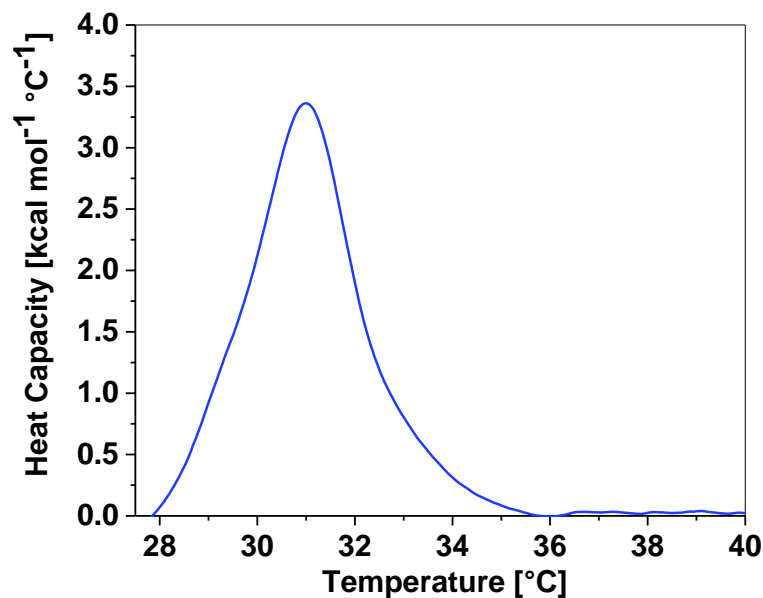


Figure 3.13 The normalised and baseline subtracted DSC thermogram for Gelatin-225 (100 mg/ml) showing a melt transition temperature of 31 °C.

3.3.3.2.2 Cavitation Rheology

The mechanical properties of single component gelatin gels were probed using cavitation rheology. Gels were prepared from gelatin-225 at concentrations ranging from 75 mg/ml to 100 mg/ml, and characterised using cavitation rheology to determine their elastic modulus. As the concentration of the gelatin was increased, the elastic modulus increased from a modulus of 7.08 Pa for a gel with volume fraction, $\phi_{\text{gel}} = 0.055$ to a modulus of 9.64 kPa for a gel with a volume fraction, $\phi_{\text{gel}} = 0.073$, figure

3.14. At concentrations below 50 mg/ml, the solutions remained liquid-like. The deformation process for all the gelatin gels proceeded by irreversible fracture, as determined by successive pressurization/depressurization cycles, and shown by the linear scaling with $1/r^{1/2}$, figure 3.14.

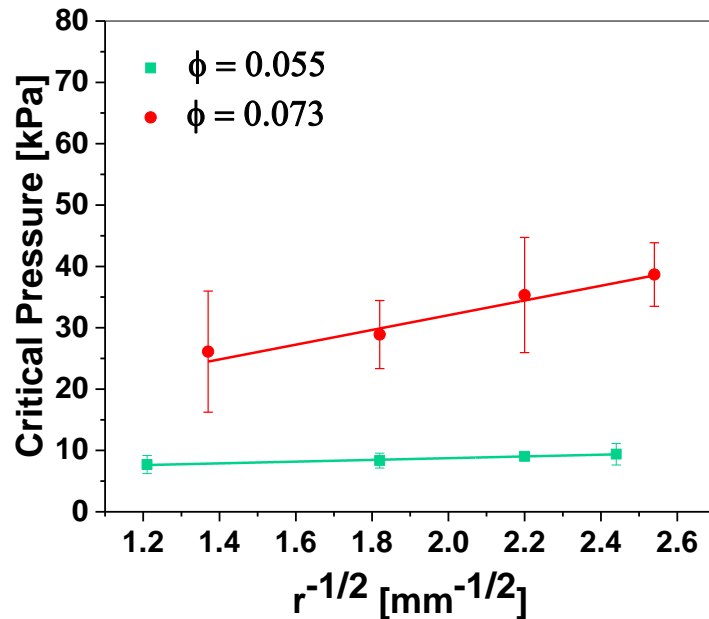


Figure 3.14: The elastic modulus of gelatin-225g at concentrations of a) gelatin-225g, $\phi = 0.055$, and b) gelatin-225g, $\phi = 0.073$, were found to be 7.08 and 9.64 kPa respectively using equation 3.2.

3.3.4 Ovalbumin/Gelatin-225g Bigels

Following the promising results regarding the mechanical properties for the single component ovalbumin and gelatin-225g proteins, these two proteins were used to create a double network gel. Since the mechanism for the gelation of OVA seemed to be similar to that of BSA, it was hoped that a discrete network could be created. The optimised bigel preparation procedure from section 1.3.5 was used for all the OVA/gelatin bigels.

3.3.4.1 Cavitation rheology

The mechanical properties of the OVA/gelatin-225 bigels were examined using cavitation rheology. As for the BSA/Gelatin-75 bigel, a gel was prepared with a total

volume fraction, $\phi = 0.139$, composed of OVA, $\phi = 0.066$ and gelatin-225g, $\phi = 0.073$. The elastic modulus of this gel was found to be 66.96 kPa, figure 3.15, approximately 4 - 5 times greater than the combined modulus of the parent gels as summarised in table 3.5 and figure 3.16.

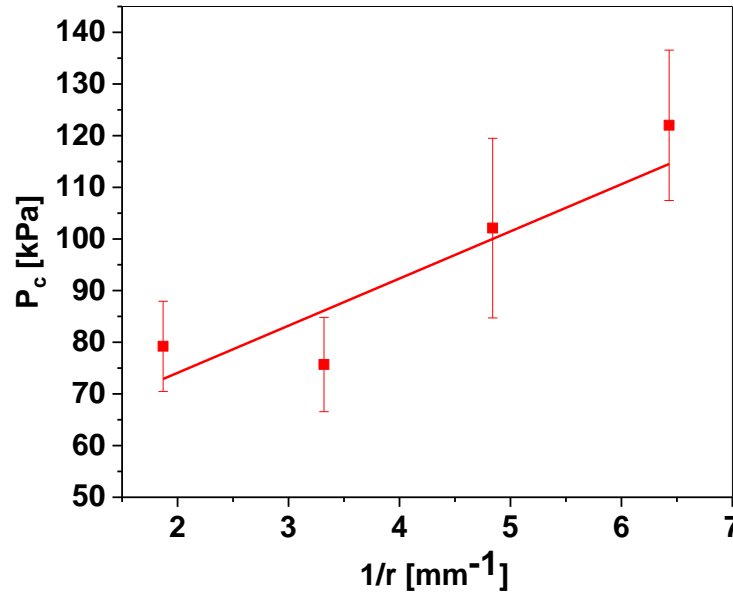


Figure 3.15: The elastic modulus of the OVA-gelatin-225 bigels at a volume fraction of 0.139 was determined to be 67kPa using equation 3.2.

This enhancement of the elastic modulus supports the idea that the two components in a bigel work synergistically to create a material with enhanced mechanical properties (Sun *et al.*, 2012; Di Michele *et al.*, 2014).

Table 3.5: A comparison of the elastic moduli obtained for the BSA/Gel-75 bigel and the OVA/Gel-225 bigel as well as for the parent gels.

Composition	E [kPa]	Composition	E [kPa]
BSA, $\phi = 0.066$	3.2	OVA, $\phi = 0.066$	5.6
Gelatin-75g, $\phi = 0.073$	2.8	Gelatin-225g, $\phi = 0.073$	9.6
BSA/Gelatin-75g bigel, $\phi = 0.139$	24.3	OVA/Gelatin-225g bigel, $\phi = 0.139$	67

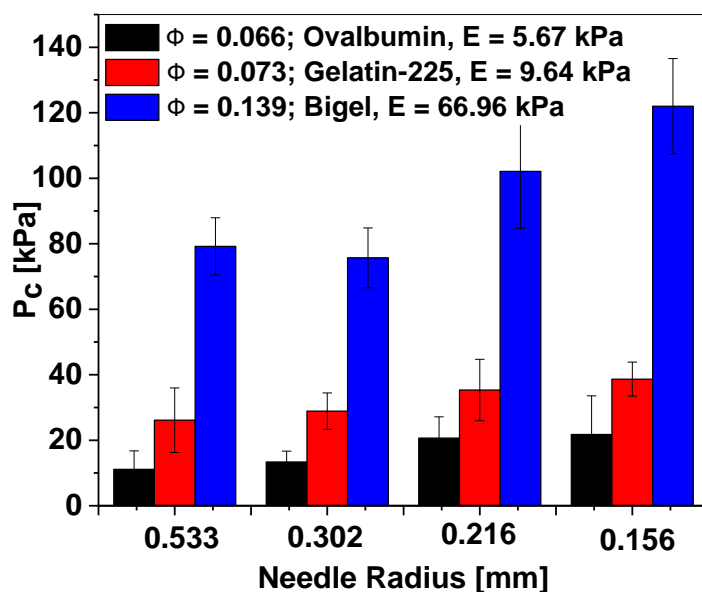


Figure 3.16: Comparison of the critical pressures obtained for a) gelatin-225, $\phi = 0.073$, b) OVA, $\phi = 0.066$ and c) Bigel, $\phi = 0.139$ across of variety of needle radii.

3.3.4.2 Reversibility

As with the single component gels, the nature of the deformation process for the bigels was explored with cavitation rheology. The bigels were subjected to successive pressurization and depressurization cycles. The measurements indicated that deformation process for the bigel was predominantly elastic with the critical pressure retuning to 85 % of its original critical pressure, figure 3.17. This is surprising since the single component ovalbumin gels only displayed 45 % elasticity and suggests a change in the behaviour of the ovalbumin in the presence of gelatin. These results are very promising for certain stress-bearing applications that require a high level of elasticity (Sun *et al.*, 2012).

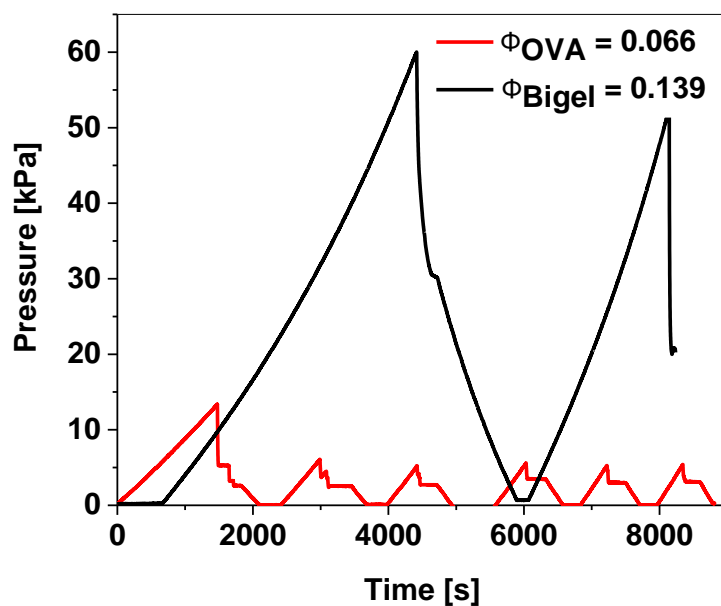


Figure 3.17: Cavitation rheology showed that the deformation process was 85 % reversible for the bigel.

3.3.4.3 Light Microscopy:

Light microscopy was used to explore the microstructure of the gels to help confirm the source of the enhanced mechanical properties. Light microscopy of the OVA/Gelatin-225 bigels revealed a percolated network of spherical aggregates, figure 3.18, similar to what was seen for the BSA/gelatin-75g bigels. The uniformity of the OVA aggregates as well as the presence of a percolated network, surrounded by the gelatin system is consistent with spinodal decomposition.

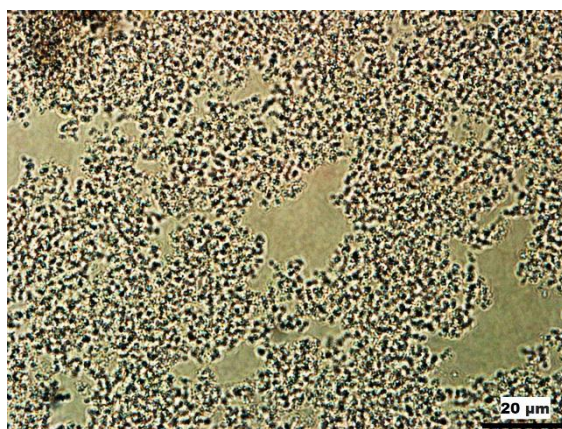


Figure 3.18: Phase contrast light microscopy image of ovalbumin/gelatin bigel, $\phi = 0.139$, at a magnification of 100x.

3.4 Discussion

New protein bigels were formed using ovalbumin and gelatin with very interesting mechanical properties. Cavitation rheology was used to determine the elastic modulus of these gels with moduli of up to 67 kPa reported for the strongest gels consisting of a bigel composed of ovalbumin and gelatin-225. The strongest gels also displayed 85 % elasticity, much higher than that of single component ovalbumin gels alone. These are very promising results for the use of these materials in a lot of biomedical applications (Hoffman, 2002). The bigel preparation procedure was also examined and standardised for all gels. Cavitation rheology was selected over standard shear rheology because the length-scale dependence of the mechanical properties of hydrogels are important for their use as cell scaffolds, since cells respond to mechanical cues at different length-scales. CR captures these properties well, since the heterogeneities of the material are also captured. These are averaged out in other type of measurements.

Tough protein bigels composed of BSA and gelatin were initially described by Blumlein and McManus in 2015. The proposed mechanism by which these gels were formed was by that of arrested spinodal decomposition of unfolded protein, figure 3.19. (Blumlein and McManus, 2015). A homologous protein mixture of BSA and gelatin was formed by heating the gelatin above its melt transition temperature, ~ 27 °C. Upon heating this solution to above 80 °C, (above the melt transition temperature of BSA), the BSA is unfolded, exposing its hydrophobic residues to the solvent, water. The system will subsequently undergo liquid-liquid phase separation via spinodal decomposition in order to minimise the free energy of the system. At specific concentrations of the BSA, this spinodal decomposition becomes dynamically arrested resulting in the formation of a percolated BSA gel network, composed of space-spanning clusters. Upon cooling the solution, the gelatin then forms a second physical gel around the BSA network (Blumlein and McManus, 2015).



Figure 3.19: The proposed mechanism for the formation of a BSA:gelatin bigel. Taken from (Blumlein and McManus, 2015).

These double network protein gels were found to have much stronger mechanical properties than either parent gel, with an elastic modulus of 24.3 kPa, four times greater than the combined modulus of both parent gels (Blumlein and McManus, 2015). These enhanced mechanical properties are consistent with the formation of a bigel, as reported by Foffi *et al.* (Di Michele *et al.*, 2014) and have the potential to overcome the biocompatibility issues that arise with synthetic hydrogels in biomedical applications.

In an attempt to reproduce the data for the BSA/gelatin bigel, some inconsistencies in the in the gel preparation procedure were observed, which led to variations in the determination of the elastic modulus. To help understand these inconsistencies, some studies were conducted on the bigel preparation procedure. The original gelation procedure involved hydrating both protein solutions, (gelatin must be heated above 30 °C to dissolve in water), mixing them and then heating the mixture to 80 °C for 1 hour. The solution was then allowed to cool at room temperature before analysis.

It was observed that the needle placement within the sample had an impact on the critical pressure (P_c) of the sample when analysed with cavitation rheology. The further into the sample the needle was inserted, the higher the critical pressure required to cause an elastic deformation in the gel. This observation was consistent with sedimentation

occurring in the sample, which would have led to a concentration gradient within the sample, and therefore inconsistencies in the determination of the elastic modulus by CR specifically, since this technique is very sensitive to local changes in elasticity. By refining the preparation conditions, greater consistency in both the gel formation and the CR measurements were achieved. The new procedure involved heating the protein mixture at 90 °C for 3 minutes followed by rapid cooling on ice. Since the sample becomes completely turbid within the first 90 seconds of heating, longer incubation times were un-necessary. For this reason, three minutes was chosen as the new incubation time and the sample was immediately quenched in ice water on removal from the heat to speed up the formation of the gelatin gel. Following these studies, the method of preparation for the bigels was optimised and standardised. Using the new procedure, the 9:10 BSA:gelatin bigel was found to have an elastic modulus of 36.2 kPa.

The effect of the pH on the bigel was also explored. The pH of the protein solutions plays a very important role in the formation of a bigel. Since one of the requirements for the formation of bigel is that the two protein networks remain discrete, it is important that there is no charge attraction between the proteins. This can be achieved by altering the solution conditions so that the pH is close to, but not at the isoelectric points of the proteins. The isoelectric point of BSA is 4.7, and gelatin at 4.7-5.2, so the pH must be maintained at around 5 to ensure this. However, to examine the importance of the pH, the pH was adjusted to 7 during the formation of the BSA/gelatin bigel. At a pH 7 the elastic modulus of the bigel was 31.02 kPa, compared to 36.26 kPa at a pH of 5.5. Due to the isoelectric points of the proteins, at a pH of 7 there is a net overall negative charge on the BSA and as a result there may have been intermolecular charge interactions occurring between the proteins which may have resulted in amorphous aggregation instead of spinodal decomposition. This would lead to a mixed gel (rather than a bigel) with less advantageous mechanical properties. The gel was less opaque when compared with the protein that underwent spinodal decomposition.

New proteins were explored for the formation of bigels with the hope of creating new gels with enhanced mechanical properties. When choosing the new bigel components it

was important to consider the properties of the proteins. As already mentioned, in order to have a system of two discrete protein networks, it is necessary that there are no intermolecular interactions occurring between the two proteins. For BSA and gelatin, this was insured by the fact that gelatin contained no cysteine residues, which were thought to be the responsible for the irreversible aggregation that occurs with the spinodally decomposed BSA as well as the fact that both proteins had a similar isoelectric point that was close to the pH of the buffer to limit charge attraction (Blumlein and McManus, 2015).

The first protein explored as a potential candidate was ovalbumin (OVA). Ovalbumin was chosen due to its similarity to BSA. Similar to BSA, OVA has an isoelectric point of 4.58 – 4.75 (Feeney, 1957) and a melt transition temperature of ~ 77 °C (Photchanachai *et al.*, 2002). OVA contains six cysteine residues with a single disulphide bond between Cys74 and Cys121 (Thompson and Fisher, 1978). The similarity to BSA suggests that OVA may also undergo spinodal decomposition resulting in very strong gels. OVA gels were initially prepared at a volume fraction of $\phi = 0.066$ with no pH adjustment. The gels were less opaque in appearance than the previously prepared BSA gels. On further investigation, it was clear that in the absence of a suitable buffer, the gels were formed at a pH of 7, meaning there was an overall net negative charge on the protein which may have resulted in amorphous aggregation rather than spinodal decomposition. The gels at pH 7 were also much weaker than the corresponding gels at pH 5.5, with elastic moduli of 0.05 kPa compared with a 5.6 kPa for the lower pH. This highlighted once more the importance of the pH for the gelation process of the single and double component gels. The mechanical properties of the OVA gel at $\phi = 0.066$ were probed further. As well as having an elastic modulus of 5.6 kPa, higher than the corresponding modulus for the BSA gel, the gels also displayed 45 % elasticity upon successive deformation cycles.

Gelatin was an ideal candidate for the original BSA gelatin-75 bigel due to the fact that it is a thermoreversible physical gel that formed independently of the BSA and has a pI of 4.7 – 5.2 (Bhattacharjee and Bansal, 2005), similar to that of BSA at 4.7 (Ge *et al.* 1998). Ferry & Eldridge showed the impact molecular weight of gelatin has on its

elastic modulus (Ferry and Eldridge, 1948). For this reason, a higher molecular weight gelatin was chosen with the anticipation it would have an even greater contribution to the overall strength of the bigel. The new gelatin had a bloom number of 225 g compared to the gelatin previously used in the protein bigel which had a bloom number of 75 g (Blumlein and McManus, 2015). The bloom value of gelatin is an indicator of its strength, defined by the weight in grams required for a 12.7 mm diameter flat bottomed cylindrical plunger to depress the surface of a 6.67% (w/w) gelatin gel. Gelatin-225 gels were formed in concentrations ranging from a volume fraction of 0.055 to 0.073. All of the gels were transparent with the elastic moduli ranging from 7 to 9.64 kPa. The reversibility of these gels was explored through successive pressurization and depressurization cycles using cavitation rheology with the results indicating deformation by fracture for all the gelatin gels.

Bigels were formed between ovalbumin and higher molecular weight gelatin, gelatin-225 with very strong mechanical properties. The gelation procedure used was identical to the optimized procedure for the BSA/gelatin-75 bigels. The bigel formed with a combined volume fraction of 0.139 was found to have an elastic modulus of 66.96 kPa, compared with 36.2 kPa for the BSA gelatin-75 bigel. This significant increase can be credited to both the higher molecular weight gelatin, as well as the ovalbumin single component gel, which was stronger than for the BSA gel at the same volume fraction. In addition, as was seen in the BSA/gelatin bigels (Blumlein and McManus, 2015), the deformation process for the gels maintained some of its elasticity. The successive pressurization and depressurization cycles indicated that the deformation process was 85 % elastic, with the bigel maintaining a critical pressure of 51 kPa following the initial cavitation event, a value which is still much higher than that of the single component ovalbumin gel at the same concentration, which only maintained 45 % elasticity with a critical pressure of 5.6 kPa. This suggests that the behaviour of the ovalbumin changes in the presence of the gelatin. These results agree with the work by Foffi and his colleagues whereby they showed how DNA bigels may withstand more stress than single component gels, with the same 4x scaling pattern observed (Di Michele *et al.*, 2014). Light microscopy of the bigels revealed a percolated network of uniform OVA aggregates surrounded by the gelatin gel. This is consistent with arrested spinodal

decomposition since it occurs rapidly and uniformly throughout the sample, unlike amorphous aggregate formation which would result in a more heterogenous gel.

3.5 Conclusion

Ovalbumin and a higher molecular weight gelatin were used to create a very strong protein bigel, consisting of two discrete interpenetrating networks, with the OVA having undergone arrested spinodal decomposition and the gelatin gel forming around the ovalbumin. Using cavitation rheology, the mechanical properties of these gels were explored, revealing very strong gels with an elastic modulus of up to 67 kPa, much higher than that of the BSA/gelatin bigels described previously. In addition, these gels displayed an extremely high elasticity of approximately 85 %, very interesting properties for the purpose of certain stress-bearing biomedical applications such as replacement cartilage. Light microscopy of these gels revealed a percolated network of uniform spherical aggregates consistent with the mechanism of arrested spinodal decomposition. The preparation procedure for the bigels was also investigated and optimised, creating a standardised procedure for all protein bigels.

Chapter 4:
Bigels as cell scaffolds

4.1 Introduction

Hydrogels are three-dimensional hydrophilic polymeric networks that are widely used in tissue engineering, wound healing and regenerative medicine (Hoffman, 2002). They are ideal for use as cellular scaffolds since their properties resembling the extracellular matrix surrounding cells *in vivo* (Zhu and Marchant, 2011).

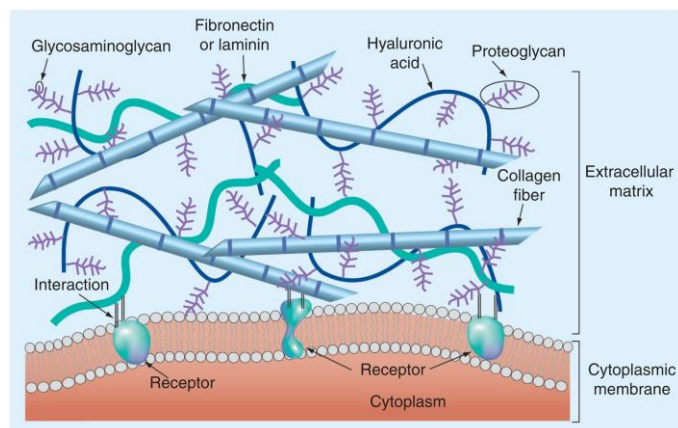


Figure 4.1: Model of the complex structure of ECM that surrounds cells *in vivo*, taken from (Zhu and Marchant, 2011).

They can be formed from natural or synthetic polymers, or a combination of both. Synthetic hydrogels often involve a chemical crosslinker that can be both toxic to the cells and can result in unreacted agent that must somehow be subsequently removed from the cells (Hoffman, 2002). Physical hydrogels involve polymer chains that are held together by non-covalent interactions such as hydrogen bonding, hydrophobic forces and electrostatic interactions (Zhu and Marchant, 2011).

Natural polymers provide a great alternative to synthetic ones, as they can avoid any biocompatibility and biodegradability issues that might arise (Zhu and Marchant, 2011). There have been hydrogel tissue scaffolds formed from polysaccharides, such as alginate (Augst *et al.*, 2006), hyaluronic acid (Leach *et al.*, 2003) and chitosan (Kim *et al.*, 2008), DNA (Wang *et al.*, 2017), and proteins, including collagen (Lee *et al.*, 2001; Levingstone *et al.*, 2014), gelatin (Sakai *et al.*, 2009) and lysozyme (Yan *et al.*, 2006). However, in general these lack the mechanical strength required for some more stress-bearing applications such as bone grafting (Hutmacher, 2001). In addition to biocompatibility, biodegradability and mechanical strength another key feature to consider in the design of three-dimensional cell scaffolds include the degree of porosity,

necessary for the cell penetration, ingrowth and distribution (El-Sherbiny and Yacoub, 2013).

Collagen is one of the most popular polymers used for cell scaffolds (Lee *et al.*, 2001; Glowacki and Mizuno, 2008). There are several collagen-based hydrogel products currently on the market for various biomedical applications. Surgacoll currently market two products, Condrocoll, and HydroxyColl, which are both collagen based, for use in tissue engineering applications (Levingstone *et al.*, 2014). Infuse Bone Graft is another collagen based product consisting of a recombinant human bone morphogenetic protein-2 (rhBMP-2) that's applied to an absorbable collagen sponge (ACS) carrier (McKay *et al.*, 2007). Matrigel® is one of the current market leading products used as a hydrogel for 2D or 3D cell culture. However, a weak elastic modulus of approximately 450 Pa was reported by Soofi and his colleagues, measured using atomic force microscopy (Soofi *et al.*, 2009).

In addition to collagen, other protein based cell scaffolds have been described including those containing gelatin, bovine serum albumin (BSA) and ovalbumin (OVA) (Sakai *et al.*, 2009; Farrar *et al.*, 2010; Shen *et al.*, 2013; Wang *et al.*, 2014; Luo and Choong, 2015; Fang *et al.*, 2016). Gelatin is another common protein used in cell culture scaffolds, in addition to its availability, biocompatibility and biodegradability, it also contains certain surface moieties, in particular Arginine-Glycine-Aspartic acid sequences that can modulate cell adhesion and encourage cell growth (Hoque *et al.*, 2014). BSA hydrogels have also been reported for use in drug delivery systems (Du *et al.*, 2013; Wang *et al.*, 2014), however these gels either lacked any mechanical strength or required a chemical crosslinker, introducing biocompatibility issues.

There have been multiple studies conducted on the efficiency of ovalbumin as a porous cell scaffold (Farrar *et al.*, 2010; Luo and Choong, 2015). Farrar *et al.* reported multiple ovalbumin hydrogels, figure 4.2, formed from chemically crosslinking the OVA with glutaraldehyde, an agent commonly used in synthetic hydrogels (Gough *et al.*, 2002; Crescenzi *et al.*, 2003).

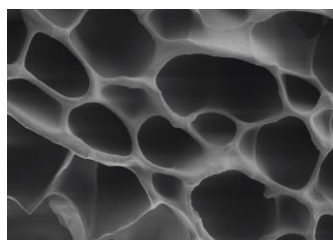


Figure 4.2: FESEM image illustrating the morphology and pore size for ovalbumin-based scaffold at magnification of 200x. Taken from (Farrar *et al.*, 2010).

Although the gels indicated significant increase in cell numbers, the mechanical strength was reported as 6.6 ± 3.6 kPa (Farrar *et al.*, 2010), lower than the OVA/gelatin-225g bigel which we have produced, which has an elastic modulus of 67 kPa. In addition, the chemical crosslinker used, glutaraldehyde, has been reported to have a negative effect on cellular response, due to its cytotoxicity (Gough *et al.*, 2002). OVA cryogels have also been described, and although there is no need for a chemical crosslinker, the elastic modulus was only reported as 15.3 kPa (Elowsson *et al.*, 2012).

The OVA/gelatin and BSA/gelatin protein-only bigels would overcome the mechanical shortcomings associated with most of the natural polymer based hydrogels, while retaining the biocompatibility and biodegradability that is sought after as well as having a naturally porous structure due to the natural voids that occur in the bigels. In addition, the inherent strength of the bigels also allow the formation of self-supporting 3D structures, which could be very useful for certain applications.

PrestoBlue (PB) is a cell viability assay that was recently developed (Lall *et al.*, 2013) to detect cell proliferation *in vitro*. It is a resazurin-based assay which is reduced to resorufin, in metabolically active cells. This conversion is accompanied by colour change from blue to red and a shift in fluorescence/absorbance which can be monitored using a spectrophotometric approach. The exact mechanism for the reduction of resazurin has not been confirmed, however it has been suggested it is from the NADH within the cell (Candeias *et al.*, 1998). PrestoBlue offers distinct advantages over other colorimetric assays including other resazurin based assays such as Alamar Blue and MTT based assays due to its high sensitivity with very low incubation times (Boncler *et al.*, 2014).

4.2 Aims of this study

The aims of this study were to examine the impact of various strong protein gels on cell growth for the potential use as cell scaffolds in biomedical applications where they would be of particular benefit to those that require mechanical strength such as cartilage and bone replacement.

4.3 Results

4.3.1 Analysis of the mechanical properties of collagen gel

Collagen gel is commonly used in cell culture as a scaffold due to its biocompatibility, biodegradability and relative abundance (Lee *et al.*, 2001). However previous studies have reported that collagen forms weak gels (Wu *et al.*, 2005). For certain stress-bearing application such as replacement bone, ligaments and cartilage, it is important that the material used has strong mechanical properties.

For this reason, the mechanical properties of collagen were explored. Collagen gel was prepared at a concentration of 2 mg/ml. Although this concentration is lower than those chosen for the bigels, it was chosen as it is the concentration typically used in cell culture. The elastic modulus of collagen was determined to be 15 Pa using cavitation rheology, figure 4.3, which is similar to some other values for the elastic modulus of Type 1 collagen (Wu *et al.*, 2005). The collagen gel was transparent and very liquid-like in appearance.

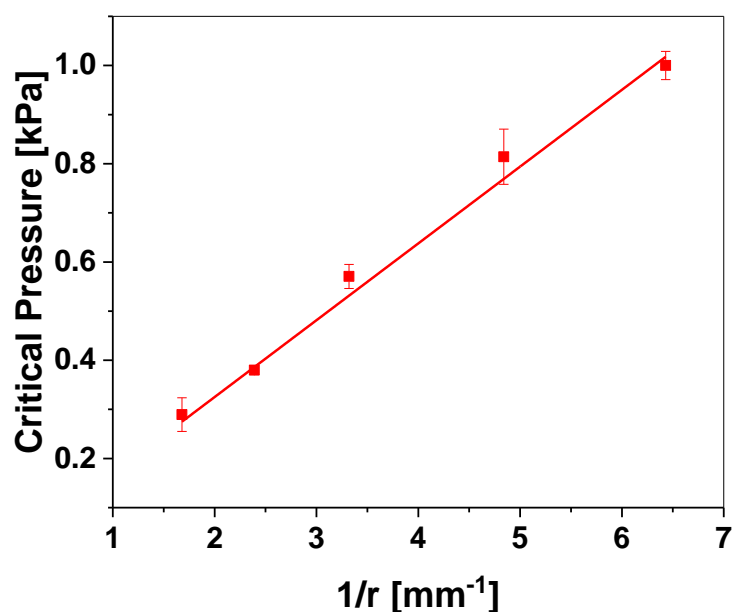


Figure 4.3: The elastic modulus Collagen at 2 mg/ml was found to be 15 P, using cavitation rheology.

In table 2, the elastic modulus for collagen is compared with that of the other scaffold materials used in the study, the OVA/gelatin-225g bigel and the BSA/gelatin-75g bigel, all determined using cavitation rheology (chapter 3). The elastic modulus for collagen is much lower than the double network protein gels.

Table 0.1: Comparison of the elastic moduli for the different scaffold materials

<i>Material</i>	<i>Elastic Modulus (kPa)</i>
BSA/Gelatin-75g bigel, $\phi = 0.141$	36.2
OVA/Gelatin-225g bigel, $\phi = 0.141$	67
Collagen, 0.2 %	0.015

4.3.2 In vitro assessment of different cell scaffolds

Hydrogels are commonly used in biomedical applications that involve tissue culture. Some of the key features to consider when designing hydrogels is biocompatibility, biodegradability, porosity and mechanical strength. The tough protein bigels described in chapter 3, OVA/gelatin and BSA/gelatin would satisfy all of these requirements, providing a great alternative to some of the traditional hydrogels that lacked the

mechanical properties required for certain stress-bearing biomedical applications. In addition, since they are completely protein based, they can be broken down enzymatically without the release of any harmful by-products. However, to qualify for use as a scaffold, the materials must support cell growth and must not exhibit any cytotoxicity towards the cells. For this reason, their efficacy as a cell scaffold was monitored using PrestoBlue assay.

4.3.2.1 Optimisation of Presto Blue assay

PrestoBlue (PB) is a reduction assay used to measure cell proliferation. Prior to use, it is necessary to determine the optimum incubation time for the cell line in use, in this instance for the HEK 273 cell line. Cells were plated in a 24 well plate, at concentrations ranging from 5×10^4 cells/ml to 2.5×10^5 cells/ml, including a control well with only CGM. 50 μ l PB was added to each well (total well volume 500 μ l) giving a 1/10 dilution. The cells were incubated for 10, 20, 30, 60 minutes respectively to determine the optimum incubation time. Experiments were conducted in triplicate. Cell viability was determined by measuring the fluorescence emission at an excitation wavelength of 560 nm and emission wavelength of 590 nm. The results from the optimisation experiments are shown in figure 4.4.

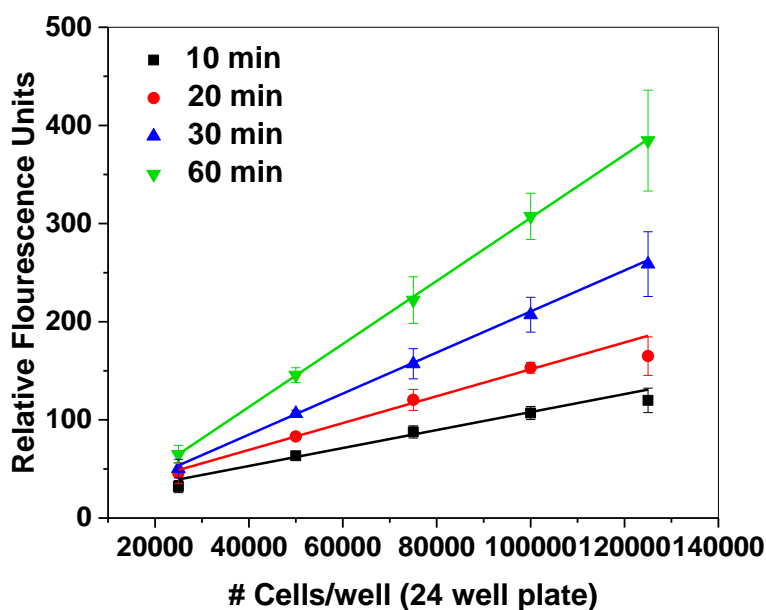


Figure 4.4: Cell proliferation assay on HEK cells using PrestoBlue. The optimal incubation time for PB on the cells was selected based on total fluorescence intensity and limit of detection.

Each data point is an average of three independent wells and corrected for any background fluorescence from the phenol red in the DMEM cell culture medium. All incubation times show good linearity and a good limit of detection (LOD), with the best linearity shown for 30 and 60 min. As the incubation time increases, the signal intensity also increases. However, beyond 30 minutes incubation, the LOD does not necessarily increase further and therefore 30 minutes is sufficient to achieve maximum sensitivity.

4.3.2.2 Preparation of bigel scaffolds for cell culture

The BSA/gelatin-75 and OVA/gelatin-225 gels were prepared using the optimised procedure as described in section 3.322. and listed in table 3.4. The entire procedure apart from any of the incubation steps, was carried out under aseptic conditions in a biological safety cabinet (BSC). Ultrapure water was used for hydrating the proteins which was previously autoclaved at 120 °C for 30 minutes to ensure sterilization. The proteins were hydrated and heated to 45 °C to ensure equilibration and mixed in the BSC. The protein mixture was aliquoted into each well in a 24-well plate. 300 µl was deemed a sufficient volume to ensure that the well surface was completely covered for the duration of the 11 days. The plate was then sealed using sealing tape to prevent any

contamination and heated at 90 °C in a water bath for 3 min and cooled in ice water. Prior to use, the gels were dialysed with 500 µl CGM three times.

4.3.2.3 Impact of various scaffolds on cell growth, determined using presto blue assay

Cell proliferation for HEK 273 was assessed on a number of different protein-based scaffolds using the PB assay and then compared. The bigel scaffolds were prepared in each well as described in section 4.3.3.2 and the collagen scaffolds were prepared as described in section 2.3.6. Experiments were conducted in triplicate. The cells were seeded at a density of 1×10^5 cells/ml in a 24-well plate (500 µl per well) and allowed to adhere for 24 hours before analysing. 50 µl PB was added to each well, including a control well for each material containing the relevant scaffold and medium with no cells. The cells were allowed to incubate with the reagent for 30 min at 37 °C. The medium containing the PB was then transferred to a 96-well plate for measurement. The fluorescence was measured at an excitation wavelength of 560 nm and an emission wavelength of 590 nm using a SpectraMax M2e plate reader each day for a total of 11 days.

The different scaffolds consisted of the OVA/gelatin-225 bigel $\phi = 0.139$, the BSA/gelatin-75 bigel, $\phi = 0.139$, three-dimensional collagen gel (0.2 %), two-dimensional collagen coating and a negative control whereby the well surface was left untreated. Figure 4.5 shows the relative fluorescence measured for the different materials each day across the 11 days. The increase in fluorescence intensity can be related to increased cell numbers. Each point in the data set is an average of three independent wells, corrected for any background fluorescence by the cell medium or from the different scaffold materials, and the error is calculated as the standard deviation of the three independent measurements. The cell growth on the gel scaffolds was compared to the cell proliferation on the untreated negative control wells.

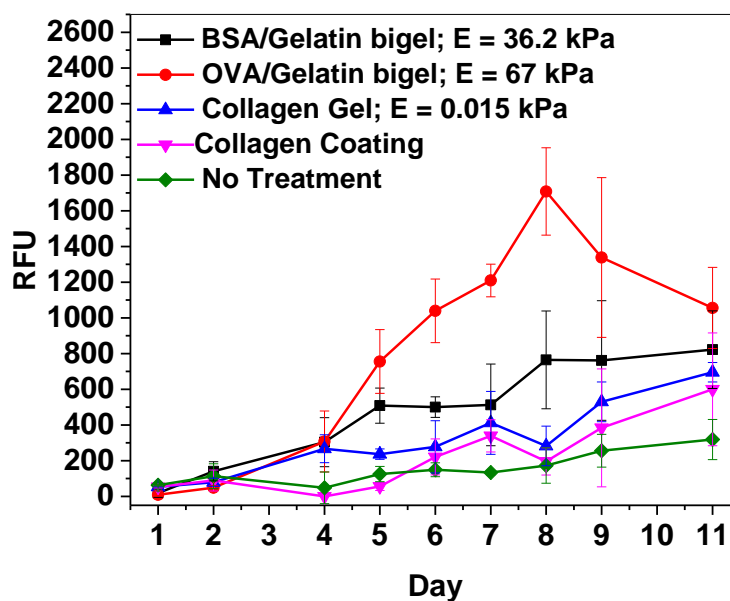


Figure 4.5: The relative fluorescence of the different scaffold materials compared with the control, over 11 days. All points taken as an average of the measurements from three independent wells and corrected for any background fluorescence from the material itself or medium.

For the first two days there was very little difference in cell proliferation on the different surfaces. On day 4, the three gel scaffolds started to show an improvement compared with the 2D collagen scaffold and the negative control (no surface treatment). The OVA/gelatin-225g showed a significant increase in fluorescence intensity over the other gels and the negative control and this trend continued until day 8. On day 8, the highest fluorescence for OVA/gelatin was recorded with RFU of 1708, 883.8 % higher than the control cells. After day 8 the relative fluorescence started to decrease for the cells with the OVA/gelatin-225g scaffold, however this can be attributed to over-confluency resulting in cell death. The cells also responded positively to the BSA/gelatin scaffold with an RFU of 882 recorded on day 11, a 177 % increase when compared with the control cells. There was a RFU of 695 recorded for collagen gel followed by an RFU of 600 for the collagen 2D scaffold.

Light microscopy was used to monitor cell growth on the bigel material. An ovalbumin/gelatin-225g bigel scaffold in the shape of a cylindrical hollow was formed in the individual well in 24 well plate as depicted in figure 4.6.

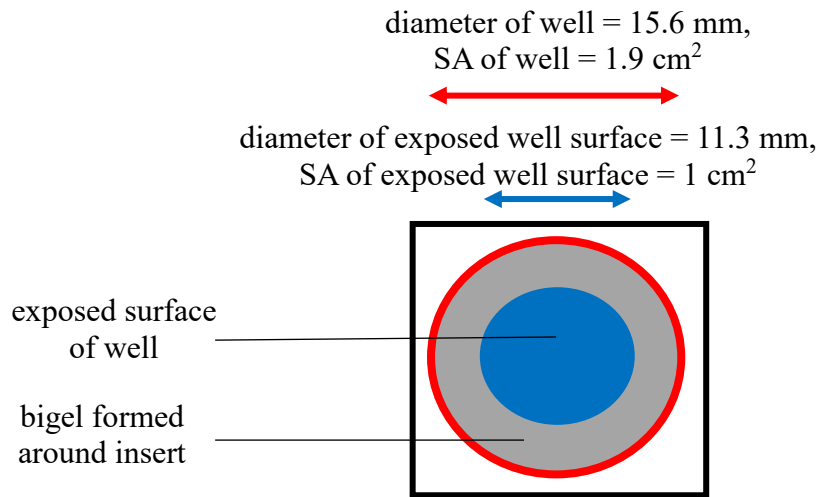


Figure 4.6: Top plan view of hollow cylindrical bigel (grey) formed around edge of well (in 24 well plate) with exposed cell surface in the centre (blue) with dimensions.

To do this, a cylindrical insert was created from layered sheets of silicone. This insert had a diameter of 11.3 mm and a surface area of 1 cm², approximately half of the total surface area of the well, 1.9 cm². This was placed in the centre of the well and the bigel was then formed around the insert. Once the bigel had fully formed and cooled, the insert was removed leaving half of the cell base exposed, as depicted in figure 4.6. Cells were seeded at a concentration of 1×10^5 cells/ml in the well, with the gel scaffold fully submerged in medium to ensure an even distribution of cells. The gels were subsequently visualised and imaged using light microscopy, figure 4.7. The cells appeared to be migrating towards the walls of the bigel, with a much higher confluency of cells visible next to the bigel, compared with the centre of the well, as seen in figure 4.7.

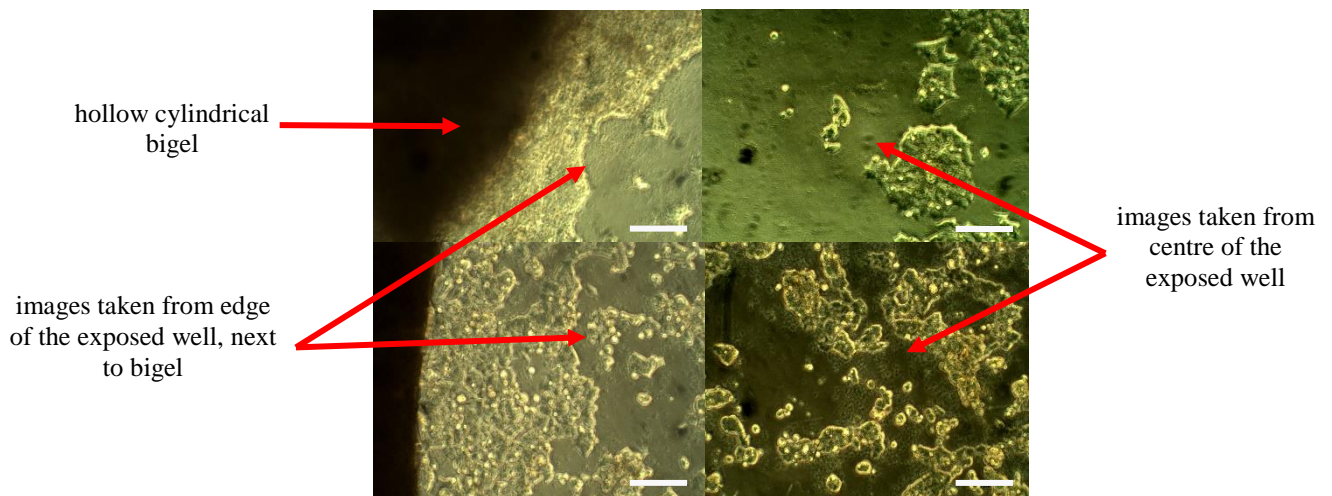


Figure 4.7: Phase contrast light microscopy images of the HEK cells migrating towards the OVA/Gelatin-225g bigel (left wall) at a magnification of 10x. Scale bar = 100 μ m.

4.4 Discussion

The impact of various cell scaffolds on cellular growth *in vitro* was assessed using the PrestoBlue (PB) assay. The ovalbumin/gelatin-225g bigel, followed by the BSA/gelatin-75g bigel had the greatest impact on cell growth when compared with both collagen and the control.

Three-dimensional cell scaffolds have been shown to have a positive impact on cell growth relative to 2D growth conditions (Edmondson *et al.*, 2014). As cells *in vivo* are surrounded by other cells as well as the extracellular matrix (ECM), 3D scaffolds are much more representative of this environment than a two-dimensional culture system and as a result, 2D cell scaffolds can often lead to inaccurate and misleading results *in vitro* (Hutchinson and Kirk, 2011).

Collagen is commonly used for 3D cell scaffolds due to its biocompatibility and biodegradability (Lee *et al.*, 2001; Glowacki and Mizuno, 2008), however, it lacks any structural integrity, forming very weak hydrogels (Wu *et al.*, 2005; Raub *et al.*, 2010), and therefore is not practical for certain applications such as biomimetics or replacement cartilage. The elastic modulus of collagen at 2 mg/ml was found to be 15 Pa using cavitation rheology, much weaker than the elastic moduli determined for the protein bigels described in chapter 3; 36.2 kPa and 67 kPa for the BSA/Gelatin-75g and OVA/Gelatin-225g bigels respectively. In addition, the collagen gel was very liquid-like and was not capable of maintaining a 3D structure, unlike the protein bigels. Although this concentration of collagen was lower than the concentrations of the bigels, 2 mg/mL was chosen as is the concentration typically used for cell culture.

Cell scaffolds containing ovalbumin, BSA and gelatin have all previously been described with promising cellular responses. Wang *et al* described BSA-PEG hydrogels with promising results for drug delivery applications, however these gels were lacking mechanical strength with elastic moduli reported around 2 kPa (Wang *et al.*, 2014). Ovalbumin-based scaffolds have also been described (Farrar *et al.*, 2010; Luo and Choong, 2015). Luo and Choong described multiple ovalbumin scaffolds with promising cellular responses and mechanical properties, however, these all involved chemical crosslinkers introducing biocompatibility and biodegradability issues (Luo and Choong, 2015). These previous findings suggest that the protein bigels described in chapter 3 would be ideal candidates for these hydrogels, overcoming the mechanical

shortcomings of most natural hydrogels, while still maintaining biocompatibility and biodegradability as there are no chemical crosslinkers involved.

To determine their efficacy as a 3D scaffold, the impact of the BSA/Gelatin-75g and the OVA/Gelatin-225g bigels on cell growth was assessed for the HEK 293 cell line, using Presto Blue (PB), a cell proliferation assay. In metabolically active cells resazurin is reduced to resorufin, which fluoresces at an excitation wavelength of 560 nm, and emission wavelength of 590 nm, where the relative fluorescence is directly proportional to cell numbers, therefore it can be used to represent cell proliferation. By comparing the treated cells to control cells, it can be used as a measure of cell viability, or cytotoxicity. Prior to use, it was necessary to determine the optimal assay incubation time for the HEK 293 cell line used in this study. Four different incubation times, 10, 20, 30 and 60 minutes were assessed, with all times showing good sensitivity and 30 and 60 minutes showing the best linearity. 30 minutes was chosen as the incubation time for this study. PB assay was applied daily for 11 days and the fluorescence was measured. All measurements were taken as an average for three separate wells and corrected for any background fluorescence from the scaffold materials or medium. Over the course of the 11 days, as expected, all of the cell scaffolds have a better impact on cell growth when compared with the control cells. However, surprisingly, the cells growing on the OVA/gelatin showed a significant increase in fluorescence compared with the control and other scaffolds, showing that the cells were responding positively to the OVA/gelatin scaffold, with the highest fluorescence recorded on day 8, with an RFU of 1708, 883.8 % higher than the control cells. The drop in fluorescence observed after day 8 for the OVA/gelatin bigel can be attributed to over-confluency. The cells also responded positively to the BSA/gelatin bigel, followed by the 3D collagen and then the 2D collagen.

These findings were supported by optical microscope images of the HEK cells growing next to the OVA/gelatin bigel scaffold. Unfortunately, since the bigels are turbid it is not possible to visualise the growth of the cells on or within the gel with optical microscopy. However, it is clear from these images that the cells were growing preferentially towards the bigel, further indication for its positive impact on cell growth.

Certain peptide sequences on the surface of the scaffold have been shown to help facilitate cellular attachment. The inclusion of the arginine-glycine-aspartic acid (RGD)

peptide for example, has been shown to contribute to cellular proliferation, migration and attachment in various cells (Hersel *et al.*, 2003; Bellis, 2011). Although this particular peptide sequence is not present in ovalbumin or bovine serum albumin, it is present in gelatin, (Zhu and Marchant, 2011; Hoque *et al.*, 2014), one of the two components present in each bigel. This could in part explain the increased cellular action observed in the presence of both bigels.

In addition, numerous recent studies have suggested that cells respond to the mechanical properties of their environment, by altering their adhesion properties (Discher, 2005; Engler *et al.*, 2006; Chang and Wang, 2011; Huebsch *et al.*, 2015). Mesenchymal stem cells for example, have been shown to respond to the stiffness of their environment (Engler *et al.*, 2006; Huebsch *et al.*, 2015). It appears from our measurements that the HEK cells have also responded positively to the high strength and elasticity of the bigels, which would explain the higher rate of cell growth for the OVA/gelatin-225 bigel, which had the highest elastic modulus of 67 kPa.

Although these results are only preliminary, the positive response of the cells to the bigels as well as their strong mechanical properties provides the potential for a range of different biomedical applications such as bone grafting, whereby previous hydrogels have failed to provide the mechanical strength and structural integrity required.

4.5 Conclusion

The two bigels described previously, BSA/gelatin-75g and OVA/gelatin-225g both had a positive impact on cell growth compared with collagen and a negative control (standard cell culture plate with no treatment), indicating promising results for potential biomedical applications. Collagen is commonly used as a hydrogel cell scaffold, due to its availability, biocompatibility and biodegradability (Lee *et al.*, 2001), however it has poor mechanical properties forming very weak gels (Wu *et al.*, 2005). The elastic modulus of collagen gel at 2 mg/ml was determined to be 15 Pa, much weaker than both protein bigels, BSA/gelatin-75g and OVA/gelatin-225g, which were found to be 36.2 and 67 kPa respectively, all determined using cavitation rheology. The impact of the protein bigels on cell growth for the HEK 273 cell line was monitored over 11 days using the PrestoBlue assay, a resazurin based assay whose reduction to resorufin is an indicator of metabolically active cells and can be quantified using fluorescence. The

OVA/gelatin-225g bigel had the greatest impact on cell growth with the highest relative fluorescence unit (RFU) of 1708 on day 8, (corrected for any background fluorescence from the gel or the medium), followed by the BSA/gelatin-75g bigel with a RFU value of 765, compared with the controls cells which had RFU of 173. Light microscopy also revealed preferential growth of the cells towards the OVA/gelatin-225g bigel. These results could be attributed to the positive response cells have been reported to have towards strong materials (Engler *et al.*, 2006; Huebsch *et al.*, 2015) as well as the surface moieties present on gelatin (Hoque *et al.*, 2014). These protein bigels could provide a promising tool for future cellular studies as well as their use for certain applications such as bone grafting and replacement cartilage.

Final Conclusions

This work explores the formation and characterisation of new protein bigels and examines their efficacy as cell scaffolds. Hydrogels are being used increasingly in applications such as tissue engineering, drug delivery and wound dressings due to their high water content and porosity. However, traditional hydrogels lack the mechanical strength required for strength bearing applications such as bone grafting and chemically synthesised hydrogels can lead to biocompatibility and biodegradability issues. Protein bigels consist of two discrete interpenetrating protein gel networks that each contribute to the overall mechanical properties of the gel producing a much stronger gel with the potential to overcome the limitations of traditional hydrogels.

Chapter 3 explores new proteins that can be used to form a bigel. The first protein bigel composed of BSA and gelatin was described in 2015 with an elastic modulus of 24.3 kPa. The mechanism of formation for the BSA component of the bigel was determined to be spinodal decomposition of unfolded BSA followed by aggregation mediated by disulphide bond formation within the spinodally decomposed state. The second thermoreversible gel network was formed by the physical entanglement of gelatin around the BSA network. The first part of my research involved examining the preparation procedure for these bigels. The preparation procedure was optimised to ensure consistency for future measurements. Solution conditions play an important role to ensure that interspecies attraction is kept at a minimum so that two discrete networks can be formed. These factors were also considered when choosing new proteins. Ovalbumin and a high molecular weight gelatin were chosen due to their chemical and physical properties. Bigels were formed with these two proteins and characterised with cavitation rheology. The elastic modulus was determined to be 67 kPa, much larger than that of the BSA/gelatin-75g bigel, at 24.3 kPa. The OVA/gelatin-225g bigel was also much stronger than the combined modulus of the parent gels, similar to what was seen for the BSA/gelatin bigel. The gels exhibited a high degree of elasticity with 85 % of the pressure retained after successive pressurisation cycles. Light microscopy also revealed a percolated network of uniform aggregates surrounded by a second network of gelatin, consistent with the mechanism of spinodal decomposition of unfolded OVA.

Chapter 4 examines the efficacy of the bigels as cell scaffolds. Hydrogels formed from natural polymers are being used increasingly in biomedical applications due to their biocompatibility and biodegradability. Collagen is commonly used, however it lacks mechanical strength. The elastic modulus for collagen at 2 mg/ml was determined to be 15 Pa, much weaker than the elastic moduli determined for the protein bigels, which would provide a great alternative to overcome these mechanical limitations. PrestoBlue cell viability assay was used to determine the impact of different scaffolds on cellular growth. The scaffolds that were compared included several three-dimensional scaffolds; BSA/gelatin bigel, OVA/gelatin bigel, collagen gel and two-dimensional scaffolds; collagen coating and untreated plate well. There was a very positive cellular response to the protein bigels, in particular the OVA/gelatin bigel, followed by the BSA/gelatin bigel when compared with the untreated well, indicating promising potential for biomedical applications.

References

- Abeyrathne, E., Lee, H. Y., and Ahn, D. U. (2013) 'Egg white proteins and their potential use in food processing or as nutraceutical and pharmaceutical agents – a review.', *Poultry Science*, 92, pp. 3292–3299.
- Ahnert, S. E., Marsh, J. A., Hernandez, H., Robinson, C. V., and Teichmann, S. A. (2015) 'Principles of assembly reveal a periodic table of protein complexes', *Science*, 350(6266), p. 1331.
- An, C., Huang, G., Yao, Y., and Zhao, S. (2017) 'Emerging usage of electrocoagulation technology for oil removal from wastewater: A review', *Science of the Total Environment*. Elsevier B.V., 579, pp. 537–556.
- Annabi, N., Nichol, J. W., Zhong, X., Ji, C., Koshy, S., Khademhosseini, A., and Dehghani, F. (2010) 'Controlling the Porosity and Microarchitecture of Hydrogels for Tissue Engineering', *Tissue Engineering Part B: Reviews*, 16(4), pp. 371–383.
- Ansar Ahmed, S., Gogal, R. M., and Walsh, J. E. (1994) 'A new rapid and simple non-radioactive assay to monitor and determine the proliferation of lymphocytes: an alternative to [3H]thymidine incorporation assay', *Journal of Immunological Methods*, 170(2), pp. 211–224.
- Asherie, N. (2004) 'Protein crystallization and phase diagrams', *Methods*, 34(3), pp. 266–272.
- Asherie, N., Lomakin, A., and Benedek, G. B. (1996) 'Phase diagram of colloidal solutions', *Physical Review Letters*, 77(23), pp. 4832–4835.
- Atkins, P. W. (1988) *Physical Chemistry*. Third. Oxford University Press.
- Augst, A. D., Kong, H. J., and Mooney, D. J. (2006) 'Alginate hydrogels as biomaterials', *Macromolecular Bioscience*, 6(8), pp. 623–633.
- Bellis, S. L. (2011) 'Advantages of RGD peptides for directing cell association with biomaterials', *Biomaterials*, 32(18), pp. 4205–4210.
- Berland, C. R., Thurston, G. M., Kondo, M., Broide, M. L., Pande, J., Ogun, O., and

Benedek, G. B. (1992) 'Solid-liquid phase boundaries of lens protein solutions.', *Proceedings of the National Academy of Sciences of the United States of America*, 89(4), pp. 1214–8.

Bhattacharjee, A. and Bansal, M. (2005) 'Collagen Structure: The Madras Triple Helix and the Current Scenario', *IUBMB Life (International Union of Biochemistry and Molecular Biology: Life)*, 57(3), pp. 161–172.

Biffi, S., Cerbino, R., Nava, G., Bomboi, F., Sciortino, F., and Bellini, T. (2015) 'Equilibrium gels of low-valence DNA nanostars: a colloidal model for strong glass formers', *Soft Matter*, 11(16), pp. 3132–3138.

Bigi, A., Panzavolta, S., and Rubini, K. (2004) 'Relationship between triple-helix content and mechanical properties of gelatin films', *Biomaterials*, 25(25), pp. 5675–5680.

Blumlein, A. and McManus, J. J. (2015) 'Bigels formed via spinodal decomposition of unfolded protein', *Journal of Materials Chemistry B. Royal Society of Chemistry*, 3(17), pp. 3429–3435.

Blumlein, A., Williams, N., and McManus, J. J. (2017) 'The mechanical properties of individual cell spheroids', *Scientific Reports*, 7(1), p. 7346.

Boncler, M., Rózsalski, M., Krajewska, U., Podswdek, A., and Watala, C. (2014) 'Comparison of PrestoBlue and MTT assays of cellular viability in the assessment of anti-proliferative effects of plant extracts on human endothelial cells', *Journal of Pharmacological and Toxicological Methods*, 69(1), pp. 9–16.

Boyan, B. D., Hummert, T. W., Dean, D. D., and Schwartz, Z. (1996) 'Role of material surfaces in regulating bone and cartilage cell response', *Biomaterials*, 17(2), pp. 137–146.

Boye, J. I., Alli, I., and Ismail, A. a. (1996) 'Interactions Involved in the Gelation of Bovine Serum Albumin', *Journal of Agricultural and Food Chemistry*, 44(4), pp. 996–1004.

Brauker, J., Carr-Brendel, V., Martinson, L., Crudele, J., and Johnson, R. (1995) 'Neovascularization of syntetic membranes directed by membrane microarchitectura', *Journal of Biomedical Materials Research*, 29, pp. 1517–1534.

- Broide, M. L., Tominc, T. M., and Saxowsky, M. D. (1996) 'Using phase transitions to investigate the effect of salts on protein interactions', *Physical Review E*, 53(6), pp. 6325–6335.
- Bruylants, G., Wouters, J., and Michaux, C. (2005) 'Differential Scanning Calorimetry in Life Science : Thermodynamics , Stability , Molecular Recognition and Application in Drug Design', *Current Medicinal Chemistry*, 12, pp. 2011–2020.
- Bryant, S. J., Nuttelman, C. R., and Anseth, K. (2000) 'Cytocompatibility of UV and visible light photoinitiating systems on cultured NIH / 3T3 fibroblasts in vitro', *Journal of Biomaterial Sciences, Polymer Edition*, 11(5), pp. 439–457.
- Caló, E. and Khutoryanskiy, V. V. (2015) 'Biomedical applications of hydrogels: A review of patents and commercial products', *European Polymer Journal*, 65, pp. 252–267.
- Candeias, L. P., MacFarlane, D. P. S., McWhinnie, S. L. W., Maidwell, N. L., Roeschlaub, C. a., Sammes, P. G., and Whittlesey, R. (1998) 'The catalysed NADH reduction of resazurin to resorufin', *Journal of the Chemical Society, Perkin Transactions 2*, 2333(2), pp. 2333–2334.
- Cardinaux, F., Gibaud, T., Stradner, A., and Schurtenberger, P. (2007) 'Interplay between spinodal decomposition and glass formation in proteins exhibiting short-range attractions', *Physical Review Letters*, 99(11), pp. 1–4.
- Carter, D. C. and Ho, J. X. (1994) 'Structure of serum albumin', *Advances in Protein Chemistry*, 45(C), pp. 153–203.
- Chambon, F. and Winter, H. H. (1987) 'Linear Viscoelasticity at the Gel Point of a Crosslinking PDMS with Imbalanced Stoichiometry', *Journal of Rheology*, 31(8), pp. 683–697.
- Chang, H.-I. and Wang, Y. (2011) 'Cell Responses to Surface and Architecture of Tissue Engineering Scaffolds', *Regenerative Medicine and Tissue Engineering - Cells and Biomaterials*, pp. 569–588.
- Chin, M. S. M., Freniere, B. B., Fakhouri, S., Harris, J. E., Lalikos, J. F., and Crosby, A. J. (2013) 'Cavitation Rheology as a Potential Method for in vivo Assessment of Skin Biomechanics', *Plastic Reconstructive Surgery*, 131(2), pp. 1–4.

- Chung, H. J. and Park, T. G. (2009) 'Self-assembled and nanostructured hydrogels for drug delivery and tissue engineering', *Nano Today*, 4(5), pp. 429–437.
- Cooper, A. (2011) *Biophysical Chemistry*. Second. Cambridge: The Royal Society of Chemistry.
- Corezzi, S., Palmieri, L., Kenny, J. M., and Fioretto, D. (2005) 'Clustering, glass transition and gelation in a reactive fluid', *Journal of Physics: Condensed Matter*, 17, pp. S3557–S3563.
- Crescenzi, V., Francescangeli, A., Taglienti, A., Capitani, D., and Mannina, L. (2003) 'Synthesis and partial characterization of hydrogels obtained via glutaraldehyde crosslinking of acetylated chitosan and of hyaluronan derivatives', *Biomacromolecules*, 4(4), pp. 1045–1054.
- Crosby, A. J. and McManus, J. J. (2011) 'Blowing bubbles to study living material', *Physics Today*, 64(2), pp. 62–63.
- Cui, J., Lee, C. H., Delbos, A., McManus, J. J., and Crosby, A. J. (2011) 'Cavitation rheology of the eye lens', *Soft Matter*, 7(17), p. 7827.
- Davis, J. S., Alkhoury, F., and Burnweit, C. (2014) 'Surgical and anesthetic considerations in histrelin capsule implantation for the treatment of precocious puberty', *Journal of Pediatric Surgery*, 49(5), pp. 807–810.
- Dhandayuthapani, B., Yoshida, Y., Maekawa, T., and Kumar, D. S. (2011) 'Polymeric scaffolds in tissue engineering application: A review', *International Journal of Polymer Science*, 2011, pp. 1–19.
- Di Michele, L., Fiocco, D., Varrato, F., Sastry, S., Eiser, E., and Foffi, G. (2014) 'Aggregation dynamics, structure, and mechanical properties of bigels.', *Soft matter*, 10(20), pp. 3633–3648.
- Discher, D. E. (2005) 'Tissue Cells Feel and Respond to the Stiffness of Their Substrate', *Science*, 310(5751), pp. 1139–1143.
- Distantina, S., Rochmadi, Fahrurrozi, M., and Wiratni (2012) 'Preparation of Hydrogel Based on Glutaraldehyde-Crosslinked Carrageenan', *3rd International Conference on Chemistry and Chemical Engineering*, 38, pp. 150–154.

- Djabourov, M., Leblond, J., and Papon, P. (1988) 'Gelation of aqueous gelatin solutions. I. Structural investigation', *Journal de Physique*, 49, pp. 319–332.
- Dragan, E. S. (2014) 'Design and applications of interpenetrating polymer network hydrogels. A review', *Chemical Engineering Journal*, 243, pp. 572–590.
- Du, C., Deng, D., Shan, L., Wan, S., Cao, J., Tian, J., Achilefu, S., and Gu, Y. (2013) 'A pH-sensitive doxorubicin prodrug based on folate-conjugated BSA for tumor-targeted drug delivery', *Biomaterials*, 34(12), pp. 3087–3097.
- Dumetz, A. C., Chockla, A. M., Kaler, E. W., and Lenhoff, A. M. (2008) 'Protein Phase Behavior in Aqueous Solutions: Crystallization, Liquid-Liquid Phase Separation, Gels, and Aggregates', *Biophysical Journal*, 94(2), pp. 570–583.
- Dumetz, A. C., Chockla, A. M., Kaler, E. W., and Lenhoff, A. M. (2008) 'Protein phase behavior in aqueous solutions: crystallization, liquid-liquid phase separation, gels, and aggregates.', *Biophysical journal*, 94(2), pp. 570–583.
- Edmondson, R., Broglie, J. J., Adcock, A. F., and Yang, L. (2014) 'Three-Dimensional Cell Culture Systems and Their Applications in Drug Discovery and Cell-Based Biosensors', *ASSAY and Drug Development Technologies*, 12(4), pp. 207–218.
- El-Sherbiny, I. and Yacoub, M. (2013) 'Hydrogel scaffolds for tissue engineering: Progress and challenges', *Global cardiology science & practice*, 2013(3), pp. 316–42.
- Elisseef, J., McIntosh, W., Anseth, K., Riley, S., Ragan, P., and Langer, R. (1999) 'Photoencapsulation of chondrocytes in poly (ether oxide) -based semi-interpenetrating networks', *Journal of Biomedical Materials Research*, 52(2), pp. 164–171.
- Elowsson, L., Kirsebom, H., Carmignac, V., Durbeej, M., and Mattiasson, B. (2012) 'Porous protein-based scaffolds prepared through freezing as potential scaffolds for tissue engineering', *Journal of Materials Science: Materials in Medicine*, 23(10), pp. 2489–2498.
- Engler, A. J., Sen, S., Sweeney, H. L., and Discher, D. E. (2006) 'Matrix Elasticity Directs Stem Cell Lineage Specification', *Cell*, 126(4), pp. 677–689.
- Everett, D. H. (2007) *Basic Principles of Colloid Science*. Royal Society of Chemistry Paperbacks.

- Fang, X., Xie, J., Zhong, L., Li, J., Rong, D., Li, X., and Ouyang, J. (2016) 'Biomimetic gelatin methacrylamide hydrogel scaffolds for bone tissue engineering', *Journal of Materials Chemistry B*, 4(6), pp. 1070–1080.
- Farrar, G., Barone, J., and Morgan, A. (2010) 'Ovalbumin-Based Porous Scaffolds for Bone Tissue Regeneration', *Journal of Tissue Engineering*, 2010, pp. 1–6.
- Ferry, J. D. and Eldridge, J. E. (1948) 'Studies of the cross-linking process in gelatin gels. I.', *Journal of Physical Chemistry*, (53), pp. 184–196.
- García De La Torre, J., Huertas, M. L., and Carrasco, B. (2000) 'Calculation of hydrodynamic properties of globular proteins from their atomic-level structure.', *Biophysical journal*. The Biophysical Society, 78(2), pp. 719–30.
- Gent, A. N. and Tompkins, D. A. (1969) 'Nucleation and growth of gas bubbles in elastomers', *Journal of Applied Physics*, 40(6), pp. 2520–2525.
- Gent, A. N. and Wang, C. (1991) 'Fracture mechanics and cavitation in rubber-like solids', *Journal of Materials Science*, 26(12), pp. 3392–3395.
- Gibaud, T., Cardinaux, F. F., Bergenholtz, J., Stradner, A., and Schurtenberger, P. (2011) 'Phase separation and dynamical arrest for particles interacting with mixed potentials—the case of globular proteins revisited', *Soft Matter*, 7(3), pp. 857–860.
- Gibaud, T. and Schurtenberger, P. (2009) 'A closer look at arrested spinodal decomposition in protein solutions.', *Journal of Physics: Condensed Matter Condensed matter*, 21(32), p. 322201.
- Gleeson, J. P., Plunkett, N. A., and O'Brien, F. J. (2010) 'Addition of hydroxyapatite improves stiffness, interconnectivity and osteogenic potential of a highly porous collagen-based scaffold for bone tissue regeneration', *European Cells and Materials*, 20, pp. 218–230.
- Glowacki, J. and Mizuno, S. (2008) 'Collagen scaffolds for tissue engineering', *Biopolymers*, 89(5), pp. 338–344.
- Gong, J. P., Katsuyama, Y., Kurokawa, T., and Osada, Y. (2003) 'Double-network hydrogels with extremely high mechanical strength', *Advanced Materials*, 15(14), pp. 1155–1158.

- Gough, J. E., Scotchford, C. A., and Downes, S. (2002) 'Cytotoxicity of glutaraldehyde crosslinked collagen/poly(vinyl alcohol) films is by the mechanism of apoptosis', *Journal of Biomedical Materials Research*, 61(1), pp. 121–130.
- Graham, F. L. and Van Der Eb, A. J. (1973) 'A New Technique for the Assay of Infectivity of Human Adenovirus 5 DNA', *Virology*, 52(2), pp. 456–467.
- Grzybowski, B. A., Wilmer, C. E., Kim, J., Browne, K. P., and Bishop, K. J. M. (2009) 'Self-assembly: from crystals to cells', *Soft Matter*, 5(6), p. 1110.
- Hayashi, A. and Oh, S.-C. (1983) 'Gelation of gelatin solution.', *Agricultural and Biological Chemistry*, 47(8), pp. 1711–1716.
- Hersel, U., Dahmen, C., and Kessler, H. (2003) 'RGD modified polymers: Biomaterials for stimulated cell adhesion and beyond', *Biomaterials*, 24(24), pp. 4385–4415.
- Hoffman, A. S. (2002) 'Hydrogels for biomedical applications', *Advanced Drug Delivery Reviews*, 43, pp. 3–12.
- Hoque, M. E., Nuge, T., Yeow, T. K., Nordin, N., and Prasad, R. G. (2014) 'Gelatin Based Scaffolds for Tissue Engineering – a Review', *Polymers Research Journal*, 9(1).
- Huebsch, N., Lippens, E., Lee, K., Mehta, M., Koshy, S. T., Darnell, M. C., Desai, R. M., Madl, C. M., Xu, M., Zhao, X., Chaudhuri, O., Verbeke, C., Kim, W. S., Alim, K., Mammoto, A., Ingber, D. E., Duda, G. N., and Mooney, D. J. (2015) 'Matrix elasticity of void-forming hydrogels controls transplanted-stem-cell-mediated bone formation', *Nature Materials*, 14(12), pp. 1269–1277.
- Hulme, E. C. and Trevethick, M. A. (2010) 'Ligand binding assays at equilibrium: Validation and interpretation', *British Journal of Pharmacology*, 161(6), pp. 1219–1237.
- Hunt, L. T. and Dayhoff, M. O. (1980) 'A surprising new protein superfamily containing ovalbumin, antithrombin-III, and alpha 1-proteinase inhibitor', *Topics in Catalysis*, 95(2), pp. 864–871.
- Huntington, J. A. and Stein, P. E. (2001) 'Structure and properties of ovalbumin', *Journal of Chromatography B: Biomedical Sciences and Applications*, 756(1–2), pp. 189–198.

- Hutchinson, L. and Kirk, R. (2011) 'High drug attrition rates—where are we going wrong?', *Nature Reviews Clinical Oncology*, 8(4), pp. 189–190.
- Hutmacher, D. W. (2001) 'Scaffold design and fabrication technologies for engineering tissues — state of the art and future perspectives', *Journal of Biomaterials Science, Polymer Edition*, 12(1), pp. 107–124.
- Israelachvili, J. (1991) *Intermolecular & Surface Forces*. Second. Academic Press.
- Johnson, C. M. (2013) 'Differential scanning calorimetry as a tool for protein folding and stability', *Archives of Biochemistry and Biophysics*, 531(1–2), pp. 100–109.
- Jones, V., Grey, J., and Harding, K. (2006) 'ABC of wound healing: Wound dressings', *British Medical Journal*, 332, pp. 777–780.
- Jonker, A. M., Löwik, D. W. P., and van Hest, J. C. M. (2012) 'Peptide- and Protein-Based Hydrogels', *Chemistry of Materials*, 24(5), pp. 759–773.
- Kallapur, S. G. and Akeson, R. A. (1992) 'The neural cell adhesion molecule (NCAM) heparin binding domain binds to cell surface heparan sulfate proteoglycans', *Journal of Neuroscience Research*, 33, pp. 538–548.
- Kim, I.-Y., Seo, S.-J., Moon, H.-S., Yoo, M.-K., Park, I.-Y., Kim, B.-C., and Cho, C.-S. (2008) 'Chitosan and its derivatives for tissue engineering applications', *Biotechnology Advances*, 26(1), pp. 1–21.
- Knipe, J. M., Chen, F., and Peppas, N. A. (2015) 'Enzymatic Biodegradation of Hydrogels for Protein Delivery Targeted to the Small Intestine', *Biomacromolecules*, 16(3), pp. 962–972.
- Knowles, T. P., Fitzpatrick, A. W., Meehan, S., Mott, H. R., Vendruscolo, M., Dobson, C. M., and Welland, M. E. (2007) 'Role of Intermolecular Forces in Defining Material Properties of Protein Nanofibrils', *Science*, 318(5858), pp. 1900–1903.
- Knowles, T. P. J., Vendruscolo, M., and Dobson, C. M. (2014) 'The amyloid state and its association with protein misfolding diseases', *Nature Reviews Molecular Cell Biology*, 15(7), pp. 496–496.
- Kundu, S. and Crosby, A. J. (2009) 'Cavitation and fracture behavior of polyacrylamide hydrogels', *Soft Matter*, 5(20), p. 3963.

- Kurotsu, M., Yajima, M., Takahashi, M., Ogawa, E., and Arai, T. (2015) 'Evaluation of human and bovine serum albumin on oxidation characteristics by a photosensitization reaction under complete binding of talaporfin sodium', *Photodiagnosis and Photodynamic Therapy*, 12(3), pp. 408–413.
- Lall, N., Henley-Smith, C. J., De Canha, M. N., Oosthuizen, C. B., and Berrington, D. (2013) 'Viability reagent, prestoblue, in comparison with other available reagents, utilized in cytotoxicity and antimicrobial assays', *International Journal of Microbiology*, 2013, pp. 1–5.
- Leach, J. B., Bivens, K. A., Patrick, C. W., and Schmidt, C. E. (2003) 'Photocrosslinked hyaluronic acid hydrogels: Natural, biodegradable tissue engineering scaffolds', *Biotechnology and Bioengineering*, 82(5), pp. 578–589.
- Lee, C. H., Singla, A., and Lee, Y. (2001) 'Biomedical applications of collagen', *International Journal of Pharmaceutics*, 221(1–2), pp. 1–22.
- Lee, C., Wacklin, H., and Bain, C. D. (2009) 'Changes in molecular composition and packing during lipidmembrane reconstitution from phospholipid–surfactant micelles', *Soft Matter*, 5(3), pp. 568–575.
- Lee, K. Y. and Mooney, D. J. (2012) 'Alginate : properties and biomedical applications', *Progress in Polymer Science*, 37(1), pp. 106–126.
- Levingstone, T. J., Matsiko, A., Dickson, G. R., O'Brien, F. J., and Gleeson, J. P. (2014) 'A biomimetic multi-layered collagen-based scaffold for osteochondral repair', *Acta Biomaterialia*, 10(5), pp. 1996–2004.
- Lewis, J. C., Snell, N. S., Hirschmann, D. J., and Fraenkel-Conrat, H. (1950) 'Amino Acid Composition of Egg Proteins', *The Journal of Biological Chemistry*, 186(1), pp. 23–35.
- Li, R., Wu, Z., Wangb, Y., Ding, L., and Wang, Y. (2016) 'Role of pH-induced structural change in protein aggregation in foam fractionation of bovine serum albumin', *Biotechnology Reports*, 9, pp. 46–52.
- Liang, Y., Hilal, N., Langston, P., and Starov, V. (2007) 'Interaction forces between colloidal particles in liquid: Theory and experiment', *Advances in Colloid and Interface Science*, 134–135, pp. 151–166.

- Lien, S. M., Ko, L. Y., and Huang, T. J. (2009) 'Effect of pore size on ECM secretion and cell growth in gelatin scaffold for articular cartilage tissue engineering', *Acta Biomaterialia*, 5(2), pp. 670–679.
- Lu, P. J. and Weitz, D. A. (2013) 'Colloidal Particles: Crystals, Glasses, and Gels', *Annual Review of Condensed Matter Physics*, 4(1), pp. 217–233.
- Lu, P. J., Zaccarelli, E., Ciulla, F., Schofield, A. B., Sciortino, F., and Weitz, D. A. (2008) 'Gelation of particles with short-range attraction.', *Nature*, 453(7194), pp. 499–503.
- Luo, B. and Choong, C. (2015) 'Porous ovalbumin scaffolds with tunable properties: A resource-efficient biodegradable material for tissue engineering applications', *Journal of Biomaterials Applications*, 29(6), pp. 903–911.
- Mahmoudi, N. and Stradner, A. (2015) 'Making Food Protein Gels via an Arrested Spinodal Decomposition', *Journal of Physical Chemistry B*, 119(50), pp. 15522–15529.
- Manley, S., Skotheim, J. M., Mahadevan, L., and Weitz, D. A. (2005) 'Gravitational collapse of colloidal gels', *Physical Review Letters*. Royal Society of Chemistry, 94(21), pp. 4300–4308.
- Manley, S., Wyss, H. M., Miyazaki, K., Conrad, J. C., Trappe, V., Kaufman, L. J., Reichman, D. R., and Weitz, D. A. (2005) 'Glasslike arrest in spinodal decomposition as a route to colloidal gelation', *Physical Review Letters*, 95(23), pp. 1–4.
- McCafferty, M. M., Burke, G. A., and Meenan, B. J. (2014) 'Mesenchymal stem cell response to conformal sputter deposited calcium phosphate thin films on nanostructured titanium surfaces', *Journal of Biomedical Materials Research - Part A*, 102(10), pp. 3585–3597.
- McKay, W. F., Peckham, S. M., and Badura, J. M. (2007) 'A comprehensive clinical review of recombinant human bone morphogenetic protein-2 (INFUSE Bone Graft)', *International Orthopaedics*, 31(6), pp. 729–734.
- McManus, J. J., Charbonneau, P., Zaccarelli, E., and Asherie, N. (2016) 'The physics of protein self-assembly', *Current Opinion in Colloid and Interface Science*, 22, pp. 73–79.
- McManus, J. J., Lomakin, A., Ogun, O., Pande, A., Basan, M., Pande, J., and Benedek,

- G. B. (2007) 'Altered phase diagram due to a single point mutation in human gammaD-crystallin.', *Proceedings of the National Academy of Sciences of the United States of America*, 104(43), pp. 16856–61.
- Morris, A. M., Watzky, M. A., and Finke, R. G. (2009) 'Protein aggregation kinetics, mechanism, and curve-fitting: A review of the literature', *Biochimica et Biophysica Acta (BBA) - Proteins and Proteomics*, 1794(3), pp. 375–397.
- Mosmann, T. (1983) 'Rapid colorimetric assay for cellular growth and survival: Application to proliferation and cytotoxicity assays', *Journal of Immunological Methods*, 65(1–2), pp. 55–63.
- Mozurkewich, E. L., Chilimigras, J. L., Berman, D. R., Perni, U. C., Romero, V. C., King, V. J., and Keeton, K. L. (2011) 'Methods of induction of labour: a systematic review', *BMC Pregnancy and Childbirth*, 11(1), p. 84.
- Nakayama, A., Kakugo, A., Gong, J. P., Osada, Y., Takai, M., Erata, T., and Kawano, S. (2004) 'High mechanical strength double-network hydrogel with bacterial cellulose', *Advanced Functional Materials*, 14(11), pp. 1124–1128.
- Ngarize, S., Herman, H., Adams, A., and Howell, N. (2004) 'Comparison of changes in the secondary structure of unheated, heated, and high-pressure-treated β -lactoglobulin and ovalbumin proteins using Fourier transform Raman spectroscopy and self-deconvolution', *Journal of Agricultural and Food Chemistry*, 52(21), pp. 6470–6477.
- O'Leary, L. E., Fallas, J. A., Bakota, E. L., Kang, M. K., and Hartgerink, J. D. (2011) 'Multi-hierarchical self-assembly of a collagen mimetic peptide from triple helix to nanofibre and hydrogel', *Nature Chemistry*, 3(10), pp. 821–828.
- Olais-Govea, J. M., López-Flores, L., and Medina-Noyola, M. (2015) 'Non-equilibrium theory of arrested spinodal decomposition', *Journal of Chemical Physics*, 143(17).
- Oldenbourg, R. (2013) 'Polarized light microscopy: Principles and practice', *Cold Spring Harbor Protocols*, 2013(11), pp. 1023–1036.
- Park, J. S., Chu, J. S., Tsou, A. D., Diop, R., Wang, A., and Li, S. (2012) 'The Effect of Matrix Stiffness on the Differentiation of Mesenchymal Stem Cells in Response to TGF- β ', *Biomaterials*, 32(16), pp. 3921–3930.
- Peters, J. P., Yelgaonkar, S. P., Srivatsan, S. G., Tor, Y., and Maher, L. J. (2013)

- ‘Mechanical properties of DNA-like polymers’, *Nucleic Acids Research*, 41(22), pp. 10593–10604.
- Philo, J. S. and Arakawa, T. (2009) ‘Mechanisms of protein aggregation.’, *Current pharmaceutical biotechnology*, 10(4), pp. 348–51.
- Photchanachai, S., Mehta, A., and Kitabatake, N. (2002) ‘Heating of an ovalbumin solution at neutral pH and high temperature.’, *Bioscience, biotechnology, and biochemistry*, 66(8), pp. 1635–1640.
- Pierschbacher, M. D. and Ruoslahti, E. (1984) ‘Cell attachment activity of fibronectin can be duplicated by small synthetic fragments of the molecule’, *Nature*, 309(5963), pp. 30–33.
- Prausnitz, J. M. and Foose, L. (2007) ‘Three frontiers in the thermodynamics of protein solutions’, *Pure and Applied Chemistry*, 79(8), pp. 1435–1444.
- Ramachandran, G. N. and Kartha, G. (1954) ‘Structure of Collagen.’, *Nature*, 174(6), pp. 269–270.
- Raub, C. B., Putnam, A. J., Tromberg, B. J., and George, S. C. (2010) ‘Predicting bulk mechanical properties of cellularized collagen gels using multiphoton microscopy’, *Acta Biomaterialia*, 6(12), pp. 4657–4665.
- Reubke, R. and Mollica, J. A. (1967) ‘Applications of differential scanning calorimetry in pharmaceutical analysis.’, *Journal of pharmaceutical sciences*, 56(7), pp. 822–5.
- Rhodes, M. B., Azari, P. R., and Feeney, R. E. (1958) ‘Analysis, fractionation, and purification of egg white proteins with cellulose cation exchanger’, *The Journal of Biological Chemistry*, 230(1), pp. 399–408.
- Riss, T. L., Moravec, R. A., Niles, A. L., Duellman, S., Benink, H. A., Worzella, T. J., and Minor, L. (2013) ‘Cell Viability Assays’, *Assay Guidance Manual [Internet]*, 114(8), pp. 785–796.
- Rosenbaum, D., Zamora, P. C., and Zukoski, C. F. (1996) ‘Phase Behavior of Small Attractive Colloidal Particles’, *Physical Review Letters*, 76(1), pp. 150–153.
- Ruoslahti, E. (1996) ‘Rgd and Other Recognition Sequences for Integrins’, *Annual Review of Cell and Developmental Biology*, 12(1), pp. 697–715.

- Ruzicka, B., Zaccarelli, E., Zulian, L., Angelini, R., Sztucki, M., Moussaïd, A., Narayanan, T., and Sciortino, F. (2011) ‘Observation of empty liquids and equilibrium gels in a colloidal clay’, *Nature Materials*, 10, pp. 56–60.
- Sakai, S., Hirose, K., Taguchi, K., Ogushi, Y., and Kawakami, K. (2009) ‘An injectable, in situ enzymatically gellable, gelatin derivative for drug delivery and tissue engineering’, *Biomaterials*, 30(20), pp. 3371–3377.
- Shen, H. J., Shi, H., Ma, K., Xie, M., Tang, L. L., Shen, S., Li, B., Wang, X. S., and Jin, Y. (2013) ‘Polyelectrolyte capsules packaging BSA gels for pH-controlled drug loading and release and their antitumor activity’, *Acta Biomaterialia*, 9(4), pp. 6123–6133.
- Shoulders, M. D. and Raines, R. T. (2009) ‘Collagen Structure and Stability’, *Annual Review of Biochemistry*, 78(3), pp. 929–958.
- Smith, M. B. (1964) ‘Studies on Ovalbumin I. Denaturation by Heat, and the Heterogeneity of Ovalbumin’, *Australian Journal of Biological Sciences*, 17(1), pp. 261–270.
- Soofi, S. S., Last, J. A., Liliensiek, S. J., Nealey, P. F., and Murphy, C. J. (2009) ‘The elastic modulus of Matrigel™ as determined by atomic force microscopy Shauheen’, *Journal of structural biology*, 167(3), pp. 216–219.
- Sperling, L. H. and Mishra, V. (1996) ‘The Current Status of Interpenetrating Polymer Networks’, *Polymers for Advanced Technologies*, 7(4), pp. 197–208.
- Suggs, L. J. and Mikos, A. G. (1999) ‘Development of poly(propylene fumarate-co-ethylene glycol) as an injectable carrier for endothelial cells’, *Cell Transplantation*, 8(4), pp. 345–350.
- Sun, J.-Y., Zhao, X., Illeperuma, W. R. K., Chaudhuri, O., Oh, K. H., Mooney, D. J., Vlassak, J. J., and Suo, Z. (2012) ‘Highly stretchable and tough hydrogels’, *Nature*, 489(7414), pp. 133–136.
- Thomas, P. and Smart, T. G. (2005) ‘HEK293 cell line: A vehicle for the expression of recombinant proteins’, *Journal of Pharmacological and Toxicological Methods*, 51, pp. 187–200.
- Thompson, E. O. P. and Fisher, W. K. (1978) ‘A Correction and Extension of the Acetylated Amino Terminal Sequence of Ovalbumin’, *Australian Journal of Biological*

Sciences, 31(5), pp. 443–446.

Tıgılı, R. S., Kazaroğlu, N. M., Maviş, B., and Gümüşderelioğlu, M. (2011) ‘Cellular Behavior on Epidermal Growth Factor (EGF)-Immobilized PCL/Gelatin Nanofibrous Scaffolds’, *Journal of Biomaterials Science, Polymer Edition*, 22(1–3), pp. 207–223.

Valente, J. J., Payne, R. W., Manning, M. C., Wilson, W. W., and Henry, C. S. (2005) ‘Colloidal behavior of proteins: effects of the second virial coefficient on solubility, crystallization and aggregation of proteins in aqueous solution.’, *Current pharmaceutical biotechnology*, 6(6), pp. 427–436.

Vargaftik, N. B., Volkov, B. N., and Voljak, L. D. (1983) ‘International Tables of the Surface Tension of Water’, *Journal of Physical and Chemical Reference Data*, pp. 817–820.

Varrato, F., Di Michele, L., Belushkin, M., Dorsaz, N., Nathan, S. H., Eiser, E., and Foffi, G. (2012) ‘Arrested demixing opens route to bigels.’, *Proceedings of the National Academy of Sciences of the United States of America*, 109(47), pp. 19155–19160.

Vekilov, P. G. (2012) ‘Phase diagrams and kinetics of phase transitions in protein solutions.’, *Journal of physics. Condensed matter*, 24(19), p. 193101.

Vernon, T. (2000) ‘Intrasite Gel and Intrasite Conformable: the hydrogel range.’, *British journal of nursing (Mark Allen Publishing)*, 9(16), pp. 1083–8.

Wang, D., Hu, Y., Liu, P., and Luo, D. (2017) ‘Bioresponsive DNA Hydrogels: Beyond the Conventional Stimuli Responsiveness’, *Accounts of Chemical Research*, 50(4), pp. 733–739.

Wang, J., Liu, K., Xing, R., and Yan, X. (2016) ‘Peptide self-assembly: thermodynamics and kinetics’, *Chemical Society Reviews*, 45(20), pp. 5589–5604.

Wang, K., Buschle-Diller, G., and Wu, Y. (2014) ‘Thermoresponsive hydrogels from BSA esterified with low molecular weight PEG’, *Journal of Applied Polymer Science*, 131(20), pp. 1–8.

Wang, W. (2005) ‘Protein aggregation and its inhibition in biopharmaceutics’, *International Journal of Pharmaceutics*, 289(1–2), pp. 1–30.

Weijers, M., Barneveld, P. A., Cohen Stuart, M. A., and Visschers, R. W. (2003) ‘Heat-

induced denaturation and aggregation of ovalbumin at neutral pH described by irreversible first-order kinetics.’, *Protein Science*, 12, pp. 2693–703.

Whitford, D. (2005) *Proteins: Structure and Function*. West Sussex: John Wiley & Sons Ltd.

Williams, C. (1996) ‘Granugel: hydrocolloid gel.’, *British journal of nursing (Mark Allen Publishing)*, 5(3), pp. 188, 190.

Wu, C.-C., Ding, S.-J., Wang, Y.-H., Tang, M.-J., and Chang, H.-C. (2005) ‘Mechanical properties of collagen gels derived from rats of different ages’, *Journal of Biomaterials Science, Polymer Edition*, 16(10), pp. 1261–1275.

Xu, M., McCanna, D. J., and Sivak, J. G. (2015) ‘Use of the viability reagent PrestoBlue in comparison with alamarBlue and MTT to assess the viability of human corneal epithelial cells’, *Journal of Pharmacological and Toxicological Methods*, 71, pp. 1–7.

Yan, H., Saiani, A., Gough, J. E., and Miller, A. F. (2006) ‘Thermoreversible protein hydrogel as cell scaffold’, *Biomacromolecules*, 7(10), pp. 2776–2782.

Yannas, I. V. (1972) ‘Collagen and Gelatin in the Solid State’, *Journal of Macromolecular Science, Part C*, 7(1), pp. 49–106.

Yu, H. G., Chung, H., Yu, Y. S., Seo, J. M., and Heo, J. W. (2003) ‘A New Rapid and Non-radioactive Assay for Monitoring and Determining the Proliferation of Retinal Pigment Epithelial Cells.’, *Korean J Ophthalmol*, 17(1), pp. 29–34.

Zaccarelli, E. (2007) ‘Colloidal Gels: Equilibrium and Non-Equilibrium Routes’, *Journal of Physics: Condensed Matter*, 19.

Zaccarelli, E., Lu, P. J., Ciulla, F., Weitz, D. A., and Sciortino, F. (2008) ‘Gelation as arrested phase separation in short-ranged attractive colloid–polymer mixtures’, *Journal of Physics: Condensed Matter*, 20(49), p. 494242.

Zhang, Y., Liu, J., Huang, L., Wang, Z., and Wang, L. (2015) ‘Design and performance of a sericin-alginate interpenetrating network hydrogel for cell and drug delivery.’, *Scientific reports*, 5(4), p. 12374.

Zhu, J. and Marchant, R. E. (2011) ‘Design properties of hydrogel tissue-engineering

scaffolds’, *Expert Review of Medical Devices*, 8(5), pp. 607–626.

Zimberlin, J. A., McManus, J. J., and Crosby, A. J. (2010) ‘Cavitation rheology of the vitreous: mechanical properties of biological tissue’, *Soft Matter*, 6(15), p. 3632.

Zimberlin, J. A., Sanabria-DeLong, N., Tew, G. N., and Crosby, A. J. (2007) ‘Cavitation rheology for soft materials’, *Soft Matter*, 3(6), p. 763.